

Synthesis and Characterisation of Amphiphilic Block Copolymers

Dissertation presented for the degree:

Doctor of Philosophy (Polymer Science)

at the University of Stellenbosch



by

Charl Ernst Morkel

Promoter: Dr A.J. van Reenen
Stellenbosch

April 2005

Declaration

I, the undersigned, hereby declare that the work contained in this dissertation is my original work and that I have not previously in its entirety or in part submitted it at any university for a degree.

Charl E. Morkel

Abstract

This study involves the synthesis and characterisation of PEG-based amphiphilic block copolymers for the hydrophilization of polysulphone ultrafiltration membranes. PEG based macro RAFT agents were synthesized and characterised. PEG-b-PS block copolymers were synthesized via the RAFT assisted controlled free radical polymerisation utilizing the synthesized PEG macro RAFT agents. The resulting polymerisation products were then analyzed by two-dimensional chromatography at the “critical conditions” for PS.

In the second phase of this study PEG-b-PSU block copolymers were synthesized via the polycondensation of bis (4-chlorophenyl) sulphone, Bisphenol A, and PEG. The resulting products were characterised by NMR spectrometry.

PEG-b-PS films and modified PSU membranes (modified by the addition of PEG-b-PSU block copolymer to the membrane casting solution) were prepared and analyzed. Surface analyses included static contact angle, AFM force-distance analysis, and FTIR-PAS analysis.

Results showed the successful synthesis of both PEG-b-PS and PEG-b-PSU amphiphilic block copolymers. Surface analysis proved the successful hydrophilization of the surface of the modified PSU membranes.

Opsomming

Hierdie studie behels die sintese en karakterisering van amfifiliese blok kopolimere gebaseer op polietileenglikol (PEG) vir die hidrofilisering van polisulfoon ultrafiltrasiemembrane. PEG-gebaseerde makro "RAFT" agente is gesintetiseer en gekarakteriseer. PEG-b-PS blok kopolimere is gesintetiseer via omkeerbare addisie-fragmentasie kettingoordrag (RAFT) polimerisasie, 'n beheerde vryradikaal polimerisasie, deur gebruik te maak van die gesintetiseerde makro RAFT agente. Die resulterende polimerisasie produkte is gekarakteriseer deur behulp van twee-dimensionele chromatografie by die kritiese toestand vir PS.

In die tweede fase van die studie is polietileenglikol-polisulfoon blok kopolimere gesintetiseer via die polikondensasie van bis (4-chlorofeniel) sulfoon, Bisfenol A, en PEG. Die resulterende produkte is gekarakteriseer met behulp van KMR spektrometrie.

PEG-PS films en gemodifiseerde polisulfoon membrane (gemodifiseer deur die byvoeging van polietileenglikol-polisulfoon blok kopolimere by die membraangietoplossing) is voorberei en geanaliseer. Oppervlakanalises sluit statiese kontakhoekmeting, atoomkragnmikroskopie, en Fourier Transform Infrarooi Foto-akoestiese spektrometrie in.

Resultate wys die suksesvolle sintese van beide die polietileenglikol-polistireen sowel as die polietileenglikol-polisulfoon blok kopolimere. Oppervlakanalise het bewys dat die oppervlak van die gemodifiseerde polisulfoon membraan suksesvol gehidrofiliseer is.

Acknowledgements

I would like to express my gratitude to:

Dr Albert van Reenen, my promoter, for entrusting me with this project; and for the necessary guidance and friendship.

Prof. Ed Jacobs, WRC Project 1268 project leader, for the opportunity to be involved in this project.

Water Research Commission of South Africa and NRF for financial assistance.

Calvin Maart, a true friend in need, always available to assist when supplies are running low. It surely did not go unnoticed and unappreciated.

Stephan Roux, Marius Pretorius and **Adèle Engelmöhr**, my coworkers on the project, for their enthusiasm and assistance.

Andre van Zyl for GPC and 2D analysis. Andre, thank you for your friendship, advice and encouragement during the past couple of years. Thank you for the time you spent in proofreading this document.

James M^cLeary, Ewan Sprong, and **Jaco (LAM) Vosloo** for advice and assistance regarding RAFT agent synthesis and for the time-to-time discussions on RAFT.

Erinda Cooper, Aneli Fourie, Johan Bonthuys and **Adam Keuler**, admin staff at the Polymer Science, for their assistance in logistics regarding the placement of orders, etc. for this project.

Elsa Malherbe and **Jean McKenzie** for NMR analysis.

Valerie Grumel for GPC and 2D chromatographic analysis.

Martina Meincken for AFM analysis.

Illana Bergh and **Lilanie Beets** from **Roediger Agencies** for contact angle measurements and FTIR analysis.

Friends I've made at Polymer Science, true friends for life, far too many to name; thank you for the times we spent together, whether at Polymer Science or under "less academic circumstances".

Table of Contents

Synthesis and Characterisation of Amphiphilic Block

Copolymers	1
Declaration	i
Abstract	ii
Opsomming	iii
Acknowledgements	iv
Table of Contents	vi
List of Acronyms	xi
List of Figures	xiii
List of Schemes	xvii
List of Tables	xviii
Chapter 1 Introduction and objectives	1
1.1 Introduction	1
1.2 Objectives	5
1.3 Layout	6
1.4 References	7
Chapter 2 Amphiphilic polymers: Introduction and overview	8
2.1 Introduction	8
2.2 Amphiphilic block copolymers	9
2.3 Amphiphilic graft copolymers	11
2.4 Amphiphilic networks	11
2.5 Conclusions	12
2.6 References	13
Chapter 3 Polystyrene-co-poly (ethylene glycol) copolymers: Historical	15
3.1. Introduction	15
3.2. PEG-b-PS block copolymers	16
3.2.1 PEG-b-PS via living anionic polymerisation	16

3.2.2	PEG-b-PS via free radical polymerisation	19
3.2.3	PEG-b-PS via living free radical polymerisation	21
3.3.	Conclusions	24
3.4.	References	26
Chapter 4 Reversible addition-fragmentation chain transfer polymerisation: An overview		32
4.1	Introduction	32
4.2	Conventional free radical polymerisation	33
4.3	Controlled free radical polymerisation	35
4.3.1	Stable free radical polymerisation	37
4.3.2	Atom transfer radical polymerisation	40
4.3.3	Reversible addition fragmentation chain transfer polymerisation	41
4.3.3.1	The mechanism of RAFT	41
4.3.3.2	Effect of the R-group	44
4.3.3.3	Effect of the Z-group	45
4.3.3.4	Advantages of the RAFT process	45
4.4	References	47
Chapter 5 PEG-b-PS block copolymer synthesis and characterisation		52
5.1	Introduction	52
5.2	Polymer characterisation	53
5.2.1	Size exclusion chromatography	53
5.2.2	Two-dimensional chromatography	54
5.2.3	NMR spectroscopy	58
5.3	RAFT agent synthesis	58
5.3.1	Chemicals	58
5.3.2	Synthesis of 4-cyano-4-[(thiobenzoyl) sulfanyl] valeric acid	59
5.3.3	Synthesis of S-1-dodecyl-S'- (α , α' dimethyl - α'' -acetic acid) trithiocarbonate	61
5.3.4	Synthesis of MPEG dithiobenzoate macro RAFT agent	63
5.3.5.	Synthesis of MPEG-tri-thiocarbonate macro RAFT agent.	67
5.4	Controlled free radical homopolymerisation of styrene	69
5.4.1	Polymerisation conditions	69
5.4.2	Experimental calculations	70
5.4.2.1	Molar mass predictions	70
5.4.2.2	Fractional conversion	71
5.4.3	Homopolymerisation of styrene with CVADTB	71
5.4.4	Homopolymerisation of styrene with DIBTC	78

5.4.5	Conclusions	82
5.5	PS-b-MPEG 350 block copolymer synthesis	82
5.5.1	Introduction	82
5.5.2	Polymerisation conditions	84
5.5.3	Copolymerisation of styrene using CVADTB MPEG 350 macro RAFT agent	85
5.5.4	Copolymerisation of styrene using DIBTC MPEG 350 macro RAFT agent	90
5.5.5	Conclusions	93
5.6	MPEG 2000-b-PS copolymer synthesis	93
5.6.1	Copolymerisation of styrene using CVADTB MPEG 2000 macro RAFT agent	93
5.6.2	Copolymerisation of styrene using DIBTC MPEG 2000 macro RAFT agent	109
5.7	PS-b-MPEG 5000 copolymer synthesis	113
5.7.1	Copolymerisation of styrene using CVADTB MPEG 5000 macro RAFT agent	113
5.8	Conclusions	117
5.9	References	119

Chapter 6 Polysulphone-b-poly (ethylene glycol) triblock copolymer synthesis and characterisation **121**

6.1	Introduction	121
6.2	Polycondensation reactions	122
6.3	Polysulphone homopolymer synthesis	125
6.3.1	Introduction	125
6.3.2	Possible synthetic routes	126
6.3.3	Polycondensation of monomers bearing sulphonyl groups	127
6.3.4	Bis (4-chlorophenyl) sulphone-bisphenol A polysulphone	128
6.3.4.1	Background	128
6.3.4.2	Reaction mechanism	129
6.3.4.3	Possible side reactions	129
6.3.4.4	Synthesis of bis (4-chlorophenyl) sulphone-bisphenol A polysulphone	130
6.3.4.5	SEC characterisation of bis (4-chlorophenyl) sulphone-bisphenol A polysulphone	132
6.3.4.6	NMR analysis of bis (4-chlorophenyl) sulphone-bisphenol A polysulphone	133
6.4	PSU-PEG block copolymers	135
6.4.1	PSU-b-PEG copolymer synthesis	138
6.4.2	PSU-PEG-PSU triblock copolymer characterisation	138
6.4.2.1	SEC analysis of PEG-b-PSU block copolymers	138
6.4.2.2	NMR characterisation	140

6.5	Summary of results	143
6.6	References	144
Chapter 7 Surface analysis of amphiphilic block copolymers		146
7.1	Introduction	146
7.2	Contact angle	146
7.2.1	Introduction	146
7.2.2	Sample preparation	148
7.2.2.1	PEG-b-PS sample preparation	148
7.2.2.2	Modified PSU membrane preparation	148
7.2.3	Results and discussion	149
7.2.3.1	PEG-b-PS films	149
7.2.3.2	Modified PSU membranes	152
7.3	Atomic force microscopy	154
7.3.1	Introduction	154
7.3.2	Force-distance analysis	154
7.3.3	Digital pulsed force mode	156
7.3.4	Experimental	157
7.3.5	Sample preparation	158
7.3.6	Results and discussion	159
7.3.6.1	PEG-b-PS films	159
7.3.6.2	Modified PSU membranes	160
7.4	FTIR-PAS	161
7.4.1	Introduction	161
7.4.2	Sample preparation	163
7.4.3	Results and discussion	163
7.4.3.1	PEG-b-PS films	163
7.4.3.2	PEG-b-PSU films and membranes	165
7.5	Summary of results	168
7.6	Conclusions	169
7.7	References	171
Chapter 8 Conclusions and recommendations		173
8.1	Conclusions	173
8.1.1	Synthesis and characterisation of hydrophilizing agents	173
8.1.2	Surface analysis	175
8.1.3	Model study	175
8.1.4	Surface analysis of hydrophilized PSU membranes	176
8.2	Recommendations	176
8.3	References	179

List of Acronyms

^{13}C NMR	Carbon-13 nuclear magnetic resonance spectroscopy
^1H NMR	Proton nuclear magnetic resonance spectroscopy
2D	Two-dimensional
3D	Three-dimensional
AIBN	Azobis(isobutyronitrile)
ATRP	Atom transfer radical polymerisation
BPO	Benzoyl peroxide
CAP	Critical adsorption point
CVADTB	4-Cyano-4-[(thiobenzoyl) sulfanyl] pentanoic acid
DCC	1,3-dicyclohexylcarbodiimide
DCM	Dichloromethane
DBTC	S-1-Dodecyl-S'-(α , α' dimethyl - α'' -acetic acid) trithiocarbonate
DMAP	4-(dimethyl amino) pyridine
DMSO	Dimethylsulfoxide
\overline{DP}_n	Degree of polymerisation
EATP	Elution adsorption transition point
EO	Ethylene oxide
EtAc	Ethyl acetate
FAD	Full adsorption chromatography
GPC	Gel permeation chromatography
h	Hours
HPLC	High performance liquid chromatography
LAC	Liquid adsorption chromatography
LC	Liquid Chromatography
LC-CAP	Liquid chromatography at the critical adsorption point
LFRP	Living free radical polymerisation
M	Monomer
MMA	Methyl methacrylate
MMD	Molar mass distribution
\overline{M}_n	Number average molar mass
$\overline{M}_{(\text{Theory})}$	Theoretically determined number average molar mass
MPEG	Poly (ethylene glycol) mono methyl ether
MPEG 2000	Poly (ethylene glycol) mono methyl ether with number average molar mass of 2000 g/mol

MPEG 350	Poly (ethylene glycol) mono methyl ether with number average molar mass of 350 g/mol
MPEG 5000	Poly (ethylene glycol) mono methyl ether with number average molar mass of 5000 g/mol
MPEG RAFT	Poly (ethylene glycol) mono methyl ether coupled to RAFT agent
NMRP	Nitroxide mediated radical polymerisation
PDI	Polydispersity index
PEB	Polyethylene-butylene copolymer
PEG	Poly (ethylene glycol)
PEG-b-PS	Ethylene glycol styrene block copolymer
PEG-PS-PEG	Tri-block copolymer of PEG and PS
PEO	Poly (ethylene oxide)
PPO	Poly (propylene oxide)
PS	Polystyrene
PSU	Polysulphone
PTSA	<i>p</i> -toluene sulphonic acid
R [•]	Radical
RAFT	Reversible addition fragmentation chain transfer
RI	Refractive Index
SEC	Size exclusion chromatography
SFRP	Stable free radical polymerisation
TEMPO	2,2,6,6-tetramethylpiperidin-2-oxyl
THF	Tetrahydrofuran
UF	Ultrafiltration
UV	Ultra violet

List of Figures

Figure 5.1: ^1H NMR spectrum of CVADTB.	60
Figure 5.2: ^{13}C NMR spectrum of CVADTB.	61
Figure 5.3: ^1H NMR spectrum of DIBTC.	63
Figure 5.4: Graph of RI response vs. log M for SEC analysis of CVADTB MPEG macro RAFT agents.	65
Figure 5.5: ^1H NMR spectrum of CVADTB MPEG 2000.	66
Figure 5.6: ^{13}C NMR of CVADTB MPEG 2000 macro RAFT agent.	67
Figure 5.7: ^1H NMR spectrum of DIBTC MPEG 2000 macro RAFT agent.	68
Figure 5.8: SEC graph of RI response vs. log M for the homopolymerisation of styrene with CVADTB at 60°C.	72
Figure 5.9: SEC graph of RI response vs. log M for the homopolymerisation of styrene with CVADTB at 70°C.	72
Figure 5.10: SEC graph of RI response vs. log M for the homopolymerisation of styrene with CVADTB at 80°C.	73
Figure 5.11: Graph of \bar{M}_n vs. time for homopolymerisation of styrene with CVADTB.	74
Figure 5.12: Graph of polydispersity vs. time for homopolymerisation of styrene with CVADTB.	75
Figure 5.13: Graph of fractional conversion vs. reaction time for the homopolymerisation of styrene with CVADTB at 70°C.	76
Figure 5.14: Graph of \bar{M}_n and polydispersity vs. fractional conversion for the homopolymerisation of styrene with CVADTB at 70°C.	77
Figure 5.15: SEC graph of RI response vs. log M for sample taken at 9 hours in the polymerisation of styrene with CVADTB at 70°C.	78
Figure 5.16: SEC graph of RI response vs. log M for the homopolymerisation of styrene with DIBTC at 70°C.	79
Figure 5.17: Graph of \bar{M}_n and polydispersity vs. fractional conversion for the homopolymerisation of Styrene with DIBTC at 70°C.	80
Figure 5.18: Graph of fractional conversion vs. reaction time for the homopolymerisation of styrene with CVADTB and DIBTC.	81
Figure 5.19: First-order kinetic plot for polymerisation of styrene with CVADTB and DIBTC.	81

Figure 5.20: SEC graph of RI response vs. log M for the copolymerisation of styrene with CVADTB MPEG 350 at 60°C.....	86
Figure 5.21: SEC graph of RI response vs. log M for the copolymerisation of styrene with CVADTB MPEG 350 at 70°C.....	86
Figure 5.22: SEC graph of RI response vs. log M for the copolymerisation of styrene with CVADTB MPEG 350 at 80°C.....	87
Figure 5.23: Graph of \bar{M}_n vs. reaction time for the copolymerisation of styrene with CVADTB MPEG 350.....	88
Figure 5.24: Graph of polydispersity vs. reaction time for the copolymerisation of styrene with CVADTB MPEG 350.	89
Figure 5.25: SEC graph of RI response vs. log M for the copolymerisation of styrene with DIBTC MPEG 350 at 70°C.	91
Figure 5.26: Comparative graph of copolymerisation of styrene with DIBTC MPEG 350 and CVADTB MPEG 350 at 70°C.....	92
Figure 5.27: SEC graph of RI response vs. log M for the copolymerisation of styrene with CVADTB MPEG 2000 at 60°C.....	94
Figure 5.28: SEC graph of RI response vs. log M for the copolymerisation of styrene with CVADTB MPEG 2000 at 60°C (reaction time: 22 h).....	95
Figure 5.29: ¹ H NMR spectrum for the copolymerisation of styrene with CVADTB MPEG 2000 at 60°C (reaction time: 22 h).	96
Figure 5.30: Three-dimensional plot of 2D chromatographic analysis for the copolymerisation of styrene with CVADTB MPEG 2000 at 60°C (reaction time: 22 h).	97
Figure 5.31: SEC graph of RI response vs. log M for the copolymerisation of styrene with CVADTB MPEG 2000 at 70°C. Macro initiator prepared by Method 1.....	99
Figure 5.32: SEC graph of RI response vs. log M for the copolymerisation of styrene with CVADTB MPEG 2000 at 70°C. Macro initiator prepared by Method 2.....	100
Figure 5.33: Three-dimensional plot of 2D chromatographic analysis for the copolymerisation of styrene with CVADTB MPEG 2000 at 70°C (Method 1). .	101
Figure 5.34: Three-dimensional plot of 2D chromatographic analysis for the copolymerisation of styrene with CVADTB MPEG 2000 at 70°C (Method 2). .	102
Figure 5.35: SEC graph of RI response vs. log M for the copolymerisation of styrene with CVADTB MPEG 2000 at 80°C.....	104

Figure 5.36: Three-dimensional plot of 2D chromatographic analysis for the copolymerisation of styrene with CVADTB MPEG 2000 at 80°C.	105
Figure 5.37: Graph of \bar{M}_n (SEC) vs. reaction time for the copolymerisation of styrene with CVADTB MPEG 2000.....	106
Figure 5.38: Graph of polydispersity vs. reaction time for the copolymerisation of styrene with CVADTB MPEG 2000.	106
Figure 5.39: Graph of \bar{M}_n and polydispersity vs. fractional conversion for the copolymerisation of styrene with CVADTB MPEG 2000 macro RAFT agent at 70°C.	107
Figure 5.40: First-order kinetic plot for reactions of CVADTB and CVADTB MPEG 2000 with styrene at 70°C.....	108
Figure 5.41 SEC graph of RI response vs. log M for the copolymerisation of styrene with DIBTC MPEG 2000 at 70°C.	109
Figure 5.42: Three-dimensional plot of 2D chromatographic analysis for the copolymerisation of styrene with DIBTC MPEG 2000 at 70°C.	110
Figure 5.43: Graph of \bar{M}_n and polydispersity vs. fractional conversion for the copolymerisation of styrene with DIBTC MPEG 2000 macro RAFT agent at 70°C.	112
Figure 5.44: Three-dimensional plot of 2D chromatographic analysis for the copolymerisation of styrene with CVADTB MPEG 5000 at 70°C.	114
Figure 5.45: Graph of fractional conversion vs. reaction time for the copolymerisation of styrene with CVADTB MPEG 5000 macro RAFT agent.	115
Figure 5.46: Comparative graph of fractional conversion vs. time for polymerisation of styrene with CVADTB- and DIBTC based RAFT initiators.....	116
Figure 5.47: Comparative first-order kinetic plot for the polymerisation of styrene with CVADTB- and DIBTC based RAFT initiators.....	117
Figure 6.1: Graph of RI response vs. log M for the polycondensation of bis (4-chlorophenyl) sulphone and Bisphenol A.	132
Figure 6.2: ^1H NMR spectrum of PSU homopolymer.....	134
Figure 6.3: ^{13}C NMR spectrum of PSU homopolymer.	135
Figure 6.4: Tetronic 304.....	136

Figure 6.5: Graph of RI response vs. log M for the polycondensation of bis (4-chlorophenyl) sulphone with Bisphenol A and MPEG 2000.....	139
Figure 6.6: ¹ H NMR spectrum of MPEG 2000-b-PSU block copolymer.	140
Figure 6.7: ¹ H NMR spectrum of MPEG 5000-b-PSU block copolymer.	141
Figure 6.8: ¹³ C NMR spectrum of MPEG 2000-b-PSU block copolymer.	142
Figure 6.9: ¹³ C NMR spectrum of MPEG 5000-b-PSU block copolymer.	143
Figure 7.1. Hydrophilicity calculation of water droplet on a surface.....	147
Figure 7.2: Static contact angle measurements of PEG-b-PS films.	151
Figure 7.3: Static contact angle measurements of modified PSU membranes.	153
Figure 7.4: AFM “force-distance” analysis.	155
Figure 7.5 a) z modulation of the piezo, b) force signal as a function of time and c) adhesion force measured for each sinus cycle. ¹⁶	157
Figure 7.6: Histogram of the voltage distribution in an adhesion image.	158
Figure 7.7 FTIR-PAS of PEG-b-PS block copolymers.....	164
Figure 7.8: FTIR-PAS of PSU membranes modified with PEG2000-b-PSU block copolymers	166
Figure A1: ¹ H NMR spectrum for the copolymerisation of styrene with CVADTB MPEG 2000 at 60°C (reaction time: 22 h).	180
Figure A2: ¹ H NMR spectrum for the copolymerisation of styrene with CVADTB MPEG 2000 at 70°C (reaction time: 24 h, Method 1).	180
Figure A3: ¹ H NMR spectrum for the copolymerisation of styrene with CVADTB MPEG 2000 at 70°C (reaction time: 11 h, Method 2).	181
Figure A4: ¹ H NMR spectrum for the copolymerisation of styrene with CVADTB MPEG 2000 at 80°C (reaction time: 22 h).	181
Figure A6: ¹ H NMR spectrum for the copolymerisation of styrene with CVADTB MPEG 5000 at 70°C (reaction time: 6.5 h).	182

List of Schemes

Scheme 1.1: Diagram of hydrophilized PSU UF membrane.	4
Scheme 4.1: Thermal decomposition of benzoyl peroxide.	33
Scheme 4.2: Thermal decomposition of azobisisobutyronitrile.....	33
Scheme 4.3: Mechanism of NMRP.....	39
Scheme 4.4: Mechanism of ATRP.....	40
Scheme 4.5: Mechanism of RAFT.....	42
Scheme 5.1: Synthesis of bis (thiobenzoyl) disulphide.....	59
Scheme 5.2: Synthesis of CVADTB.	60
Scheme 5.3: Synthesis of DIBTC	62
Scheme 5.4: MPEG-CVADTB macro RAFT agent synthesis.....	65
Scheme 5.5: MPEG-DIBTC macro RAFT agent synthesis.....	68
Scheme 5.5: Synthesis of PEG-b-PS with a CVADTB MPEG macro RAFT agent. ..	84
Scheme 6.1: Bimolecular elimination-addition mechanism.	127
Scheme 6.2: Etherification by nucleophilic substitution.....	128
Scheme 6.3: Bis (4-chlorophenyl) sulphone-bisphenol A polysulphone synthesis. .	128
Scheme 6.4: (Bis (4-chlorophenyl) sulphone-bisphenol A polysulphone)-b-PEG block copolymer synthesis.	137

List of Tables

Table 3.1: Various methods for the preparation of PS-b-PEG via anionic polymerisation	18
Table 3.2: Preparation of PS-b-PEG via conventional free radical polymerisation....	20
Table 3.3: Preparation of PS-b-PEG via controlled free radical polymerisation	23
Table 5.1: Formulations for the synthesis of different MPEG-macro RAFT agents... 64	
Table 5.2: Composition of reagents for the RAFT assisted homopolymerisation of styrene	69
Table 5.3: Composition of reagents for the RAFT assisted synthesis of PEG-b-PS block copolymers	85
Table 5.4: Composition of polymerisation product obtained from the copolymerisation of styrene with CVADTB MPEG 2000 at 60°C	97
Table 5.5: Composition of polymerisation product obtained for the copolymerisation of styrene with CVADTB MPEG 2000 at 70°C (Method 1)	101
Table 5.6: Composition of polymerisation product obtained for the copolymerisation of styrene with CVADTB MPEG 2000 at 70°C (Method 2)	103
Table 5.7: Composition of polymerisation product obtained for the copolymerisation of styrene with CVADTB MPEG 2000 at 80°C	105
Table 5.8: Composition of polymerisation product obtained for the copolymerisation of styrene with DIBTC MPEG 2000 at 70°C	111
Table 5.9: Composition of polymerisation product obtained for the copolymerisation of styrene with CVADTB MPEG 5000 at 70°C	115
Table 6.1: Effect of variation in r on \bar{x}_n	125
Table 6.2: Typical quantities of reagents used for PSU preparation	131
6.3: Typical composition of reagents for PEG-b-PSU preparation	138
Table 6.3 PEG-b-PSU compositions	141
Table 7.1: Contact angle measurements of PEG-b-PS block copolymer films.....	150
Table 7.2: Contact angle measurement of PSU membranes modified with MPEG-b-PSU block copolymers	153
Table 7.3: AFM analysis of PEG-b-PS block copolymers.....	159
Table 7.4: AFM analysis of PSU membranes modified with PEG-b-PSU block copolymers	161

Table 7.5: Results of FTIR analysis of PEG-b-PS block copolymers	165
Table 7.6: Results of FTIR analysis of PEG-b-PSU block copolymers.....	166
Table 7.7: Results of FTIR analysis of PSU membranes modified with PEG-b-PSU block copolymers	167
Table 7.8: Summary of results of surface analysis of PEG-b-PS block copolymers	168
Table 7.9: Summary of results of surface analysis of modified PSU membranes ...	169

Chapter 1

Introduction and objectives

1.1 Introduction

The world population is increasing annually. Technology is advancing by leaps and bounds and filling the needs of an ever-demanding market. With this increase in the world population and concurrent industrial development, an ever-increasing demand is being placed on the world's natural resources, the major natural resource being water. A high premium is placed on the supply of potable water. With the boom in the world population, potable water is soon to become a commodity item. Also, an increasing amount of pressure is being placed on industry to clean up industrial effluent, thereby preventing the pollution of rivers and dams. Water purification by membrane processes plays an important role in producing potable water, whether it is by cleaning up industrial effluent, or by removing pollutants from water in rural areas. Membrane processes can be divided into different groups, according to the molecular size of the pollutants in the water to be treated. Ultrafiltration (UF) classically can be employed to remove pollutants in the range of 10^{-1} to 10^{-3} microns.¹

Polysulphone (PSU) is widely used as substrate for UF membranes due to its advantageous characteristics.¹ These include: usage over a wide temperature range, a broad pH tolerance (pH 1 to 13), and fairly good resistance to chlorine and other chemicals. Ease of fabrication and control of pore size of the resulting membranes further favours the use of PSU as a membrane material. One of the advantages of polysulphone in terms of being a suitable membrane substrate is the hydrophobicity of polysulphone. This is unfortunately also one of the disadvantages of the material as, being hydrophobic, the water sorption capability of PSU is limited, and the possibility of biological attack by bacterial substances in the water to be treated is increased.

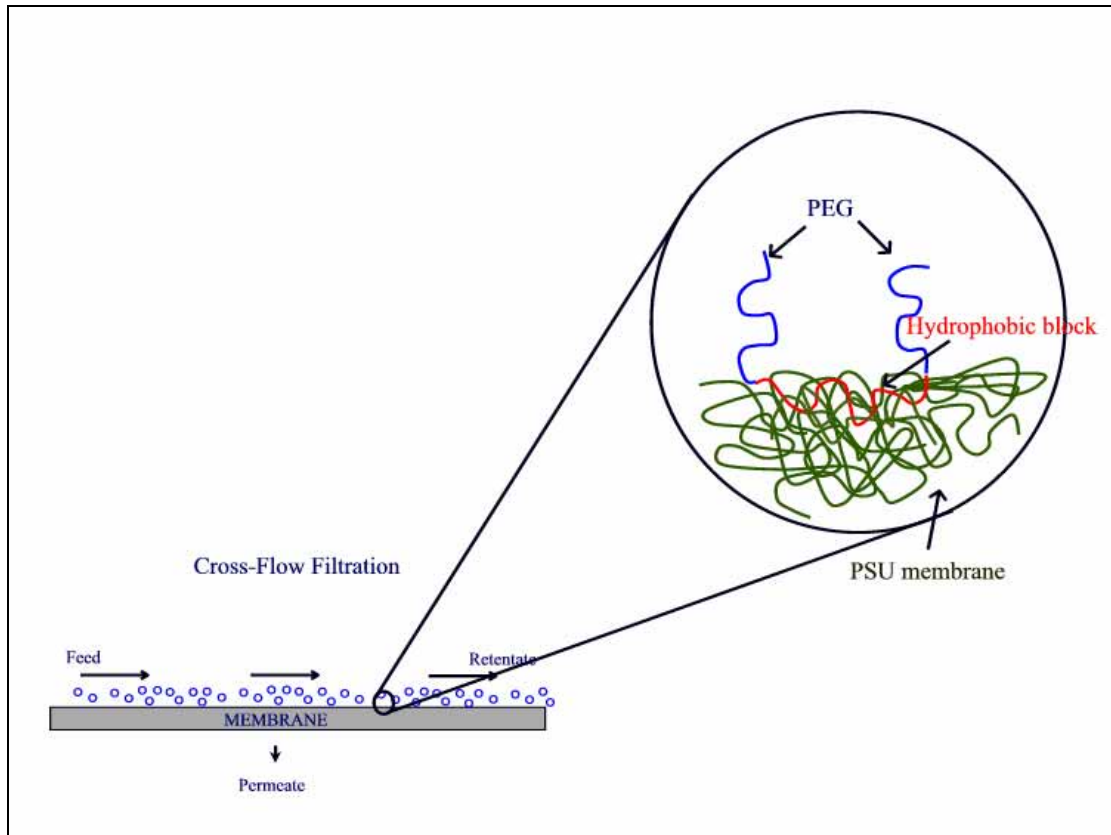
Fouling, which manifests as a resistance to transport, is a phenomenon that features in all membrane processes. Whereas fouling that results from concentration polarization in pressure-driven membrane operations can be reduced through process engineering, fouling that results from adsorption cannot. Fouling is particularly predominant in the case of membranes prepared from the more hydrophobic materials such as polysulphone, poly(ether sulphone) and poly(ether imide).

Semi-permeable membranes play an important role in biomedical applications, including hemodialysis, plasma separators, membrane oxygenators and bioartificial organs. These devices are designed to bring large artificial membrane surface areas into direct contact with body fluids, such as blood or plasma, in order to perform the desired function of that specific device. Prevention or minimization of blood trauma is of paramount importance when blood is exposed to artificial membranes. It is well documented that membrane devices with less hydrophobic membranes are more effective in such applications² and part of the research on such devices is directed towards minimization of protein adsorption and interaction of cellular components with the surfaces of the membranes used.

In many of the studies carried out to produce more hydrophilic membranes, poly(ethylene oxide) (PEO) has been incorporated into the membrane structure. Surface immobilization of PEG or PEO is a commonly used technique for achieving minimal protein-surface interaction.²⁻⁶ The passivity of PEG-modified surfaces in biological fluids is most likely due to the properties of PEG. These properties include the low interfacial free energy of the hydrated surface, the unique structural interactions of the soluble chains within the water matrix, high chain mobility, and the steric stabilization (repulsion) effect.⁷⁻⁹ Techniques for the modification of surfaces of artificial membranes with PEO include free radical crosslinking,³ blending,^{2, 4} and grafting.^{5, 6} However, none of these techniques is applied without problems. Coating and surfactant adsorption techniques are vulnerable to dissolution and displacement of the adsorbate, while chemical and irradiative processes are more effective when applied to two-dimensional substrates. Membranes, and internally skinned capillary membranes in particular, present an intricate three-dimensional morphology that makes them an extremely difficult substrate for surface modification.²

The focus of more recent developments to modify membrane contact surfaces is aimed towards physical incorporation of the hydrophilization agent(s) into the membrane structure.⁴ By synthesizing PEO-b-PSU copolymers, a composite material becomes available for membrane manufacturing that favours surface segregation of the relatively hydrophobic block copolymer. During wet-phase inversion membrane fabrication, the membrane-forming solution is immersed in a non-solvent, eg. water. This process controls precipitation of the polymer as a porous network. Other factors that control the morphology and pore size of the resulting membrane include: the concentration of the membrane-forming polymer, additives, solvent/non-solvent interactions and temperature.²

During the phase inversion process, the amphiphilic nature of the PEO-b-PSU copolymers favours surface segregation, whereby the PEO segments arrange at the membrane surface due to their solubility in the aqueous coagulant (water). The most important advantage derived from homogeneous modification of both internal and external membrane surfaces during the phase inversion process results in a membrane with hydrophilic external and internal surfaces as result of PEO enrichment. The advantages of this type of membrane modification compared to those mentioned earlier include: homogeneity of the surface modification, achieving membrane modification by simply blending the PEO-b-PSU copolymer into the membrane-forming solution, elimination of costly and elaborate post-treatment processes and the preservation of the integrity of the membrane surface during use. This latter advantage is derived from the covalent linkage between the hydrophilic block and the hydrophobic membrane-forming block that anchors the hydrophilic block in the membrane surface structure. This process also avoids problems associated with slowly desorbing adsorbates during use and loss of initial hydrophilization.^{2, 4} A schematic diagram of a hydrophilized PSU membrane is given in Scheme 1.1.



Scheme 1.1: Diagram of hydrophilized PSU UF membrane.

These membrane modification techniques that have been mentioned are not limited to the biomedical industry; they can be applied with equal success to any process where membranes are used, and lower hydrophobicity of the membrane surface is a requirement to reduce fouling. This, particularly, holds true for ultrafiltration and microfiltration membranes where the preferred material of construction is hydrophobic in nature.

This dissertation forms part of *Project K5/1268* of the Water Research Commission (WRC) of South Africa with the title: *Hydrophilization of hydrophobic Ultrafiltration and Microfiltration Membranes*. The aim of *Project K5/1268* is to improve the properties of commercial PSU UF membranes in terms of the useful lifetime and the separation properties of these membranes.

Certain guidelines are critical for suitable hydrophilizing agents for PSU membranes. These guidelines include:

- the conformational structure of the hydrophilizing agent;

- the precise chemical architecture of the proposed hydrophilizing agents; and
- the most suited method of synthesis.

The hydrophilizing agent to be used should be compatible with the membrane substrate, being PSU. Furthermore, it is important that a certain section of this hydrophilizing agent is hydrophilic in order to hydrophilize the surface of the substrate membrane. It is important that an even distribution of the hydrophilic groups on the surface of the membrane is obtained to ensure the complete hydrophilization of the surface of the membrane. Amphiphilic polymers as used by Hancock *et al.*^{2, 4} comprising both hydrophilic and hydrophobic segments, are ideal materials for this purpose. In order to optimize the hydrophilization process, it is necessary to investigate the influence of the hydrophilic:hydrophobic ratio within the amphiphilic polymer. Certain critical lengths of the hydrophilic and/or hydrophobic groups can have an influence on the hydrophilization process. It is therefore important to study the influence of this hydrophilic/hydrophobic ratio on the hydrophilization capabilities of the hydrophilizing agents. In order to perform this investigation on the influence of the hydrophilic:hydrophobic ratio on the hydrophilization process, it is of importance to synthesize polymers with exact chemical architecture in terms of molar mass and molar mass distribution.

1.2 Objectives

This dissertation will therefore focus on the synthesis of polymers with controlled chemical architecture in order to investigate the influence of the hydrophilic/hydrophobic ratio on the hydrophilization process. The objectives of the dissertation is therefore as follows

1. The controlled synthesis and characterisation of amphiphilic polymers with exact chemical architecture.
2. Surface analysis of the synthesized amphiphilic polymers.
3. A model study on the effects of the hydrophilic:hydrophobic ratio will lead to a better understanding of the hydrophilization process. The construction of a model in terms of the influence of the chemical architecture (molar mass and molar mass distribution of both the hydrophilic and hydrophobic segments) of the hydrophilizing agents on the hydrophilizing properties of these hydrophilizing agents.
4. Surface analysis of hydrophilized PSU UF membranes.

1.3 Layout

In Chapter 2 an overview on amphiphilic polymers is given: what they are, what their chemical nature is, and what different types of amphiphilic polymers are available.

In Chapter 3 a historical review is given of PEG-b-PS diblock copolymers in terms of the different synthetic routes available to produce these hydrophilizing agents. Recommendations are made in terms of the most suited method by which to synthesize these copolymers.

In Chapter 4 the basic theoretical principles of free radical chemistry are discussed, highlighting the advantages and disadvantages of conventional free radical polymerisation. An introduction to modern-day controlled free radical polymerisation is given. Special focus is placed on the RAFT (reversible addition-fragmentation chain transfer) polymerisation process. The mechanism of the process and factors that might influence the effectivity of the RAFT agents are discussed.

In Chapter 5 the RAFT-assisted controlled free radical copolymerisation of styrene with PEG-based macro RAFT agents to form the resulting PEG-b-PS block copolymers is described. RAFT agent were synthesized, characterised and evaluated in terms of their ability to produce polystyrene homopolymers with narrow molar mass distributions. The synthesis and characterisation of RAFT agents for the synthesis of PEG-b-PS block copolymers is discussed. The synthesis and characterisation of the said PEG-b-PS block copolymers concludes this chapter.

In Chapter 6 an overview of polycondensation reactions is given. An overview on the synthesis of PEG-b-PSU block copolymers is given. The synthesis and characterisation of these PEG-b-PSU block copolymers are discussed.

In Chapter 7 results of the surface analysis (in terms of the hydrophilicity of that surface) of the amphiphilic block copolymers, synthesized as described in Chapters 5 and 6, are given. The hydrophilizing agents described in Chapter 6 are also used as hydrophilizing agents for PSU ultrafiltration membranes. Surface analysis techniques as well as results obtained in the surface analysis of the different copolymers are discussed.

In Chapter 8 conclusions are summarized and recommendations for future investigations are made.

1.4 References

1. Munir, C., Ultrafiltration and microfiltration handbook, **1998**, Technomic Publishing, (ISBN No. 1-56676-598-6).
2. Hancock, L. F., Fagan, S. M. and Ziolo, M. S., Hydrophilic, semipermeable membranes fabricated with poly(ethylene oxide)-polysulfone block copolymer, *Biomaterials*, **2000**, 21, 725-733.
3. Lee, J. H., Ju, Y. M. and Kim, D. M., Platelet adhesion onto segmented polyurethane film surfaces modified by addition and crosslinking of PEO-containing block copolymers, *Biomaterials*, **2000**, 21, 683-691.
4. Hancock, L. F., Phase inversion membranes with an organised surface structure from mixtures of polysulfone and polysulfone-poly(ethylene oxide) block copolymers, *Journal of Applied Polymer Science*, **1997**, 66, 1353-1358.
5. Efremova, N. V., Sheth, S. R. and Leckband, D. E., Protein-Induced changes in poly(ethylene glycol) brushes: Molecular weight and temperature dependence, *Langmuir*, **2001**, 17, 7628-7636.
6. Branch, D. W., Wheeler, B. C., Brewer, G. J. and Leckband, D. E., Long-term stability of grafted poly (ethylene glycol) surfaces for use with microstamped substrates in neuronal cell culture, *Biomaterials*, **2001**, 22, 1035-1047.
7. Jeon, S. I., Lee, J. H., Andrade, J. D. and De Gennes, P. G., Protein-surface interactions in the presence of poly ethylene oxide, *Journal of Colloid and Interface Science*, **1991**, 142, 149-166.
8. Lee, J. H., Kopecek, J. and Andrade, J. D., Protein-resistant surfaces prepared by PEO-containing block copolymer surfactants, *Journal of Biomedical Materials Research*, **1989**, 23, 351-368.
9. Litauszki, L., Howard, L., Salvati, L. and Tarcha, P. J., Surfaces modified with PEO by the Williamson reaction and their affinity for proteins, *Journal of Biomedical Materials Research*, **1997**, 35, 1-8.

Chapter 2

Amphiphilic polymers: Introduction and overview

2.1 Introduction

Polymers are complex materials and their properties (physical and chemical) rely on their chemical compositions. Of particular interest to this investigation are the polymers that, while being insoluble in water, still maintain a high affinity towards water, and are simultaneously compatible with a hydrophobic membrane substrate. The above requirements would therefore need a polymer with dual characteristics. Amphiphilic copolymers are macromolecular substances containing segments of opposite philicity, i.e. hydrophilic and hydrophobic, which are covalently bonded. If a material is classified as hydrophilic it has a high affinity for water, therefore meaning that water can be adsorbed by the material. Conversely, if a material is hydrophobic, it has no affinity for water and water is therefore not adsorbed by such a material.

Amphiphilic copolymers have molecular architectures in which different domains, both hydrophilic and hydrophobic, are present within the polymer molecules. This gives rise to unique properties of these materials in selected solvents, at surfaces as well as in the bulk, due to microphase separation.¹ The characteristic self-organization of these materials in the presence of selective media often results in the formation of aggregates such as micelles, microemulsions, and adsorbed polymer layers.² Amphiphilic copolymers can be divided into different groups, namely non-ionic, ionic, and synthetic polymer/natural polymer hybrids, the latter being designed mainly for special medical applications. The investigation into amphiphilic copolymers in this dissertation will be limited to non-ionic compounds. Any reference to amphiphilic polymers will therefore be limited to non-ionic amphiphilic polymers.

The application of these non-ionic amphiphilic polymers depends on the composition of the copolymers in terms of molar mass, molar mass distribution (MMD) and the ratio of hydrophilic to hydrophobic groups. Control, in terms of chemical architecture, is required in the synthesis of these materials to obtain the desired properties for each application. An even bigger advantage than the control of the molar mass of these copolymers is the ability to design systems where one is possible to predetermine the resulting molar mass

of each of the blocks of the copolymerisation product. Starting materials in the synthesis of these amphiphilic copolymers are macromonomers and telechelics.

Macromonomers refer to macromolecules with a functional group, that participate in a polymerisation reaction.³ These functional groups include unsaturation, which can participate in radical or ionic polymerisation, heterocycles that are active in ring-opening polymerisation reactions, or functional groups that can participate in polycondensation reactions. Depending on the nature of the functionality, the polymerisation of macromonomers generally results in graft copolymers or networks.

Telechelic polymers are defined as linear macromolecules bearing reactive functional groups at both ends. Macromonomers and telechelics participate in chain extension reactions, which lead to the formation of linear block copolymers or networks.

Amphiphilic copolymers are typically used as emulsifiers, surface-active agents, phase transfer catalysts, solid polymer electrolytes (after complexing with alkali salts), and antistatic agents.³

Non-ionic amphiphilic copolymers can therefore be divided into three general classes of copolymers

- 1 Linear block copolymers
- 2 Graft copolymers
- 3 Star/network polymers.

2.2 Amphiphilic block copolymers

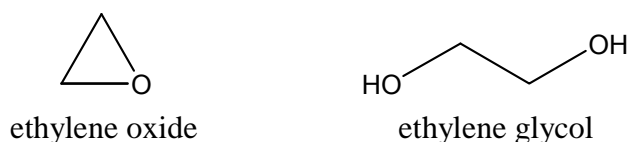
Traditionally, amphiphilic block copolymers, having well-defined character, are formed by a number of synthetic routes including:

- living anionic or sequential cationic polymerisation;
- reaction of telechelics having different backbones and suitable reactive end groups; and
- chain extension of macromonomers.

Recent advances in controlled “living” free radical polymerisation have also led to the introduction of a new route for the synthesis of these materials. Controlled radical polymerisation includes techniques such as RAFT (reversible addition-fragmentation

chain transfer) polymerisation,⁴⁻¹⁴ ATRP (atom transfer radical polymerisation),^{15, 16} and NMRP (nitroxide mediated radical polymerisation).¹⁷ (Refer to Chapter 3 for a discussion on controlled free radical polymerisation techniques.)

Amphiphilic block copolymers are mainly di- or tri-block copolymers where the different blocks are incompatible, therefore giving the polymer its unique properties. The most extensively studied and industrially significant amphiphilic polymers contain PEG or PEO as hydrophilic segment. PEG and PEO have the same repeat unit ($\text{CH}_2\text{CH}_2\text{O}$), but the starting monomer and method of synthesis of the two differ. PEO is synthesized from ethylene oxide, while PEG is synthesized from ethylene glycol. The polymerisation of these different monomers generally yields a higher molar mass for the PEO compounds than for the PEG compounds.



Other polymers used as hydrophilic segment in amphiphilic block copolymers include poly (2-alkyl-2-oxazoline), poly (vinyl ether), polyacetal and poly (methyl) acrylate.

In terms of hydrophobic segments, the most generally used polymers are poly (propylene oxide) and polystyrene.¹⁸

Velichkova and Christova¹⁸ reported that the first amphiphilic block copolymers were prepared in the early 1950s by Lundsted on the basis of ethylene oxide and propylene oxide. A series of AB and ABA type block copolymers were developed under the trademark *Pluronic*[®]. These polymers were prepared by sequential addition of monomers. At first the dependence of the lengths of the hydrophilic and hydrophobic blocks on the surfactant and detergent properties was established for the *Pluronic*[®]. It was found that wettability increased with an increase in the length of the PEO block, while the best surface activity was achieved with the poly (propylene oxide) (PPO) block. *Pluronics* were shown to exhibit emulsifying properties, phase transfer catalyst properties, complexing abilities with alkali salts and also ionic conducting behavior. Recently it was also found that *Pluronics* prevented protein adsorption and platelet adhesion.¹⁹

Since the introduction of *Pluronics* into the market, various advances have been made in the synthesis of amphiphilic block copolymers. These advances have been reviewed by Velichkova and Christova.¹⁸

2.3 Amphiphilic graft copolymers

Tailor-made graft copolymers can be prepared by a macro monomer technique or by grafting telechelics onto preformed polymer backbones that contain sufficient reactive functional groups randomly distributed along the polymer backbone. While these methods offer full control over the graft length, there are disadvantages in using this technique to synthesize well-defined copolymers. In the grafting process, although being able to control the graft length, it is difficult to determine the amount of grafts and the distribution thereof along the polymer backbone.

A proper orientation of the hydrophilic and hydrophobic components of these materials in the solid state and in solution favours phase separation and micelle formation, and affords surface activity, similar to the corresponding linear copolymers. However, because of their specific structures, in some features they differ considerably. Amphiphilic graft copolymers have found applications as polymeric surfactants, phase transfer catalysts, biocompatible materials, drug carriers, blending agents and thickening agents.¹⁸

2.4 Amphiphilic networks

Among the variety of methods for the synthesis of polymer networks, attempts have been made to synthesize networks with controlled structures. The use of telechelics makes it possible to separate the polymerisation process from network formation. The first stage is directed towards the preparation of linear prepolymers with well-defined chemical architecture in terms of structure, functionality, molar mass, and molar mass distribution. The primary obstacle, especially in the case of blocks with opposite philicity, is to endlink these prepolymers in a defect-free network structure.¹⁸

Of particular interest is the sol-gel process. This process offers a unique advantage of producing multi-component materials, in particular new mixed organic-inorganic hybrids.¹⁸

2.5 Conclusions

In terms of the current investigation into the synthesis and characterisation of amphiphilic copolymers to be used as hydrophilizing agent for polysulphone ultrafiltration membranes, certain key factors have to be taken into account:

- 1 It is necessary to control as many variables (molar mass and MMD of both hydrophilic and hydrophobic segments) in the process as possible. With linear block copolymers the number of variables are less than with graft- or network structures. Linear block copolymers therefore seem to be the obvious choice of chemical architecture here.
- 2 The single most important disadvantage of graft copolymers is the fact that the only control in the reaction is the control of the length of the graft molecule. The lack of control of the amount of grafts and the distribution thereof is a disadvantage in the preparation of tailored polymers for specific applications. Without being able to control the amount and distribution of grafts, it would not be possible to perform a model study on the influence of the hydrophilic:hydrophobic ratio on the surface properties of the synthesized copolymers.
- 3 The difficulties in linking polymers with different philicities into network structures is a disadvantage of this technique for preparing the desired copolymers.
- 4 PEG is to be employed as hydrophilic block whilst polystyrene will be used as the hydrophobic segment. It is envisaged that the aromatic nature of PS would be miscible with polysulphone, the membrane substrate material.

2.6 References

1. Noshay, A. and McGrath, J. E., Block copolymers, overview and critical survey, *Academic Press, New York*, **1977**.
2. Halperin, A., Tirrell, M. and Lodge, T. P., Tethered chains in polymer microstructures, *Advances in Polymer Science*, **1992**, 100, 31-71.
3. Riess, G., Micellization of block copolymers, *Progress in Polymer Science*, **2003**, 28, 1107–1170.
4. Barner-Kowollik, C., Quinn, J. F., Morsley, D. R. and Davis, T. P., Modeling the reversible addition-fragmentation chain transfer process in cumyl dithiobenzoate-mediated styrene homopolymerisations: Assessing the rate coefficients for the addition-fragmentation equilibrium, *Journal of Polymer Science: Part A: Polymer Chemistry*, **2001**, 39, 1353-1365.
5. Chiefari, J., Chong, Y. K., Ercole, F., Krstina, J., Jeffery, J., Le, T. P. T., Mayadunne, R. T. A., Meijs, G. F., Moad, C. L., Moad, G., Rizzardo, E. and Thang, S., Living free radical polymerisation by reversible addition-fragmentation chain transfer: The RAFT process, *Macromolecules*, **1998**, 31, 5559-5562.
6. De Brouwer, H., RAFT memorabilia: living radical polymerisation in homogeneous and heterogeneous media, *PhD dissertation, Eindhoven*, **2001**.
7. De Brouwer, H., Schellekens, M. A. J., Klumperman, B., Monteiro, M. J. and German, A. L., Controlled radical copolymerisation of styrene and maleic anhydride and the synthesis of novel polyolefin-based block copolymers by reversible addition-fragmentation chain transfer polymerisation, *Journal of Polymer Science: Part A: Polymer Chemistry*, **2000**, 38, 3596-3603.
8. Matyjaszewski, K. and Xia, J., Atom transfer radical polymerisation, *Chemical Reviews*, **2001**, 101, 2921-2990.
9. Mayadunne, R. T. A., Rizzardo, E., Chiefari, J., Moad, G., Chong, Y. K. and Thang, S., Living radical Polymerisation with reversible addition-fragmentation chain transfer (RAFT Polymerisation) using dithiocarbamates as chain transfer agents, *Macromolecules*, **1999**, 32, 6977-6980.

10. McLeary, J. B., Reversible addition-fragmentation transfer polymerisation in heterogeneous aqueous media, *PhD dissertation, University of Stellenbosch*, **2004**.
11. Moad, C. L., Moad, G., Rizzardo, E. and Thang, S., Chain transfer activity of ω -unsaturated methyl methacrylate oligomers, *Macromolecules*, **1996**, 29, 7717-7726.
12. Moad, G., Chiefari, J., Chong, Y.-K., Krstina, J., Mayadunne, R. T. A., Postma, A., Rizzardo, E. and Thang, S., Living free radical polymerisation with reversible addition-fragmentation chain transfer (the life of RAFT), *Polymer International*, **2000**, 993-1001.
13. Moad, G. and Moad, C. L., Use of chain length distributions in determining chain transfer constants and termination mechanisms, *Macromolecules*, **1996**, 29, 7727-7733.
14. Monteiro, M. J. and de Barbeyrac, J., Free radical polymerisation of styrene in emulsion using reversible addition-fragmentation chain transfer agent with a low transfer constant: Effect of rate, particle size, and molecular weight, *Macromolecules*, **2001**, 34, 4416-4423.
15. Cheng, S.-K., Xu, Z., Yuan, J., Ji, P., Xu, J., Ye, M. and Shi, L., Synthesis and characterisation of PS-PEO-PS triblock copolymers by ATRP, *Journal of Applied Polymer Science*, **2000**, 77, 2882-2888.
16. Neugebauer, D., Zhang, Y., Pakula, T., Sheiko, S. S. and Matyjaszewski, K., Densely-grafted and double-grafted PEO brushes via ATRP. A route to soft elastomers, *Macromolecules*, **2003**, 36, 6746-6755.
17. Greszta, D. and Matyjaszewski, K., Mechanism of controlled/"living" radical polymerisation of styrene in the presence of nitroxyl radicals. Kinetics and simulation, *Macromolecules*, **1996**, 29, 7661-7670.
18. Velichkova, R. S. and Christova, D. C., Amphiphilic polymers from macromonomers and telechelics, *Progress in Polymer Science*, **1995**, 20, 819-887.
19. Lee, J. H., Ju, Y. M. and Kim, D. M., Platelet adhesion onto segmented polyurethane film surfaces modified by addition and crosslinking of PEO-containing block copolymers, *Biomaterials*, **2000**, 21, 683-691.

Chapter 3

Polystyrene-co-poly (ethylene glycol) copolymers: Historical

3.1. Introduction

In Chapter 2 an overview of amphiphilic polymers was presented. Different amphiphilic polymers exist, namely: block copolymers, graft copolymers, interpenetrating networks, and star copolymers. The most frequently used hydrophilic segment is PEG or PEO, while polystyrene (PS) is one of the most frequently used hydrophobic segments.¹ The goal of this study is the synthesis of amphiphilic polymers with a possible application of these copolymers being the hydrophilization of polysulphone membranes. PSU offers unique properties (Chapter 1) that make PSU the ideal material to be used for ultrafiltration membranes. PSU membranes are, however, subjected to fouling due to protein adsorption on the surface of the membranes. PEG exhibit properties such as low interfacial free energy of the hydrated surface, unique structural interaction of the soluble chains within the matrix, high chain mobility, and steric stabilization.^{2, 3} These properties make PEG passive towards biological fluids and therefore make it the ideal candidate for the hydrophilic segment of the proposed amphiphilic block copolymer.

It is important that the hydrophobic segment of the amphiphilic block copolymer is compatible with PSU. The structures of PS and PSU are compatible, in terms of the aromatic structure of both these species.

In Chapter 2 the different methods of synthesizing amphiphilic block copolymers were discussed. The synthesis of amphiphilic copolymers containing PEO as hydrophilic and PS as hydrophobic groups has been widely published in literature and recently reviewed by Velichkova and Christova.¹ Several different routes have been used to synthesize these polymers. Apart from block copolymers, research efforts have also been directed at the synthesis of graft copolymers.⁴⁻¹⁴ These methods mainly include on the copolymerisation of styrene end-functional PEG mono methyl ether (MPEG), with the functional group on the MPEG being methacrylate or maleate.

Lately there have been several reports on the synthesis of heteroarm copolymers of styrene and ethylene glycol for specific applications.¹⁵⁻²⁰

This investigation will focus mainly on linear MPEG-*b*-PS diblock copolymers.

3.2. PEG-*b*-PS block copolymers

It was stated in Chapter 2 that the most suitable amphiphilic copolymer configuration selected for use in this study is block copolymers. This study will focus on amphiphilic block copolymers and any reference to amphiphilic polymers will be restricted to linear amphiphilic block copolymers. More specifically, as will be discussed in Chapter 5 and Chapter 6, this study will focus on diblock and triblock copolymers, therefore excluding multi-block copolymers. For the PEG-*b*-PS block copolymers, the focus will remain on diblock copolymers, where better control in terms of the hydrophilic:hydrophobic ratio will be possible compared to other amphiphilic copolymer configurations.

Different methods exist for the synthesis of these PEG-*b*-PS block copolymers, the most commonly used being

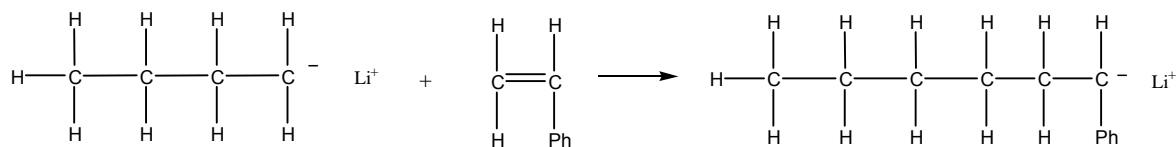
- 1 anionic polymerisation;
- 2 free radical polymerisation; and
- 3 controlled living free radical polymerisation.

Each of these methods has advantages and disadvantages. With the control of the molar mass and the hydrophilic:hydrophobic ratio being of importance in these polymers, certain factors will prove to be of the utmost importance in the selection of a suitable method of synthesis.

3.2.1 PEG-*b*-PS via living anionic polymerisation

Traditionally, anionic polymerisation was the only method suitable for the synthesis of polymers with controlled architecture. Even today, companies like Polymer Source (Dorval, Canada) and Polymer Laboratories (France) use this method to synthesize PEG-*b*-PS di- and triblock copolymers on a commercial scale.²¹⁻²⁶

The major advantage that anionic polymerisation offers over conventional free radical polymerisation is the excellent control of molar mass and the MMD of the polymer products obtained. A variety of anionic initiators exist, but probably the most common are the alkali-metal salts and, in particular, *n*-butyl lithium (as described below).²⁷



The anionic chain end propagates by adding another monomer molecule. This process continues until all monomer is exhausted. In anionic polymerisation, unlike conventional free radical polymerisation, the rate of initiation is comparable with the rate of propagation. This means that the initiator starts chain growth immediately. In the absence of impurities, there is no termination step.²⁷ This means that the chains grow until the monomer is exhausted. The growing chain is then perfectly stable and will start to grow again as soon as new monomer is introduced into the system. This is extremely useful in block copolymer synthesis, whereby the first monomer is exhausted from the system and a new one introduced to form a perfect block copolymer.

Living anionic polymerisation, however, remains a technique that is highly sensitive to any impurities and normally demands severe polymerisation conditions and long reaction times.

The main contributions towards the living anionic polymerisation in the synthesis of PEG-*b*-PS block copolymers can be divided into two different groups, namely: sequential anionic polymerisation; and anionic macro initiators.

In sequential anionic copolymerisation the one monomer is added to the system and, once fully reacted, the second monomer is introduced into the system to form a block copolymer.

Anionic macro initiators make use of a macromonomer that is transformed into an anionic macro initiator. Upon reaction with a second monomer the resulting block copolymer is formed.

Contributions towards the synthesis of PEG-*b*-PS block copolymers via anionic polymerisation are listed in Table 3.1.

Table 3.1: Various methods for the preparation of PS-*b*-PEG via anionic polymerisation

Polymerisation method	Initiator	Author	Notes
Sequential anionic	Cumylpotassium	O'Malley and Marchessault ²⁸	
Sequential anionic	α -phenyl ethyl potassium	Xie and Zhou ²⁹	
Sequential anionic	2-(1-phenyl)naphthalene	Qiurck <i>et al.</i> ³⁰	
Sequential anionic	Cumylpotassium	Calderare <i>et al.</i> ³¹	
Sequential anionic	Naphthalenyl sodium	Richards and Szwarc ³²	
Sequential anionic	Disodium compound of α -methyl styrene tetramer	Finaz <i>et al.</i> ³³	
Sequential anionic	Biphenyl potassium	Zgonnik <i>et al.</i> ³⁴	
Sequential anionic	Dipotassium compound of α -methyl styrene tetramer	Marti <i>et al.</i> ³⁵	
Sequential anionic	Alkali metal naphthalene	Xie <i>et al.</i> ³⁶	1
Sequential anionic	Cumylpotassium	Yu and Eisenberg ³⁷	
Sequential anionic	Sec-butyl lithium	Jialanella <i>et al.</i> ³⁸	
Sequential anionic	Cumylpotassium	Hruska <i>et al.</i> ³⁹	
Sequential anionic	Sec-butyl lithium	Khan <i>et al.</i> ⁴⁰	
Anionic	PS anion with COCl ₂	Finaz <i>et al.</i> ³³	
Anionic macro initiator	LiOCH ₂ CH ₂ -PS	Quirck and Seung ⁴¹	
Anionic macro initiator	CH ₃ O(CH ₂ CH ₂ O) _n Na + CBr ₃ COCl + Mn ₂ (CO) ₁₀	Niwa and Higashi ⁴²	
Anionic macro initiator	Alkali metal oxides	Stolarzewicz <i>et al.</i> ⁴³	2
Anionic and photo-induced charge transfer	p-Amino phenol	Huang <i>et al.</i> ⁴⁴	3

Notes:

- 1 In a two-stage process styrene was polymerised with the aid of lithium α -methyl naphthalene, followed by addition of ethylene oxide. Water and hot cyclohexane proved to be effective in extracting the homopolymers (PEO and PS) respectively.
- 2 A recent study showed the use of hydroxyl terminated PEG with potassium to initiate the polymerisation of styrene. Although alkali metal oxides do not initiate polymerisation of vinyl monomers, some exceptions can be found. Here it was stated that styrene could be polymerised by potassium alkoxides without the addition of a ligand. The reaction occurred when the alkoxide possessed one or more additional oxygen atoms in the molecule.
- 3 Starting with *p*-amino phenol, the phenol group was protected with benzaldehyde. The phenol group was transformed to a phenoxy anion and EO was polymerised via anionic polymerisation using the formed phenoxy anionic initiator. Upon termination, the amino group was deprotected, followed by the photo-induced charge transfer polymerisation of styrene to form the resulting PEO-*b*-PS block copolymer.

3.2.2 PEG-*b*-PS via free radical polymerisation

The basic principles of free radical polymerisation will be discussed in Chapter 4 with specific attention to the mechanism of polymerisation. The major contributions towards the synthesis of PEG-*b*-PS block copolymers via conventional free radical polymerisation are reported here. Careful consideration has to be given to use of the free radical technique by which to synthesize these copolymers. It is important to distinguish between making use of macro initiators to produce block copolymers, while making use of macromonomers will result in the formation of graft copolymers.

Macro initiators are macromolecules that contain at least one end-functional group, that is transformed into a free radical initiating species. Macromonomers are macromolecules that contain a polymerisable group (a double bond) that is able to take part in free radical polymerisation reactions. Where only one macro initiator can be incorporated into a polymer chain as an initiating species, any number of macromonomers can be incorporated into a growing polymer chain as monomer reactants.

Reaction conditions in free radical polymerisation are mild compared to anionic polymerisation. One of the major advantages of free radical polymerisation in terms of

industrial applicability is that it is possible to conduct polymerisations in water. Conventional free radical chemistry is, however, limited in that there is less control over the molar mass and the distribution thereof.

Macro initiators are formed via ester- or isocyanate linkages between hydroxy-terminated macromolecules (either PEG or PS)

Table 3.2: Preparation of PS-*b*-PEG via conventional free radical polymerisation

Polymerisation method	Initiator	Author	Notes
Free Radical macro initiator	4,4'-azo bis(4-cyanopentanoyl chloride) and PEG	Hazer <i>et al.</i> ¹¹	1
Free Radical macro initiator	4,4'-azo bis(4-cyanopentanoyl chloride) and PEG	Ueda and Nagai ⁴⁵	2
Free Radical	4,4'-azo bis(4-cyanopentanoyl chloride)	Cheng <i>et al.</i> ⁴⁶	3
Free radical	Azocarbamate	Yürük and Özdemir ⁴⁷	4
Radical + condensation	Isophorone diisocyanate + t-BuOOH	Unyanik and Baysal ⁴⁸	5
Radical + condensation	Diisocyanate	Orhan <i>et al.</i> ⁴⁹	
Coupling reaction	Butadiene di-epoxide	Seiler <i>et al.</i> ⁵⁰	6
Coupling reaction	Isocyanate	Lundberg and Thame ⁵¹	
Coupling reaction	Isocyanate	Xie and Xie ⁵²	

Notes:

- 1 4,4'-azo bis(4-cyanopentanoyl chloride) was reacted with PEG and with either benzyl chloride, acetyl chloride or acryloyl chloride. The resulting macro initiator was used for the bulk polymerisation of styrene.

- 2 Block copolymers of styrene and EO were synthesized by condensation of 4,4'-azo bis(4-cyanopentanoyl chloride) and PEG, followed by thermal decomposition in the presence of styrene.
- 3 Styrene and 4,4'-azo bis(4-cyanopentanoyl chloride) were dissolved in THF, the product was purified and then treated with SOCl_2 . PEG was added to the product to yield the copolymer. Note that the order of synthesis was reversed in that the polystyrene segment of the block copolymer was formed prior to the reaction of the initiator with PEG.
- 4 PEG was reacted with a diisocyanate to form an isocyanate-capped prepolymer. The *NCO* group was reacted with dihydrogenperoxide to form peroxy carbamate, which then initiated the radical polymerisation of styrene.
- 5 A block copolymer was prepared by using polymeric azocarbamate as an initiator, which was obtained by capping PEG with aliphatic diisocyanate and subsequently by reacting this intermediate with azobiscyanopentanol. The product was then used to polymerise styrene.
- 6 The triblock copolymer was obtained by coupling an AB diblock copolymer with one hydroxyl endgroup, using butadiene di-epoxide as coupling agent.

3.2.3 PEG-*b*-PS via living free radical polymerisation

Tables 3.1 and 3.2 show a trend towards the use of macro monomers as starting blocks for the synthesis of block copolymers. The end-functionalised macro monomers are converted to form nuclei for polymerisation by ionic polymerisation. Using hydroxyl-terminated PEG and transforming the hydroxyl group to a suitable ion which can initiate polymerisation to form the PS segment of the polymer. In starting with a known hydrophilic macro monomer, the ratio of hydrophilic:hydrophobic segments are controlled by controlling the length of the hydrophobic segment of the polymer.

Free radical polymerisation offers more favorable conditions for polymerisation, but the lack of control of the molar mass distribution renders this technique inefficient to produce block copolymers. The reason for the lack of control is due to termination reactions taking place in the reaction.

Recent advances in controlled or “living” free radical polymerisation have also introduced techniques to reduce the amount of “active” radicals and turn them into “dormant” species, a process that is in equilibrium. By keeping the amount of “active” radicals low, the probability of termination by self reaction is reduced, thereby giving better control of the final molar mass. These processes therefore offer a new route for the synthesis of block copolymers with narrow MMDs. Although more time consuming than conventional free radical polymerisation, controlled radical polymerisation yields products of much narrower MMD than conventional radical polymerisation. Controlled radical polymerisation also offers more favorable polymerisation conditions than those required for anionic polymerisation.

Controlled radical polymerisation includes techniques such as ATRP, NMRP, and RAFT.

NMRP and ATRP were the first controlled free radical techniques to be devised. NMRP was used especially for styrene polymerisation,⁵³ but had less utility for other monomers. ATRP is more versatile, but it requires more unconventional initiating systems. NMRP initiators have poor solubility in certain media and cannot be used with a wide variety of monomers. An advantage of RAFT with regards to ATRP and NMRP is that conditions similar to conventional free radical polymerisation can be employed. RAFT polymerisation is performed by adding a chosen quantity of a thiocarbonylthio compound to a conventional free radical polymerisation mixture. Another advantage of the RAFT process over the other processes for living/controlled radical polymerisation is that it is compatible with a wide variety of monomers, including functional monomers containing, for example, acid, acid salt or tertiary amino groups.

The main efforts towards the synthesis of PEG-*b*-PS via controlled radical polymerisation are given in Table 3.3.

Table 3.3: Preparation of PS-*b*-PEG via controlled free radical polymerisation

Polymerisation method	Initiator	Author	Notes
Controlled Radical	Thiuram disulfide	Nair <i>et al.</i> ⁵⁴	1
Iniferter	Bis (2-hydroxyethyl) thiuram disulfide	Cakmak ⁵⁵	2
Iniferter	Benzyl N,N-diethyl dithiocarbamate	Nakayama <i>et al.</i> ⁵⁶	3
NMRP	2,2,6,6-tetramethyl-piridinyl-1-oxy (TEMPO)	Chen <i>et al.</i> ⁵⁷	4
ATRP	2-Bromo (chloro) propionyl chloride	Jankova <i>et al.</i> ⁵⁸	5
ATRP	α -Chlorophenylacetylchloride, 2-chloroacetylchloride	Reining <i>et al.</i> ⁵⁹	6
RAFT	4-(Cyano)-4-(thiobenzoylthio)pentanoic acid	Rizzardo <i>et al.</i> ^{53, 60-62}	7

Notes

- 1 The terminal OH groups of PEG were converted to amine groups and then to thiuram disulfide via thiocarbamylation. The amine-terminated iniferters were then used as polymeric initiators for styrene.
- 2 Bis (2-hydroxyethyl) thiuram disulfide was reacted with PEG to form the resulting macroiniferter, whereafter the macroiniferter was used for the polymerisation of styrene.
- 3 PEG mono methyl ethers were end-capped with benzyl N,N-diethyl dithiocarbamate. The products were then UV irradiated in the presence of styrene.
- 4 MPEG was tosylated with p-toluenesulfonyl chloride. The product was coupled to HO-TEMPO to form the macro initiator MPEG-TEMPO. The resulting product was then added to styrene to form a diblock copolymer.
- 5 A macro initiator was formed by reacting 2-bromo (chloro) propionyl chloride with PEG. After purification, the macro initiator was added to styrene and CuBr to form the resulting copolymer.

- 6 PEG mono methyl ether (MPEG) was added to the acid chlorides to form the PEO macro initiator. The product was used with styrene to form the block copolymer.
- 7 MPEG was reacted with 4-(cyano)-4-(thiobenzoylthio)pentanoic acid with a suitable catalyst (DMAP). The product was washed with water to yield a pure macro initiator, which was then used for the preparation of the block copolymer.

3.3. Conclusions

Different synthetic routes are available by which to synthesize PEG-*b*-PS block copolymers, including: living anionic polymerisation, RAFT polymerisation, NMRP, and ATRP.

Limiting synthesis to linear diblock copolymers further reduces the variables in terms of the synthesis of materials with well-defined chemical architecture.

The proposed method of hydrophilization, as described in Chapter 1, will involve the addition of a hydrophilizing agent to the PSU membrane casting solution. This hydrophilizing agent should therefore have a specific chemical architecture, in order to investigate the influence of the hydrophilic:hydrophobic ratio on the hydrophilizing capability of these compounds. It is therefore necessary to control as many variables (molar mass and MMD of both the hydrophilic and hydrophobic segments) in the process as possible. Linear block copolymers seem to be the obvious choice of chemical architecture to be synthesized in terms of this investigation.

Literature shows a trend towards the use of macro molecules as starting blocks for the synthesis of block copolymers. By converting functional macromonomers into macro initiators and then polymerising a second block onto the macro initiator, the number of variables are reduced, whereby the molar mass and MMD of only one segment of the amphiphilic polymer has to be controlled.

An advantage of RAFT with regards to ATRP and NMRP is that conditions similar to conventional free radical polymerisation can be employed. RAFT polymerisation is performed by adding a chosen quantity of a thiocarbonylthio compound to a conventional free radical polymerisation mixture.

Another advantage of the RAFT process over the other processes for living/controlled radical polymerisation is that it is compatible with a wide variety of monomers including functional monomers containing, for example, acid, acid salt or tertiary amino groups.

This provides the ability to synthesize a wide range of narrow polydispersity polymers containing end or side chain functionality in one step without any need for protection or deprotection. This can be advantageously used in the synthesis of block copolymers and other products of more complex structure.

3.4. References

1. Velichkova, R. S. and Christova, D. C., Amphiphilic polymers from macromonomers and telechelics, *Progress in Polymer Science*, **1995**, 20, 819-887.
2. Lee, J. H., Kopecek, J. and Andrade, J. D., Protein-resistant surfaces prepared by PEO-containing block copolymer surfactants, *Journal of Biomedical Materials Research*, **1989**, 23, 351-368.
3. Jeon, S. I., Lee, J. H., Andrade, J. D. and De Gennes, P. G., Protein-surface interactions in the presence of poly ethylene oxide, *Journal of Colloid and Interface Science*, **1991**, 142, 149-166.
4. Lee, Y.-S., Wang, Y. and Byun, J.-W., The synthesis of grafted PS resins with PEG using ozone oxidation and their application to enzyme immobilization, *Chemical Abstract*, **1997**, CA133: 43778.
5. Ishizu, K. and Shen, X. X., Radical copolymerisation reactivity of maleate-terminated poly(ethylene glycol) with vinylbenzyl-terminated polystyrene macromonomers, *Polymer*, **1999**, 40, 3251-3254.
6. Lui, J., Chew, C. H., Wong, S. Y., Gan, L. M., Lin, J. and Tan, K. L., Dispersion polymerisation of styrene in aqueous ethanol media using poly(ethylene oxide) macromonomer as a polymerisable stabiliser, *Polymer*, **1998**, 39, 283-289.
7. Tuncel, A., Emulsion copolymerisation of styrene and poly(ethylene glycol) ethyl ether methacrylate, *Polymer*, **2000**, 41, 1257-1267.
8. Capek, I., Radical polymerisation of polyoxyethylene macromonomers in disperse systems, *Advances in Polymer Science*, **1999**, 145, 1-55.
9. Riza, M., Mstapha, S. and Dewi, R., Dispersion copolymerisation of methacraloyl-poly(ethylene glycol) macromonomer with styrene, *Malaysian Journal of Chemistry*, **2004**, 6, 24-28.
10. Chen, M.-Q., Liu, X.-Y., Yang, C. and Zhang, M., Synthesis of PEG macromonomer and preparation of nanoparticles based on PEG grafted PS copolymers., *Chemical Abstracts*, **2001**, 136:54161.

11. Hazer, B., Erdem, B. and Lenz, R. W., Styrene polymerisation with some new macro or macromonomeric azoinitiators having PEG units, *Journal of Polymer Science: Part A: Polymer Chemistry*, **1994**, 32, 1739-1746.
12. Park, B. D. and Lee, Y.-S., The effect of PEG groups on swelling properties of PEG-grafted-polystyrene resins in various solvents, *Reactive & Functional Polymers*, **2000**, 44, 41-46.
13. Ishizu, K., Shen, X. X. and Tsubaki, K.-I., Radical copolymerisation of methacryloyl-terminated poly(ethylene glycol methylether) with vinylbenzyl-terminated polystyrene macromonomers, *Polymer*, **2000**, 41, 2053-2057.
14. Gibanel, S., Heroguez, V. and Forcada, J., Surfactant characteristics of polystyrene/poly(ethylene glycol) macromonomers in aqueous solutions and on polystyrene latex particles: Two-step emulsion polymerisations, *Journal of Polymer Science: Part A: Polymer Chemistry*, **2001**, 39, 2767-2776.
15. Peleshanko, S., Jeong, J., Gunawidjaja, R. and Tsukruk, Amphiphilic heteroarm PEO-*b*-PS star polymers at the air-water interface: Aggregation and surface morphology, *Macromolecules*, **2004**, 37, 6511-6522.
16. Tsistikianis, C. and Papanagopoulos, D., Amphiphilic heteroarm star copolymers of polystyrene and poly(ethylene oxide), *Polymer*, **1995**, 36, 3745-3752.
17. Tian, L., Yam, L., Zhou, N., Tat, H. and Urich, K. E., Amphiphilic scorpion-like macromolecules: design, synthesis, and characterisation, *Macromolecules*, **2004**, 37, 538-543.
18. Francis, R., Skolnik, A. M., Carino, S. R., Logan, J. L., Underhill, R. S., Angot, S., Taton, D., Gnanou, Y. and Duran, R. S., Aggregation and surface morphology of a poly(ethylene oxide)-block-polystyrene three-arm star polymer at the air/water interface studied by AFM, *Macromolecules*, **2003**, 35, 6483-6485.
19. Francis, R., Taton, D., Logan, J. L., Masse, P., Gnanou, Y. and Duran, R. S., Synthesis and surface properties of amphiphilic star-shaped dendrimer-like copolymers based on PS core and PEG corona, *Macromolecules*, **2003**, 36, 8253-8259.

20. Neugebauer, D., Zhang, Y., Pakula, T., Sheiko, S. S. and Matyjaszewski, K., Densely-grafted and double-grafted PEO brushes via ATRP. A route to soft elastomers, *Macromolecules*, **2003**, 36, 6746-6755.
21. Yeh, S. W., Wei, K.-H., Sun, Y.-S., Laing, K. S. and Jeng, U.-S., Morphological transformation of PS-*b*-PEO diblock copolymer by selectively dispersed colloidal CdS quantum dots, *Macromolecules*, **2003**, 36, 7903-7907.
22. Dorgan, J. R., Stamm, M., Toprakcioglu, C., Jerome, R. and Fetters, L. J., End-attaching copolymer adsorption: Kinetics and effects of chain architecture, *Macromolecules*, **1993**, 26, 5321-5330.
23. Patel, N. P. and Spontak, R. J., Gas-transport and thermal properties of a microphase-ordered poly(styrene-*b*-ethylene oxide-*b*-styrene) triblock copolymer and its blends with PEG, *Macromolecules*, **2004**, 37, 2829-2838.
24. Patel, N. P. and Spontak, R. J., Mesoblends of polyether block copolymers with PEG, *Macromolecules*, **2004**, 37, 1394-1402.
25. Rivillon, S., Muñoz, M. G., Monroy, F., Ortega, F. and Rubio, R. G., Experimental study of the dynamic properties of monolayers of PS-PEO block copolymers. The attractive monomer surface case, *Macromolecules*, **2003**, 36, 4068-4077.
26. Polymer Source Catalog, **2004**.
27. Rosen, S. L., Fundamental principles of polymeric materials, *Wiley Interscience, United States of America*, **1993**.
28. O'Malley, J. J. and Marchessault, R. H., Block copolymers of styrene and ethylene oxide, *Macromolecular Synthesis*, **1972**, 4, 35-39.
29. Xie, H.-Q. and Zhou, P. G., Multicomponent chemical materials, *Advances in Chemistry*, **1986**, 211, 139.
30. Quirck, R. P., Kim, J., Rodrigues, K. and Mattice, W. L., Anionic synthesis and characterisation of poly(styrene-*block*-ethylene oxide) polymers with fluorescent probes at the block junctions, *Chemical Abstracts*, **1990**, 113: 153349x.

31. Calderara, F., Hruska, Z., Hurtrez, G., Nugay, T., Reiss, G. and Winnik, M. A., Synthesis of chromophore-labeled polystyrene/poly(ethylene oxide) diblock copolymers, *Chemical Abstracts*, **1993**, 113:28698h.
32. Richards, D. H. and Szwarc, M., Block copolymers of ethylene oxide and its analogs with styrene, *Chemical Abstracts*, **1959**, 54:9350g.
33. Finaz, G. P., Rempp, P. and Parrod, J., Preparation of copolymeric chains of styrene and ethylene oxide, *Chemical Abstracts*, **1962**, 57: 1055f.
34. Zgonnik, V. N., Shibaev, L. A. and Nikolaev, N. I., Synthesis of block copolymers with alternating amorphous and crystalline blocks, *Chemical Abstracts*, **1969**, 64363b.
35. Marti, S., Nervo, J., Periard, J. and Reiss, G., Stability of reversed emulsions. Water-in-oil emulsions prepared by the use of block copolymers, *Colloidal Polymer Science*, **1975**, 253, 220-224.
36. Xie, H.-Q., Liu, Z.-S. and Guo, J.-S., Synthesis and properties of oxymethylene-linked oxypropylene-styrene multiblock copolymers, *Polymer*, **1994**, 35, 4914-4919.
37. Yu, K. and Eisenberg, A., Multiple morphologies in aqueous solutions of aggregates of polystyrene-b-poly(ethylene oxide) diblock copolymers, *Macromolecules*, **1996**, 29, 6359-6361.
38. Jlalanelia, G. L., Firer, E. M. and Piirma, I., Synthesis of polystyrene-b-polyoxyethylene for use as a stabilizer in the emulsion polymerisation of styrene, *Journal of Polymer Science: Part A: Polymer Chemistry*, **1992**, 30, 1925-1933.
39. Hruska, Z., Hurtrez, G., Walter, S. and Riess, G., An improved technique of cumylpotassium preparation: application in the synthesis of spectroscopically pure PS-PEG diblock copolymers, *Polymer*, **1992**, 33, 2447-2449.
40. Khan, T. N., Mobbs, R. H., Quintana, J. R. and Stubbersfield, R. B., Synthesis and colloidal behavior of a PS-b-PEO block copolymer, *European Polymer Journal*, **1986**, 23, 191-194.
41. Quirck, R. P. and Seung, N. S., Anionic polymerisation of ethylene oxide with lithium catalysts. Solution properties of styrene-ethylene oxide polymers, *ACS Symposium Series*, **1985**, 286, 37-45.

42. Niwa, M. and Higashi, N., Reversible interpolymer complexation between poly(oxyethylene)-based amphiphilic block polymer and poly(acrylic acid) at the air-water interface, *Macromolecules*, **1989**, 22, 1000-1002.
43. Stolarzewicz, A., Czaja, M. and Neugebauer, D., Polymerisation of styrene in the presence of oligo(ethylene glycol) alkoxides: a new route to amphiphilic polymers?, *Polymer*, **2000**, 41, 7865-7869.
44. Huang, J., Huang, X. and Zhang, S., Block copolymerisation of ethylene oxide and styrene by sequential initiation of an snion and a photoinduced charge transfer complex, *Macromolecules*, **1995**, 28, 4421-4425.
45. Ueda, A. and Nagai, A., Block copolymers derived from azobiscyanopentanoic acid. VI. Synthesis of a poly(ethylene glycol)-polystyrene block copolymer, *Journal of Polymer Science: Part A: Polymer Chemistry*, **1986**, 24, 405-418.
46. Cheng, S.-K., Wang, C.-C. and Chen, C.-Y., Synthesis of block copoly(polyethylene glycol-styrene) by the macromonomer and macroinitiator method, *Materials Chemistry and Physics*, **2002**, 78, 581-590.
47. Yürük, H. and Özdemir, A. B., Preparation of block copolymers with polymeric azocarbamate as an initiator, *Journal of Applied Polymer Science*, **1986**, 31, 2171-2183.
48. Unyanik, N. and Baysai, B. M., Preparation of polystyrene-block-(ethylene oxide)s and characterisation of the products, *Journal of Applied Polymer Science*, **1990**, 41, 1981-1993.
49. Orhan, E. H., Yilgor, I. and Baysal, B. M., Block copolymers from PEG and styrene, *Polymer*, **1977**, 18, 286-290.
50. Seiler, E., ., Fahrbach, G., Gerberling, K. and Stein, P., Ethylene oxide block copolymers, *Ger Offen 2,301,224*, **1974**.
51. Lundberg, R. D. and Thame, N. G., Multiphase block and graft copolymers, *Ger. Offen. 2,403,934*, **1973**.
52. Xie, H.-Q. and Xie, D., Molecular design, synthesis and properties of block and graft copolymers containing polyoxyethylene segments, *Progress in Polymer Science*, **1999**, 24, 275-313.

53. Rizzardo, E., Chiefari, J., Chong, Y. K., Ercole, F., Krstina, J., Jeffery, J., Le, T. P. T., Mayadunne, R. T. A., Meijs, G. F., Moad, C. L., Thang, S. and Moad, G., Tailored polymers by free radical processes, *Macromolecular Symposia*, **1999**, 143, 291-307.
54. Nair, C. P. R., Chaumont, P. and Clouet, G., A-B-A triblock and (A-B)_n segmented block copolymers of styrene and ethylene oxide via thermal iniferters, *Journal of Macromolecular Science: Chemistry*, **1990**, 27, 791-806.
55. Cakmak, I., Synthesis of multiblock copolymers via macroiniferter, *European Polymer Journal*, **1998**, 34, 1561-1563.
56. Nakayama, Y., Miyamura, M., Goto, K. and Matsuda, T., Preparation of poly(ethylene glycol)-polystyrene block copolymers using photochemistry of dithiocarbamate as a reduced cell-adhesive coating material, *Biomaterials*, **1999**, 20, 963-970.
57. Chen, X., Gao, B., Kops, J. and Batsberg, W., Preparation of polystyrene-poly(ethylene glycol) diblock copolymer by 'living' free radical polymerisation, *Polymer*, **1998**, 39, 911-915.
58. Jankova, K., Chen, X., Kops, J. and Batsberg, W., Synthesis of amphiphilic PS-*b*-PEG-*b*-PS by atom transfer radical polymerisation, *Macromolecules*, **1998**, 31, 528-541.
59. Reining, B., Keul, H. and Hocker, H., Chloro-telechelic poly(ethylene oxide)s as initiators for the atom transfer radical polymerisation (ATRP) of styrene and methyl methacrylate: Structural features that affect the initiation efficiency, *Polymer*, **1999**, 40, 3555-3563.
60. Rizzardo, E., Synthesis of dithioester chain transfer agents and the use of bis(thioacyl) disulfides or dithioesters as chain transfer agents, *WO 99/05099*, **1998**.
61. Rizzardo, E., Solomon, D. H. and Cacioli, P., *US Patent*, **1985**, 4581429, *Chemical Abstracts* **1985**, 102:221335q.
62. Rizzardo, E., Thang, S., Moad, G., Chiefari, J., Chong, Y. K., Krstina, J., Mayadunne, R. T. A. and Postma, A., Living free radical polymerisation with reversible addition-fragmentation chain transfer, *Polymer International*, **2000**, 49, 993-1001.

Chapter 4

Reversible addition-fragmentation chain transfer polymerisation: An overview

4.1 Introduction

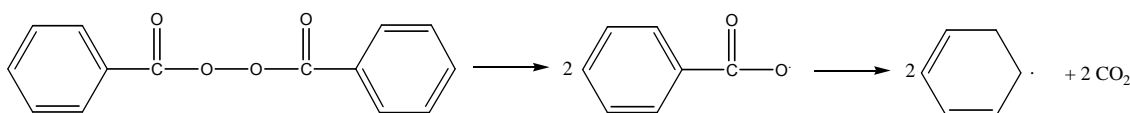
Conventional free radical polymerisation is one of the most important types of addition polymerisation. Polymers are being increasingly used, daily, in products ranging from domestic appliances to ultra high technology equipment. Technology is placing an ever increasingly higher demand on the physical properties of polymeric components. These physical properties are, to a large extent, determined by the chemical architecture of the polymer, as well as the structural design of the components. To produce macromolecules with specific chemical architecture therefore places a high premium on the ability to control the synthetic process by which these materials are prepared. A large percentage of all plastics are synthesized via conventional free radical polymerisation,¹ which has the following advantages:

1. the process is adaptable to many monomers under mild conditions,
2. no specialized equipment is necessary,
3. there is no need for monomer purification or removal of initiator, and
4. the process can be performed in bulk and suspension, which are major advantage in industrial processes.

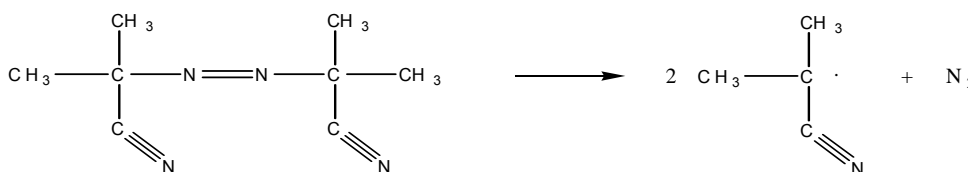
The major disadvantage of conventional free radical polymerisation is the inability to convert unsaturated monomers to well-defined polymers with precise control of molar mass and MMD.¹ Termination and transfer reactions (Section 4.2) have limited the ability to control the molar mass and the MMD of the desired products. It is also virtually impossible to synthesize block copolymers with specific chemical architecture (one of the primary objectives of this investigation) via sequential addition of monomers in a conventional free radical system. With the limitations (stringent reaction conditions) of living anionic polymerisation, researchers in recent years focused on breathing “livingness” into free radical polymerisation. The development and advances in the new controlled (“living”) free radical polymerisation (LFRP) will be discussed in Section 4.3.

4.2 Conventional free radical polymerisation

In order to fully understand the developments in controlled free radical chemistry it is necessary to briefly look at the fundamental principles of conventional free radical polymerisation to gain insight as to the limitations thereof in the synthesis of tailored products. Conventional free radical polymerisation is an addition polymerisation in which initiation occurs by the action of free radicals (as the name states), which are electrically neutral species with an unshared electron.² Free radicals for the initiation of addition polymerisation in bulk or solution are usually generated by thermal decomposition of organic peroxides or azo compounds. Two commonly used organic free radical initiators are benzoyl peroxide (BPO) and azobisisobutyronitrile (AIBN).



Scheme 4.1: Thermal decomposition of benzoyl peroxide.



Scheme 4.2: Thermal decomposition of azobisisobutyronitrile.

Conventional free radical polymerisation can be divided into 4 different steps:

- 1 initiation (creation of a radical);
- 2 propagation (successive addition of monomer units);
- 3 termination (reaction of two radicals to produce an inactive polymer); and
- 4 transfer (termination of one polymer chain and the subsequent initiation of a new polymer chain).

Initiation occurs when the initiator molecule, I , undergoes first-order decomposition to produce two free radicals, R^\bullet :



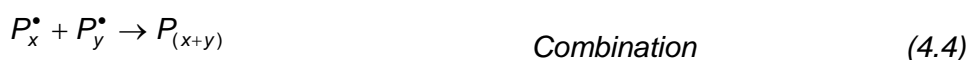
The radicals (R^\bullet) can add to monomer (M) by grabbing an electron from the electron-rich double bond, forming a single bond with the monomer, but leaving an unshared electron at the other end:



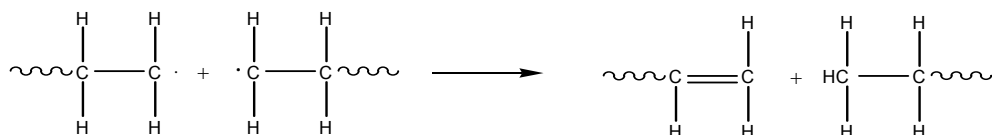
The product (P_1^\bullet) is therefore still a free radical and the process proceeds by adding another monomer unit. In general it can be written as follows:



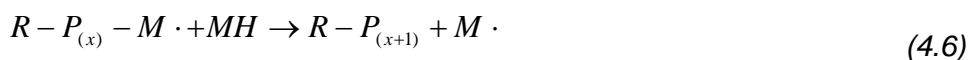
Termination can occur by either combination or disproportionation. In combination, two growing polymer chains can collide and the unshared electrons can combine to form a single bond:



where $P_{(x+y)}$ is a *dead* polymer chain with, $(x+y)$ repeating units. In disproportionation, two growing polymer chains can collide, leading to proton (H) abstraction from the penultimate carbon of one of the chains:



Chain transfer takes place in free radical polymerisation where a growing chain is terminated and a new chain starts to grow in its place:



Normally, all the radical processes occur simultaneously and the molar mass of the resulting polymer is statistically determined by the competition of *propagation* with *termination* and *transfer*.¹ The resulting MMD is therefore broad. This excludes this method for the preparation of polymers with complex chemical architectures.

4.3 Controlled free radical polymerisation

Traditionally, copolymers are prepared mainly by either living polymerisation or by the combination of macromonomers with end functionalities. These processes suffer from many disadvantages in terms of the stringent conditions in which these reactions take place as well as the limited variety of monomers than can be used. Anionic polymerisation is a process that is normally associated with true living polymerisation. The difference between the mechanisms of conventional and ionic polymerisation is that with free radical polymerisation the growing chain-ends recombine or disproportionate, whereas in ionic polymerisation the charges on the growing chain-ends repel each other and no termination is possible.¹ The protocol in controlled free radical chemistry is the restriction of transfer and/or termination reactions, which result in a system where the active growing polymer chains will continue growing as long as there is monomer present in the system. When looking at ideal living polymerisation, only two processes, namely *initiation* and *propagation*, should occur, hence all growing polymer chains in the system should be active. Recent investigations into the advancement of controlled free radical processes therefore targeted the elimination of transfer and termination reactions.

Otsu³ and Otsu and Yoshida⁴ reported the use of an *iniferter* (an agent that act as *initiators*, *transfer* and *termination* agents) in order to obtain living free radical polymerisation.

A simplified reaction scheme would therefore be as follows:



Earlier investigations by Otsu and Yoshida⁵ involving the addition of certain compounds (dithiocarbamates, disulfides) to free radical systems, which exhibited living conditions, marked the start of investigations into controlled free radical polymerisation. Although the

MMD of the products obtained by Otsu and Yoshida⁵ were relatively high (compared to ideal living polymerisations), the main interest in their findings was the concept of reversible activation and deactivation.

Subsequently, different free radical processes offering controlled growth have been developed in recent years. These processes all rely on the reversible deactivation of the growing polymer chains but, because not all chains are actively growing, cannot be classified as ideal living polymerisation processes. Although there has been a call for uniform terminology, terms like quasi-, pseudo-, truly or apparently living systems are all being used to describe these processes.^{1, 6} The criteria for livingness has not yet been well-defined, but it has been stressed that the chain breaking (termination) mechanism should not be observed (<5%) at the time of complete conversion (>99%) for a synthetically convenient reaction.⁷

Certain experimental criteria have been assigned to living polymerisation processes:

- the synthesis of polymers with MMDs of less than 1.5 is evidence of a living system (with 1.5 being the lower limit MMD obtainable by conventional free radical polymerisation),^{8, 9}
- the first-order rate plot ($\ln[M]_0/[M]$ vs time) should give a linear relationship;⁹
- \bar{M}_n vs. fractional conversion plot should give a linear relationship;^{1, 9} and
- $[P\cdot]$ vs. time should give a linear relationship.¹

Penczek *et al.*^{10, 11} and Quirck and Lee¹² reviewed the scope and limitations of the experimental criteria for living conditions as stated above. According to these authors, linear plots of \bar{M}_n vs. fractional conversion are not sufficient criteria for living polymerisation. Although a linear relationship in the plot of \bar{M}_n vs. fractional conversion requires that no transfer is taking place, a linear plot does not provide information on the non-existence of transfer reactions. The only information given in the linearity of the plot is that the number of growing chains remains constant in the reaction and that there are growing chains present in the system at full conversion.

Control in free radical polymerisation involves the *reversible deactivation* of the growing polymer chains, therefore forming a reversible dormant species in the system. To be effective in controlling a radical polymerisation reactions, two necessary conditions have to be met.^{5, 13}

- 1 The equilibrium between the active and dormant species must be in favor of the dormant species to ensure that the overall concentration of propagating radicals remains low and that the rate of irreversible termination will be negligible to the apparent rate of polymerisation.
- 2 The rate of exchange between the dormant and active species must be faster than the rate of propagation to assure that all polymer chains have equal probability of adding monomer.

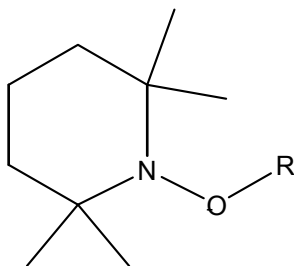
These prerequisites have been confirmed by Goto and Fukuda¹⁴ who investigated the kinetics of LFRP in 2004.

Considerable progress has been made in the last decade in the development of controlled free radical processes including the development of stable free radical polymerisation (SFRP), ATRP, and RAFT.^{3, 15-21} These processes all aim to simulate ideal living conditions in that irreversible termination and transfer reactions are replaced by reversible transfer reactions.

In this dissertation, the RAFT process will be used to synthesize block copolymers of ethylene glycol and styrene. The history and theory behind the RAFT process will therefore be discussed. SFRP and ATRP will be discussed briefly as controlled free radical processes, alternative to RAFT, that can be used to synthesize block copolymers with controlled molar mass and MMD.

4.3.1 Stable free radical polymerisation

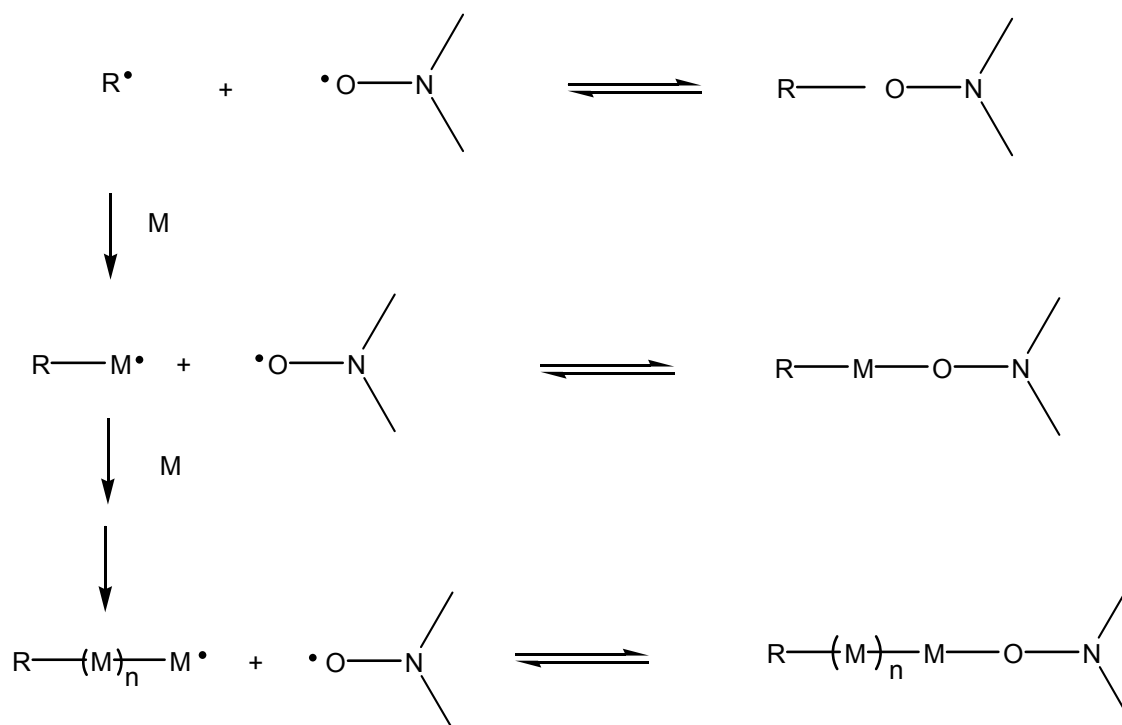
NMRP, also known as SFRP was first reported by Rizzardo *et al.*²² in 1984. Stable nitroxide radicals were used as deactivators in free radical polymerisation. The authors reported that nitroxides offered activation and deactivation rate constants superior to those of iniferters as utilised by Otsu and Yoshida.^{4, 5} High deactivation rates imply the rapid deactivation of growing chains, which implies that the equilibrium is shifted towards the dormant side. Georges *et al.*²³ investigated the polymerisation and copolymerisation of styrene in the presence of 2,2,6,6-tetramethylpiperidin-2-oxyl (TEMPO) and reported that low polydispersity polymers with well-defined structure could be obtained.



2,2,6,6-tetramethylpiperidin-2-oxyl (TEMPO)

Greszta and Matyjaszewski²⁴ reported on the TEMPO-mediated polymerisation of styrene and concluded that the polymerisation rates in the presence and absence of alkoxyamines were nearly the same. The presence of the alkoxyamines led to a reduction of the polydispersity of the formed products. Self-initiation was found to be responsible for maintaining a reasonable polymerisation rate. They also found that the polymerisation rate would have been three times lower without thermal initiation. They concluded that transfer to monomer occurred at elevated temperatures, with the effect thereof being significant for high molar mass polymers.

The key step in the mechanism of NMRP is the reversible coupling of the propagating radicals with nitroxides to form the corresponding alkoxyamines (dormant chains). This can be presented according to Scheme 4.3:²⁰



Scheme 4.3: Mechanism of NMRP.

where R^\bullet refers to the radical initiator and M to a vinyl monomer. Although being able to control chain growth in the reaction, there are certain disadvantages associated with the use of TEMPO: the availability of nitroxides (expensive or difficult to synthesize) and limitations in terms of monomer type (only certain monomers produce narrow MMD polymers). Side reactions also occur with the use of TEMPO and reactions normally have to be conducted at high temperatures.

In 1999, Chong *et al.*²⁰ reported on the use of imidazolidinone nitroxides in controlled radical polymerisation. They concluded that the imidazolidinone nitroxides offered the following advantages over the use of TEMPO:

- polymers with lower polydispersities were obtained,
- fewer side reactions took place,
- synthesis from readily available precursors, and
- non-volatility (TEMPO is odorous).

Chen *et al.*²⁵ produced PS-co-PEG copolymers with NMRP. They prepared a macro initiator by reacting tosylated MPEG with HO-TEMPO. The macro initiator, MPEG-TEMPO, was then used in the controlled radical polymerisation of styrene to produce a

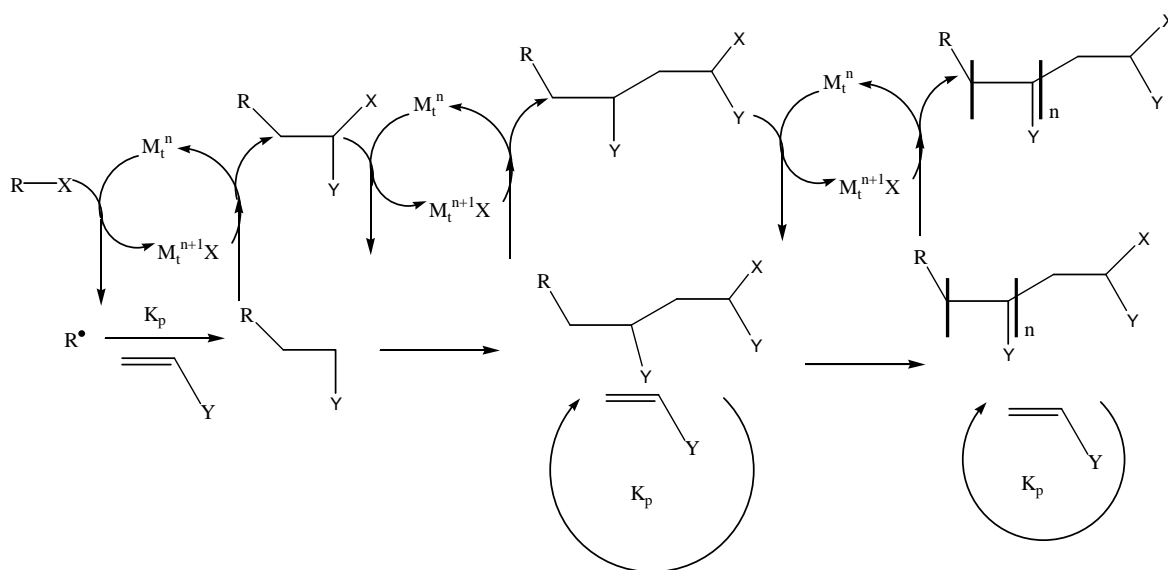
diblock copolymer. They reported that a large amount of PS homopolymer with narrow polydispersity also formed during the reaction.

One of the disadvantages of NMRP is that the process is limited to only a few monomers, such as styrene and acrylates.

Advances in NMRP have been reviewed by Hawker *et al.*²⁶ and Otsu and Matsumoto²⁷.

4.3.2 Atom transfer radical polymerisation

ATRP utilises a transition metal complex to deactivate a propagating radical by transfer of a halogen atom to the growing polymer chain end. During this process the metal ion complex is reduced. The most commonly used metal is copper, but nickel, palladium, ruthenium and iron are also suitable for the ATRP process. Typical halogens used are chlorides and bromides. The general mechanism for the process is as follows.²⁸



Scheme 4.4: Mechanism of ATRP.

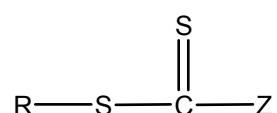
There are two disadvantages of the ATRP process: a) the removal of the catalyst is costly, and b) oxygen may have a large influence on the polydispersity of the product.

PS-co-PEG copolymers synthesized using ATRP have been reported by several authors.^{19, 29-31}

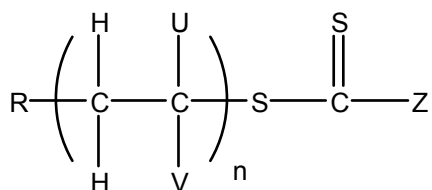
Recent advances in ATRP have been reviewed by Matyjaszewski *et al.*³² and Otsu *et al.*²⁷

4.3.3 Reversible addition fragmentation chain transfer polymerisation

The RAFT process was first patented by Le *et al.*,³³ it was claimed that if free radical polymerisations are carried out in the presence of a compound of the structure



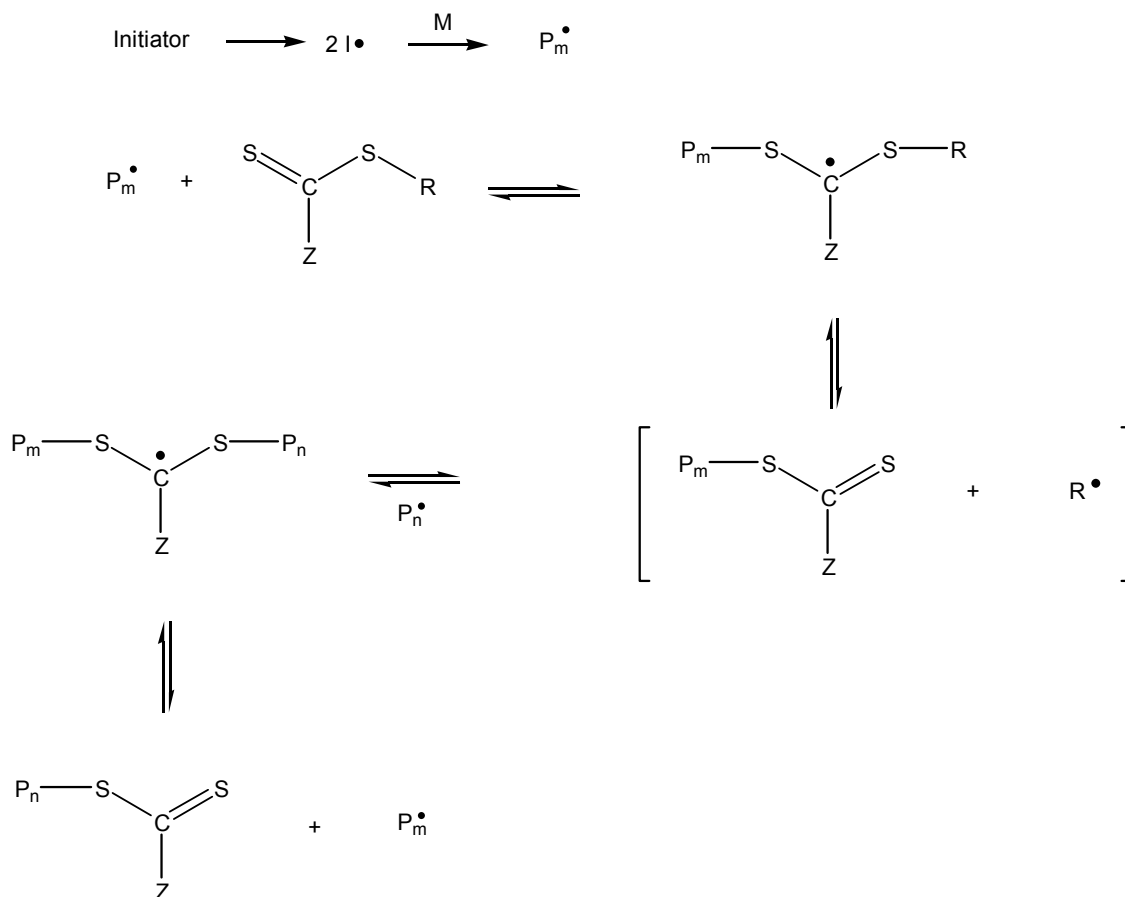
the resulting products will have controlled molar mass and narrow polydispersities. Rizzardo^{34, 35} further elaborated on this, and at the same time, patented the use of a similar type of compound, namely



for the LFRP of a variety of monomers. R must be a free radical leaving group and Z an activating group in order for the C=S bond to have a high reactivity towards free radical addition, while not slowing down the rate of fragmentation.¹⁸ The basic mechanism of the RAFT process entails initiation of a radical species, followed by the propagation step and subsequently a reversible transfer reaction.

4.3.3.1 The mechanism of RAFT

The basic mechanism of the RAFT process is given as follows:^{17, 36, 37}



Scheme 4.5: Mechanism of RAFT.

The process of reversible addition-fragmentation chain transfer involves the homolytic cleavage of a weak carbon-sulfur bond and the reversible endcapping of propagating polymer chains with a dithioester moiety. In the early stages of the polymerisation addition of the propagating radical (P_n^\bullet) to the dithio compound ($\text{S}=\text{C}(\text{Z})\text{SR}$), followed by the fragmentation of the intermediate radical, gives rise to a polymeric compound ($\text{P}_n\text{S}(\text{Z})\text{C}=\text{S}$) and a new radical (R^\bullet). Reaction of the newly formed radical (R^\bullet) with monomer will form a new propagating chain (P_m^\bullet). In the presence of monomer the equilibrium between the active propagating radicals (P_m^\bullet and P_n^\bullet) and the dormant dithio compound provides equal probability of growth for all chains.

It is of primary importance that the rate of transfer is higher than the rate of propagation. This ensures that only one monomer unit is incorporated into a growing chain before transfer takes place, which results in a system where all chains grow at a similar rate.²⁸ According to De Brouwer³⁸ the number of chains produced in a RAFT assisted polymerisation is given by the following equation:

$$[chains] = [RAFT] + 2f([I] - [I]_0) \quad (4.12)$$

where $[RAFT]$ is the concentration of the RAFT agent used and the second term of the equation refers to the amount of chains produced by initiator radicals. $([I] - [I]_0)$ refers to the concentration of the species that initiated, f is the initiator efficiency and, because each initiator molecule produces two radicals, the term has to be multiplied by a factor of two. The first term in the equation refers to the dormant chains, while the second term refers to the actively growing chains. It is important to maintain a high ratio of $[RAFT]:[Initiator]$, therefore $[dormant\ chains]:[active\ chains]$, to ensure that most of the polymer chains initiated remain in the dormant form. The lower the $[RAFT]:[Initiator]$ ratio, the higher the probability for uncontrolled termination reactions, which will lead to higher polydispersity. The number of chains in the polymerisation system will then not remain constant, which should be avoided. In the event of having a system where the rate of transfer to RAFT agent is higher than the propagation rate of the reaction, and the $[RAFT]:[Initiator]$ ratio is high, it is possible to produce polymers with a narrow MMD (low polydispersity).

In 2000 Moad *et al.*¹⁵ reported on a) the livingness of RAFT, b) the factors influencing the activity of the RAFT agent, and c) the rate of RAFT polymerisation vs. conventional free radical polymerisation. The investigation was done by studying the thermal polymerisation of styrene in the presence of cumyl dithiobenzoate. The obtained results can be summarised as follows:¹⁵

- 1 Size exclusion chromatography (SEC) results revealed that a decrease in the concentration of RAFT agent result in an increase in the polydispersity of the formed product. The number of dead polymer chains also indicated the livingness of the RAFT process.
- 2 It was found that the transfer rates varied according to the functionality of the R- and Z-groups in the RAFT agent, as well as the monomer used.
- 3 Many RAFT agents behave as ideal chain-transfer agents and rates of polymerisation similar to conventional free radical polymerisation (without RAFT agents) were found. Retardation occurred in some circumstances, which could have resulted from:
 - slow fragmentation of the intermediate species from the initial RAFT agent in the chain transfer step,

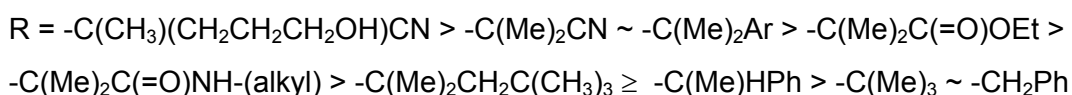
- slow fragmentation of the intermediate species formed by the polymeric RAFT agent in the chain equilibrium step,
- slow initiation of the radical R^\bullet ,
- preferential addition of the expelled radical to the RAFT agent rather than re-initiation of monomer,
- preferential addition of the propagating radical species P_n^\bullet to the RAFT agent rather than to monomer.

With a high transfer rate from growing chain to RAFT agent being a prerequisite for an effective RAFT polymerisation, it is important to determine what factors influence this transfer reaction. As stated previously in this section, the R- and Z-groups in the RAFT agent have been assigned specific characteristics by various authors. It is important that the Z-group is able to modify the activity of the thiocarbonyl group towards free radical addition and that the R-group is a good free radical leaving group.^{17, 18, 39}

4.3.3.2 Effect of the R-group

Chong *et al.*⁴⁰ investigated the efficiency of RAFT agents and extensively studied the influence of the variation in the R-group in terms of RAFT agent efficiency. The rate of addition to the dithiocarbonyl group should not be affected by the nature of the R-group since it is remote from the C=S double bond and not directly conjugated to it. The R-group is relevant in the partitioning of the intermediate species and to reinitiate polymerisation through the radical species R^\bullet . As in conventional chain transfer, the rate of reinitiation should be equal to or greater than the rate of propagation, to avoid retardation. In RAFT polymerisation it is therefore necessary to consider the rate of reinitiation in relation to the rate of reaction of R^\bullet with the polymeric RAFT agent. The properties of the R-group are determined by steric, polar and bond strength terms. More stable, electrophilic and bulky radicals are better leaving groups and will also contribute to the partitioning of R^\bullet between adding to polymeric RAFT and monomer (re-initiate), which has an effect on the consumption of RAFT agent.

For MMA polymerisation, control decreases as the R-group is changed in the following sequence:



For the polymerisation of styrene, it was found that all R-groups used were successful in assisting controlled polymerisation

R = -C(Me)₂Ph, -C(Me)₂CO₂Et, -C(Me)₂CH₂C(Me)₃

4.3.3.3 **Effect of the Z-group**

The Z-group modifies the reactivity of the thiocarbonylthio compound and the derived adduct radical.⁴¹ This groups therefore determines the rate of addition of free radical addition to the thiocarbonylthio compound, that is the rate of free radical addition to the C=S double bond. In general, the transfer coefficients of the RAFT agents decrease in the order dithiobenzoates > trithiocarbonates > dithioalkanoates > dithiocarbonates > dithiocarbamates. RAFT agents with electrophilic Z substituents with lone pairs directly conjugated to the C=S double bond have low transfer coefficients. Electron withdrawing groups on N and O (in particular groups able to delocalize the nitrogen lone pair in the case of dithiocarbamates) can sufficiently enhance the activity of the RAFT agents and modify the mentioned order.

The effectivity of the Z-group for the polymerisation of styrene is as follows:

Z= -Ph > -SCH₂Ph ~ SMe ~ N-pyrrolo >> OC₆F₅ > N-lactam > OC₆H₅ > O(alkyl) >> -N(alkyl)₂

Rizzardo *et al.*⁴² investigated the feasibility of conducting the RAFT process at room temperature. At room temperature known RAFT agents retarded polymerisation due to the stability of the intermediate species. By decreasing the stability of the intermediate species, the equilibrium is shifted to increase the concentration of propagating polymer chains. In the study, the authors changed the Z-group from phenyl to benzyl, therefore the radical in the RAFT intermediate was changed from being in a sulfur benzylic position to a less stable disulfur alkyl position. It was therefore possible to produce polystyrene with narrow polydispersity. The authors also found that the experimental \bar{M}_n values correlated well with theoretically determined values.

4.3.3.4 **Advantages of the RAFT process**

The RAFT process has certain advantages over other controlled free radical processes (NMRP and ATRP). The primary advantage that it affords is the ability to conduct polymerisation reactions in conditions similar to conventional free radical polymerisation.

This method of LFRP is therefore more robust than SFRP and ATRP in terms of reaction conditions. The RAFT process can also be employed to polymerise a wide range of monomers, where NMRP is restricted to only a few monomers. In terms of industrial applicability, it is also possible to employ the RAFT process in emulsion polymerisation.⁴³

⁴⁴ In the RAFT process it is also not necessary to remove the catalyst (as with the metal compounds in ATRP) from the products formed.

4.4 References

1. Colombani, D., Chain-growth control in free radical polymerisation, *Progress in Polymer Science*, **1997**, 22, 1649-1720.
2. Rosen, S. L., Fundamental principles of polymeric materials, *Wiley Interscience, United States of America*, **1993**.
3. Otsu, T., Iniferter concept and living radical polymerisation, *Journal of Polymer Science: Part A: Polymer Chemistry*, **2000**, 38, 2121-2136.
4. Otsu, T. and Yoshida, M., Role of initiator-transfer agent-terminator (iniferter) in radical polymerisation: polymer design by organic disulfides as iniferters, *Makromolekulare Chemie, Rapid Communication*, **1982**, 3, 127-132.
5. Otsu, T. and Yoshida, M., A model for living polymerisation, *Makromolekulare Chemie, Rapid Communication*, **1982**, 3, 133-140.
6. Darling, T. R., Davis, T. P., Fryd, M., Gridnev, A. A., Haddleton, D. M., Ittel, S. D., Matheson, R. R., Moad, G. and Rizzardo, E., Living polymerisation: Rationale for uniform terminology, *Journal of Polymer Science: Part A: Polymer Chemistry*, **2000**, 38, 1706-1708.
7. Greszta, D., Mardara, D. and Matyjaszewski, K., "Living" radical polymerisation. 1. Possibilities and limitations, *Macromolecules*, **1994**, 27, 638-644.
8. Odian, G. G., Principles of polymerization, *3rd Edition*, **1991**, Wiley Interscience, New York, 293-296.
9. Haddleton, D. M., Kukulj, D., Duncalf, D. J., Heming, A. M. and Shooter, A. J., Low-temperature living "radical" polymerisation (atom transfer polymerisation) of methyl methacrylate mediated by copper (I) N-alkyl-2-pyridylmethanimine complexes, *Macromolecules*, **1998**, 31, 5201-5205.
10. Penczek, S., Kubisa, P. and Szymanski, R., On diagnostic criteria for livingness of polymerisations, *Makromolekulare Chemie, Rapid Communication*, **1991**, 77-80.

11. Penczek, S., Terminology of kinetics, thermodynamics, and mechanisms of polymerisation, *Journal of Polymer Science: Part A: Polymer Chemistry*, **2002**, 40, 1665-1676.
12. Quirck, R. P. and Lee, B., Experimental criteria for living polymerisations, *Polymer International*, **1992**, 27, 359-367.
13. Madruga, E. L., From classical to living/controlled statistical free radical copolymerisation, *Progress in Polymer Science*, **2002**, 27, 1879-1924.
14. Goto, A. and Fukuda, T., Kinetics of living free radical polymerisation, *Progress in Polymer Science*, **2004**, 29, 329-385.
15. Rizzardo, E., Thang, S., Moad, G., Chiefari, J., Chong, Y. K., Krstina, J., Mayadunne, R. T. A. and Postma, A., Living free radical polymerisation with reversible addition-fragmentation chain transfer, *Polymer International*, **2000**, 49, 993-1001.
16. Boutevin, B., From telomerisation to living radical polymerisation, *Journal of Polymer Science: Part A: Polymer Chemistry*, **2000**, 38, 3235-3243.
17. Rizzardo, E., Chiefari, J., Chong, Y. K., Ercole, F., Krstina, J., Jeffery, J., Le, T. P. T., Mayadunne, R. T. A., Meijs, G. F., Moad, C. L., Thang, S. and Moad, G., Tailored polymers by free radical processes, *Macromolecular Symposia*, **1999**, 143, 291-307.
18. Chiefari, J., Chong, Y. K., Ercole, F., Krstina, J., Jeffery, J., Le, T. P. T., Mayadunne, R. T. A., Meijs, G. F., Moad, C. L., Moad, G., Rizzardo, E. and Thang, S., Living free radical polymerisation by reversible addition-fragmentation chain transfer: The RAFT process, *Macromolecules*, **1998**, 31, 5559-5562.
19. Jankova, K., Chen, X., Kops, J. and Batsberg, W., Synthesis of amphiphilic PS-*b*-PEG-*b*-PS by atom transfer radical polymerisation, *Macromolecules*, **1998**, 31, 528-541.
20. Chong, Y.-K., Ercole, F., Moad, G., Rizzardo, E. and Thang, S., Imidazolidinone nitroxide-mediated polymerisation, *Macromolecules*, **1999**, 32, 6895-6903.
21. Velichkova, R. S. and Christova, D. C., Amphiphilic polymers from macromonomers and telechelics, *Progress in Polymer Science*, **1995**, 20, 819-887.

22. Rizzardo, E., Solomon, D. H. and Cacioli, P., *US Patent*, **1985**, 4581429, *Chemical Abstracts* **1985**, 102:221335q.
23. Georges, M. K., Veregin, R. P. N., Kazmaier, P. M. and Hamer, G. K., Narrow molecular weight resins by a free radical polymerisation process, *Macromolecules*, **1993**, 26, 2987-2988.
24. Greszta, D. and Matyjaszewski, K., Mechanism of controlled/"living" radical polymerisation of styrene in the presence of nitroxyl radicals. Kinetics and simulation, *Macromolecules*, **1996**, 29, 7661-7670.
25. Chen, X., Gao, B., Kops, J. and Batsberg, W., Preparation of polystyrene-poly(ethylene glycol) diblock copolymer by 'living' free radical polymerisation, *Polymer*, **1998**, 39, 911-915.
26. Hawker, C. J., Bosman, A. W. and Harth, E., New polymer synthesis by nitroxide mediated living radical polymerisations, *Chemical Reviews*, **2001**, 101, 3661-3688.
27. Otsu, T. and Matsumoto, A., Controlled synthesis of polymers using the iniferter technique: developments in living radical polymerisation, *Advances in Polymer Science*, **1998**, 136, 77-129.
28. McLeary, J. B., Reversible addition-fragmentation transfer polymerisation in heterogeneous aqueous media, *PhD dissertation, University of Stellenbosch*, **2004**.
29. Reining, B., Keul, H. and Hocker, H., Chloro-telechelic poly(ethylene oxide)s as initiators for the atom transfer radical polymerisation (ATRP) of styrene and methyl methacrylate: Structural features that affect the initiation efficiency, *Polymer*, **1999**, 40, 3555-3563.
30. Francis, R., Taton, D., Logan, J. L., Masse, P., Gnanou, Y. and Duran, R. S., Synthesis and surface properties of amphiphilic star-shaped dendrimer-like copolymers based on PS core and PEG corona, *Macromolecules*, **2003**, 36, 8253-5259.
31. Neugebauer, D., Zhang, Y., Pakula, T., Sheiko, S. S. and Matyjaszewski, K., Densely-grafted and double-grafted PEO brushes via ATRP. A route to soft elastomers, *Macromolecules*, **2003**, 36, 6746-6755.

32. Matyjaszewski, K. and Xia, J., Atom transfer radical polymerisation, *Chemical Reviews*, **2001**, 101, 2921-2990.
33. Le, T., Moad, G., Rizzardo, E. and Thang, S., Polymerisation with living characteristics, *WO 98/01478*, **1998**.
34. Rizzardo, E., Synthesis of dithioester chain transfer agents and the use of bis(thioacyl) disulfides or dithioesters as chain transfer agents, *WO 99/05099*, **1998**.
35. Chiefari, J., Mayadunne, R. T. A., Moad, G., Rizzardo, E. and Thang, S., Polymerisation process with living characteristics and polymers made therefrom, *WO 99/31144*, **1998**.
36. Barner-Kowollik, C., Quinn, J. F., Morsley, D. R. and Davis, T. P., Modeling the reversible addition-fragmentation chain transfer process in cumyl dithiobenzoate-mediated styrene homopolymerisations: Assessing the rate coefficients for the addition-fragmentation equilibrium, *Journal of Polymer Science: Part A: Polymer Chemistry*, **2001**, 39, 1353-1365.
37. Goto, A., Sato, K., Tsujii, Y., Fukuda, T., Moad, G., Rizzardo, E. and Thang, S., Mechanism and kinetics of RAFT-based living radical polymerisations of styrene and methyl methacrylate, *Macromolecules*, **2001**, 34, 402-408.
38. De Brouwer, H., RAFT memorabilia: living radical polymerisation in homogeneous and heterogeneous media, *PhD dissertation, Eindhoven*, **2001**.
39. Chong, Y.-K., T.P.T., L., Moad, G., Rizzardo, E. and Thang, S., A more versatile route to block copolymers and other polymers of complex architecture by living radical polymerisation: The RAFT process, *Macromolecules*, **1999**, 32, 2071-2074.
40. Chong, Y.-K., Krstina, J., Le, T. P. T., Moad, M., Postma, A., Rizzardo, E. and Thang, S., Thiocarbonylthio compounds (S=C(Z)S-R) in free radical polymerisation with reversible addition-fragmentation chain transfer (RAFT polymerisation). Effect of the free radical leaving group R, *Macromolecules*, **2003**, 36, 256-2272.
41. Chiefari, J., Mayadunne, R. T. A., Moad, C. L., Moad, G., Rizzardo, E., Postma, A., Skidmore, M. A. and Thang, S., Thiocarbonylthio compounds (S=C(Z)S-R) in free radical polymerisation with reversible addition-fragmentation chain transfer (RAFT polymerisation). Effect of the activating group Z, *Macromolecules*, **2003**, 36, 2273-2283.

42. Rizzardo, E., Thang, S., Moad, G., Chong, Y.-K., T.P.T., L., Quirck, R. P. and Davis, T. P., Ambient temperature reversible addition-fragmentation chain transfer polymerisation, *Chemical Communications*, **2001**, 1044-1045.

43. Monteiro, M. J. and de Barbeyrac, J., Free radical polymerisation of styrene in emulsion using reversible addition-fragmentation chain transfer agent with a low transfer constant: Effect of rate, particle size, and molecular weight, *Macromolecules*, **2001**, 34, 4416-4423.

44. Farmer, S. C. and Patten, T. E., (Thiocarbonyl- α -thio)carboxylic acid derivatives as transfer agents in reversible addition-fragmentation chain transfer polymerisations, *Journal of Polymer Science: Part A: Polymer Chemistry*, **2002**, 40, 555-563.

Chapter 5

PEG-b-PS block copolymer synthesis and characterisation

5.1 Introduction

Recent advances in controlled radical polymerisations indicate a tendency towards the use of macro RAFT agents for the synthesis of PEG-b-PS block copolymers (Chapter 4). The end-functionalised macro monomers are converted to form nuclei for polymerisation by controlled/“living” radical polymerisation. In this study, the main aim is to determine the influence of the hydrophilic:hydrophobic ratio (A:B, where A refers to the hydrophilic segment and B refers to the hydrophobic segment of the copolymer) on the physical properties of the polymerisation products. It is therefore important that good control be exercised in the synthesis of these polymers. In order to minimise the amount of variables regarding the A:B ratio of the block copolymer, the following general method of synthesis is proposed:

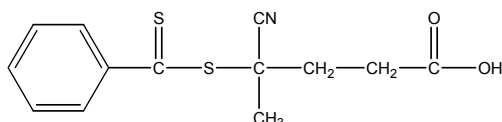
- 1 use a known mono-functional PEG as starting material for the synthesis of a macro RAFT agent (hydrophilic segment, A),
- 2 transform this mono-functional PEG into the required macro RAFT agent,
- 3 use the macro RAFT agent to polymerise the styrene block of the copolymer (hydrophobic segment, B).

By using hydroxy-terminated PEG and transforming the hydroxyl group to a suitable ion/radical, the PS segment of the polymer can be grown onto the macro RAFT agent. Using a mono-functional PEG results in the formation of a di-block copolymer (AB block copolymer), therefore further limiting the number of variables. A di-functional PEG will result in the formation of a di-functional macro RAFT agent, which will in turn lead to the formation of a tri-block copolymer (BAB block copolymer). This will result in the addition of more variables to the process of controlling the structure of the copolymer and it will therefore be more difficult to draw conclusions on the A:B ratio of the copolymer. By starting with a known hydrophilic macro monomer, the A:B ratio is controlled by controlling the length of the hydrophobic segment of the polymer.

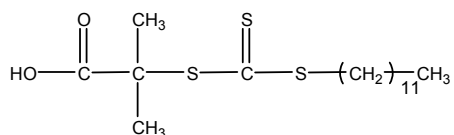
In Chapter 4 the relevance of the RAFT polymerisation process for the synthesis of PEG-b-PS AB type block copolymers is stated. By making use of MPEG, a suitable RAFT agent will be one with functionality that is able to react with the hydroxy-group of MPEG, to form the desired macro RAFT agent. A suitable RAFT agent should therefore be able to react with MPEG to form the MPEG-macro RAFT agent under conditions that will not destroy the RAFT functionality. Reacting the hydroxy group of MPEG with an acid-functional RAFT agent will lead to the formation of a desired macro RAFT agent for the formation of a PEG-b-PS block copolymer.

The following acid-functional RAFT agents were selected as targets for the formation of macro RAFT agents for copolymer synthesis:

4-Cyano-4-[(thiobenzoyl) sulfanyl] valeric acid (CVADTB)



Dodecyl isobutyric acid trithiocarbonate (DIBTC)



The following general steps were performed, using each RAFT agent, in copolymer synthesis:

- 1 RAFT agent synthesis and characterisation;
- 2 homopolymerisation with styrene and characterisation of polymer formed;
- 3 MPEG macro RAFT agent synthesis and characterisation; and
- 4 copolymerisation and characterisation.

5.2 Polymer characterisation

5.2.1 Size exclusion chromatography

Molar mass and the distribution thereof were determined by SEC.

Samples for SEC analysis were prepared according to the following procedure:

- A sample of 30 mg dried polymer product was dissolved in 30 mL THF (HPLC grade).
- The solution was filtered through a 0.45 μm nylon filter.
- The volume of the injected sample was 100 μL .

Analyses were conducted with a SEC system comprising

- A Waters 610 Fluid Unit.
- A Waters 717_{plus} Autosampler.
- A Waters 600E System Controller.
- The oven temperature was set at 30°C.
- Millenium³²® software was used for data acquisition and analysis (calibrated with narrow PS standards ranging from 800 to 2x10⁶ g/mol).

Mobile phase:

- THF (HPLC grade). Flow rate: 1.00 mL/min

Columns:

- Precolumn: PLgel 5 μm Guard
- Two Mixed-C columns: PLgel 5 μm

Detector:

- Waters 410 Differential Refractometer at 30°C

5.2.2 Two-dimensional chromatography

SEC is very effective in giving relative value in terms of the molar mass and the MMD of a polymeric material. However, one of the disadvantages of conventional SEC of polymers with complex architecture, such as blocks, grafts, etc., is the fact that SEC is based solely on the separation of polymer chains in terms of the hydrodynamic volume of the polymer chains in the eluent system being used. Polymers with different chemical compositions as well as different molar masses might have similar hydrodynamic volumes in a specific eluent and therefore have the same elution time within the system. Baran *et al.*¹ reported that, for example, in adsorption mode (THF-hexane, 40:60 wt%) ω -hydroxyl-PS of \bar{M}_n

10 000 g/mol and a non-functional PS standard with \bar{M}_n 30 000 g/mol are both eluted at the same retention time of 6 minutes. Conventional SEC therefore only give a relative value of molar mass based on the hydrodynamic size of the polymerisation product. Even with the correct selection of an eluent system, complete analysis of the different components within the product would not be possible in SEC analysis.

Further, copolymers are complex macromolecular systems, which, in addition to MMD, have to be characterised by a certain distribution in chemical composition. This complex molar mass chemical composition distribution of copolymers requires separation in more than one direction. Advances in the field of the analysis of block- and graft copolymers has led to advanced separation techniques like liquid chromatography at critical adsorption point (LC-CAP), eluent gradient liquid adsorption chromatography (LAC), and full adsorption-desorption with size exclusion chromatography (FAD/SEC).^{2, 3}

The principle of LC-CAP is the combination of exclusion and adsorption of polymeric molecules in an appropriate eluent system, including temperature and column packing. At the CAP macromolecules of a certain architecture and/or composition elute simultaneously, irrespective of their molecular size. To describe this phenomenon the term “chromatographic invisibility” is used, meaning that the chromatographic behaviour is not directed by the size but by the heterogeneities (chemical structure) of the macromolecules.⁴ These species are then “chromatographically invisible”, while other species present elute in the normal SEC mode according to their hydrodynamic volume. Although this technique is able to separate different species, there are some disadvantages associated with LC-CAP. With all “chromatically invisible” samples being eluted at once, the hydrodynamic size of these blocks remains undetermined. Furthermore, if the grafted chains in graft copolymers are made “invisible”, the homopolymer will most probably co-elute with a graft copolymer due to the similar hydrodynamic volumes of each species.

In LAC the sample is injected into an adsorptive column and flushed with an adsorption promoting liquid (adsorli). Molecules are therefore adsorbed at the entrance of the column. The eluent composition is gradually changed, introducing and gradually increasing the amount of a desorption promoting liquid (desorli). Molecules start to move along the column according to their chemical composition and not their hydrodynamic volume.

FAD/SEC was developed by Nguyen *et al.*³ to analyse multi-component polymer blends. In this process the macromolecules are fully adsorbed onto the column, followed by the stepwise selective desorption of the different components within the sample. Desorption of macromolecules is controlled by the control of the adsorli/desorli mixtures. Nguyen *et al.*³ reported on the analysis of the polymerisation products of styrene with polyethylene oxide methacraloyl-terminated macro monomer applying FAD/SEC and LAC approaches. According to the authors the complete separation of the graft copolymer according to its composition would be complicated with molar mass interference, as desorption of macromolecules from solid surfaces is by chemical structure as well as molar mass of the polymeric species. They stated that FAD/SEC is the method of choice for the separation of the graft copolymer from homopolymers when determining the amount and molecular characteristics of the homopolymers. It was reported that LAC separated the grafted products from the homopolymers, but did not give any information on the molar masses of the fractions. The authors concluded that LAC coupled with SEC was an appropriate procedure for the complete analysis of the components in the reaction mixture.

In 2000 Pasch reviewed hyphenated techniques in liquid chromatography with emphasis on the basics of two dimensional (2D) chromatography and the use of 2D chromatography to analyse complex macromolecular compounds.⁴ The combination of two selective analytical techniques is assumed to yield two-dimensional information on molecular heterogeneity. Of special interest is the combination of liquid chromatography at “critical conditions” (critical adsorption point, CAP) combined with SEC, where the sample to be analysed is first fractionated according to the chemical composition distribution. The different fractions can then be analysed by SEC according to molar mass and the MMD of each fraction. Applying this technique to AB-type block copolymers would entails that the separation be conducted under the critical conditions of either block A or block B. With the conditions corresponding to the critical conditions of homopolymer A, block A in the copolymer will be “chromatographically invisible”, and the block copolymer will be eluted with respect to the MMD of block B. Pasch concluded that gradient HPLC coupled to SEC yielded quantitative information on the chemical composition distribution and the MMD, while coupling LC CAP and SEC is useful for the analysis of functional homopolymers and block copolymers in terms of functional type distribution, MMD, and chemical composition MMD.

Baran *et al.*¹ used liquid chromatography at the **exclusion adsorption transition point** (LC-EATP), the so-called “critical conditions”, to separate PS, functional polystyrenes, PEOs

as well as their copolymers. Of particular interest is the separation of copolymers of PS and PEO of varying block lengths. The authors reported the use of THF-water as eluent system for this separation. The precise composition of the eluent mixture depends on the length of the different blocks in the copolymer. The authors tabled a range of critical mixtures employed in the analysis of the copolymers of PS and PEO. They concluded that LC-EATP is useful in separating block copolymers of PS and PEO under the “critical conditions” of PS.

With the limitations of SEC in the analysis of the obtained polymeric products, the following 2D chromatographic system was used in the analysis of the PS-b-PEG block copolymers:

Sample preparation:

- Samples were prepared by dissolving 20 mg of the corresponding product in 60 mL of a THF:water (90:10) mixture.

Chromatographic system:

- A modular chromatographic system comprising two chromatographs connected via one electrically-driven, eight-port injection valve (Valco) and two storage loops was used.
- Chromatograph 1 (first separation step): Waters 2690 separation module Alliance.
- Chromatograph 2 (second separation step): Waters 515 HPLC pump.
- The operation of the injection valve was controlled by PSS Win GPC7 software, which was used for data collection. Processing was performed by PSS Win GPC4. (Software from Polymer Standards Service, Mainz, Germany)

Mobile phase:

- Chromatograph 1: THF:water (90:10). Flow rate: 0.03 mL/min
- Chromatograph 2: THF. Flow rate: 4 mL/min

Columns:

- Chromatograph 1: Critical conditions for PS: Supelco Nucleosil C18 100 Å, 5 µm average particle size, 250 mm x 4.6 mm. Temperature: 30°C.

- Chromatograph 2: PSS SDV linear M, 5 μm average particle size, 50 mm x 20 mm.

Detector:

- Evaporative light scattering detector (ELSD) PL-ELS 1000 from Polymer Labs.

5.2.3 NMR spectroscopy

Samples were prepared for NMR analysis by dissolving 50 mg of the corresponding polymer in 0.6 ml deuterated chloroform (CDCl_3). The ^1H and ^{13}C NMR analyses were performed on a 300 MHz Varian VXR spectrometer equipped with a Varian magnet (7.0 T) operating at 300 MHz for ^1H and 75 MHz for ^{13}C analysis. The analyses were performed at 25°C. Standard pulse sequences were used for all spectra.

5.3 RAFT agent synthesis

5.3.1 Chemicals

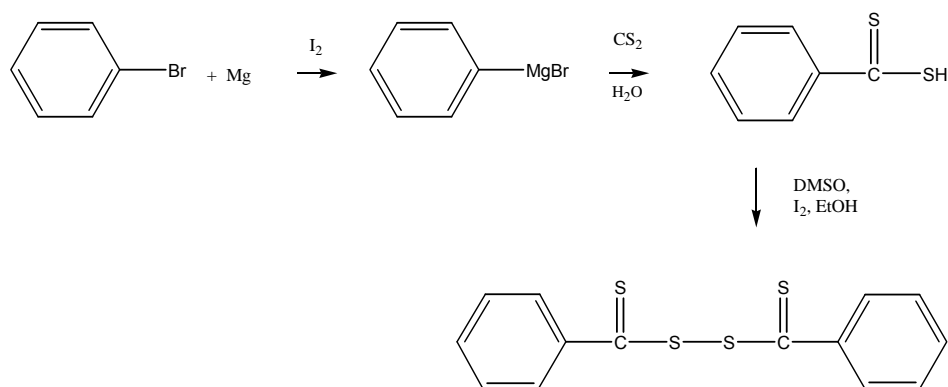
Azo bis (cyanovaleric acid) [2638-94-0] 75%(Sigma-Aldrich), 2,2' azo bis (isobutyronitrile) [78-67-1] (AIBN, Riedel de Haen), Aliquot 336 [5137-55-3] (Fluka), n-dodecyl mercaptan [112-55-0] 98%+ (Aldrich), diethyl ether [60-29-7] 99.5% (Merck), chloroform [67-66-3] 99% (Labchem), sodium hydroxide [1310-73-2] 50% solution (Aldrich), HCl [7647-010] 32% (ACE), bromobenzene [108-86-1] 99% (Aldrich), carbon disulfide (CS_2) [75-15-0] 99.9% (Aldrich), acetone [67-64-1] 99.5% (SAARChem), p-toluene sulphonic acid [98-59-9] 98.5%, (Sigma-Aldrich), carbon tetrachloride [56-23-5] (CCl_4) 99.9% (Aldrich), ethyl acetate [141-78-6] CP, isopropanol [67-63-0] CP, pentane [109-66-0] CP, heptane [142-82-5] CP (ACE), sodium hydroxide CP (SAARChem), THF [109-99-9] was distilled from LiAlH_4 [16853-85-3], iodine [7553-56-2] 99%(Aldrich), magnesium 98% [7439-95-4] (Aldrich), dichloromethane [75-09-2] (Aldrich), 4-(dimethyl amino) pyridine [1122-58-2] 99% (Aldrich), 1,3-dicyclohexylcarbodiimide [538-75-0] 99.9% (Fluka), methyl sulfoxide [67-68-5] 99.9% (Aldrich), poly(ethylene glycol) monomethyl ether [9004-74-7] (Aldrich).

Unless otherwise stated, all syntheses were carried out under anhydrous nitrogen atmosphere. CAS numbers for all chemicals used are given in parentheses.

5.3.2 Synthesis of 4-cyano-4-[(thiobenzoyl) sulfanyl] valeric acid

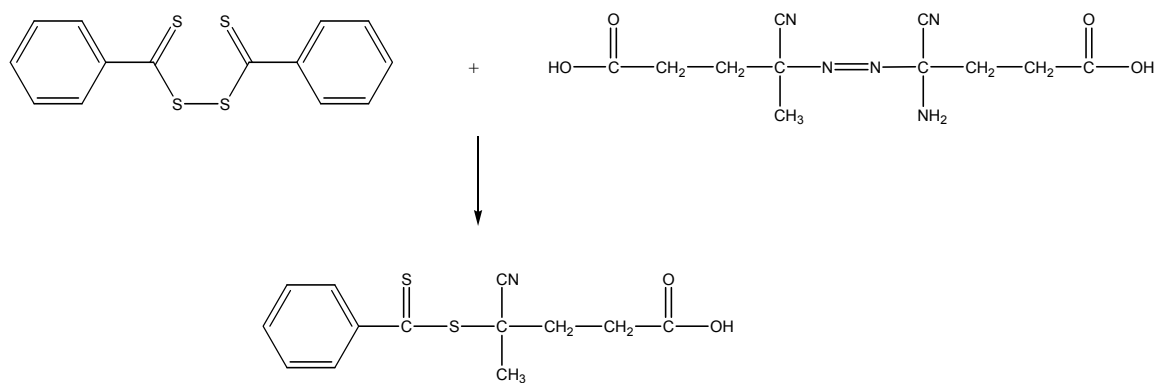
CVADTB was prepared according to the method as used by Rizzardo *et al.*^{5, 6} as follows:

Bromo-benzene (62.8 g, 0.4 mol) was reacted with magnesium metal (10.0 g, 0.411 mol) in the presence of iodine to form the resulting Grignard compound with THF (300 mL) was used as solvent. The reaction temperature was kept below 40°C with an ice bath. Carbon disulfide (30.5 g, 0.40 mol) was added to the reaction mixture, again keeping the reaction temperature below 40°C. Water was added slowly to neutralise the Grignard reagent, whereafter the magnesium salts were filtered from the solution. The water and THF was removed under vacuum, whereafter with product was acidified by slowly adding HCl. The acid was extracted by washing with diethyl ether, where after the ether was removed under vacuum. DMSO (62.5 g, 0.80 mol) and a catalytic amount of iodine were added in a medium of absolute ethanol. The solvent was then removed on a rotary evaporator to isolate the bis (thiobenzoyl) disulfide (Scheme 5.1).



Scheme 5.1: Synthesis of bis (thiobenzoyl) disulphide.

The CVADTB was synthesized by adding bis (thiobenzoyl) disulphide and azo bis [4-cyano valeric acid] (1:1 ratio) in ethyl acetate (Scheme 5.2). The reaction mixture was refluxed for 24 h at 85°C. The resulting product was purified by liquid chromatography using a silica gel column (Kieselgel 90) with ethyl acetate:hexane (2:3) as eluent. The concentrated product was crystallised and stored at 0°C.



Scheme 5.2: Synthesis of CVADTB.

The structure of CVADTB was confirmed by ^1H NMR as shown in Figure 5.1:

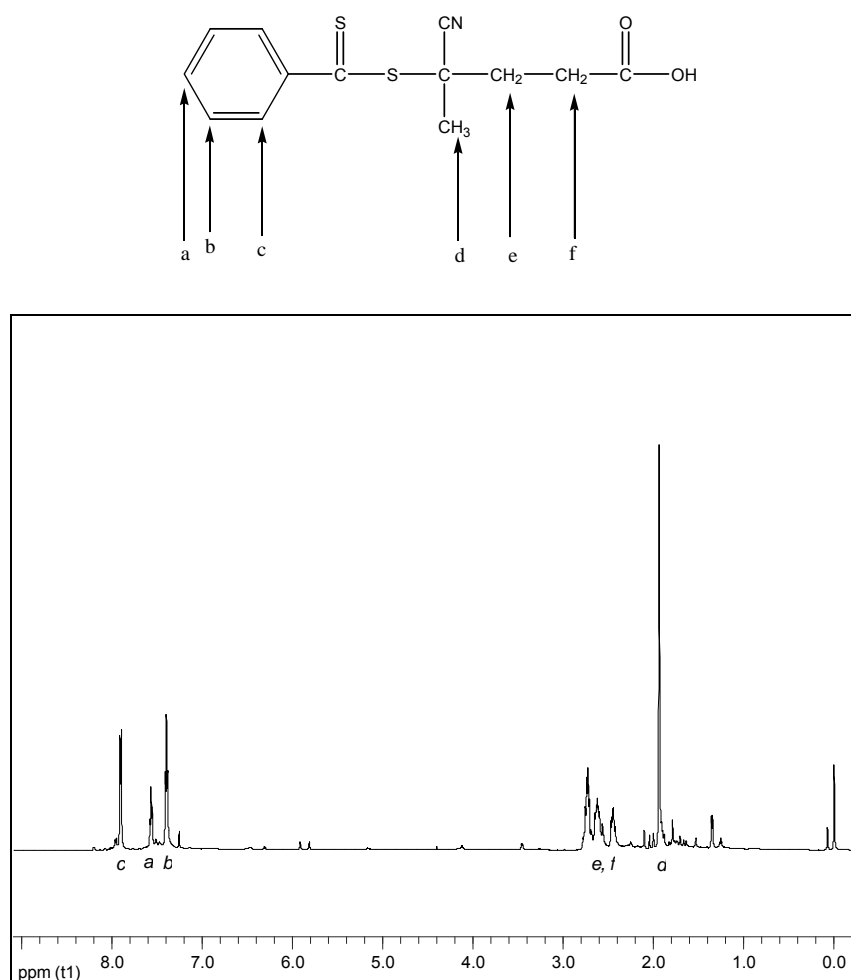


Figure 5.1: ^1H NMR spectrum of CVADTB.

Estimated purity >98%; impurities include trace water. ^1H NMR (CDCl_3) δ : 2.00, 3H, H_{methyl} ; 2.4-2.8, 4H, $\text{H}_{\text{methylene}}$; 7.5, 2H, H_{meta} ; 7.6, 1H, H_{para} ; 7.95, 2H, H_{ortho} .

The ^{13}C NMR of CVADTB is shown in Figure 5.2, of importance was the peak at 222 ppm, representing the C=S bond, the dithiocarbonyl functionality necessary for reversible addition-fragmentation chain transfer reactions.

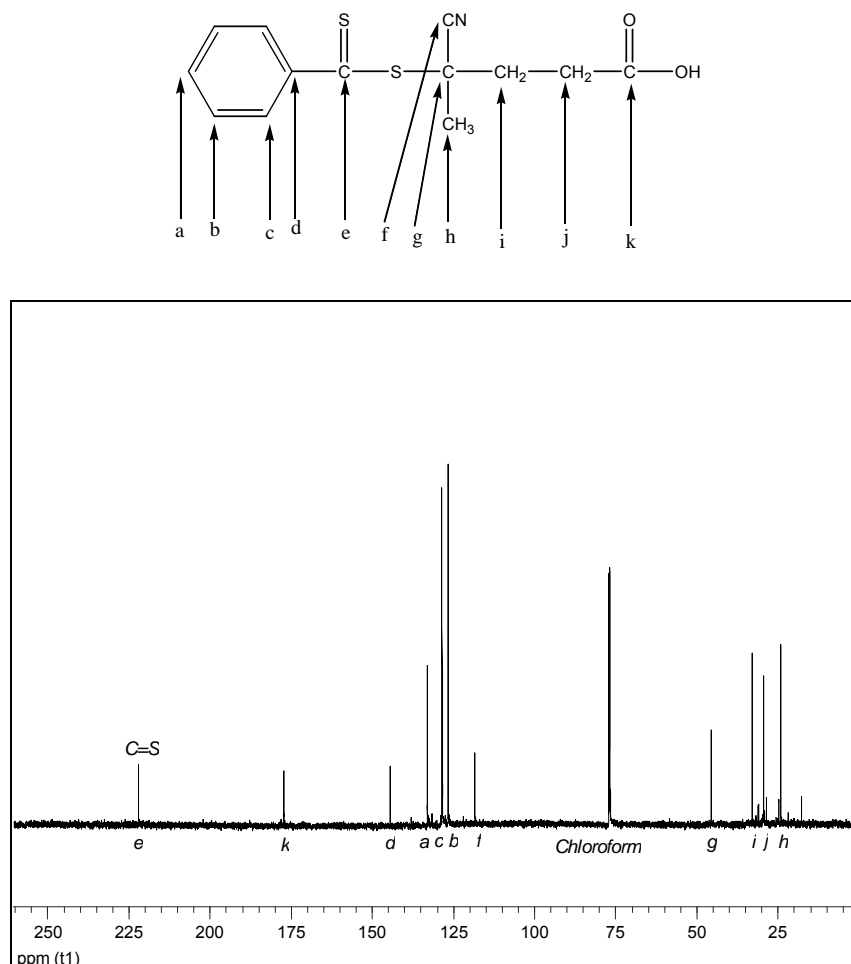
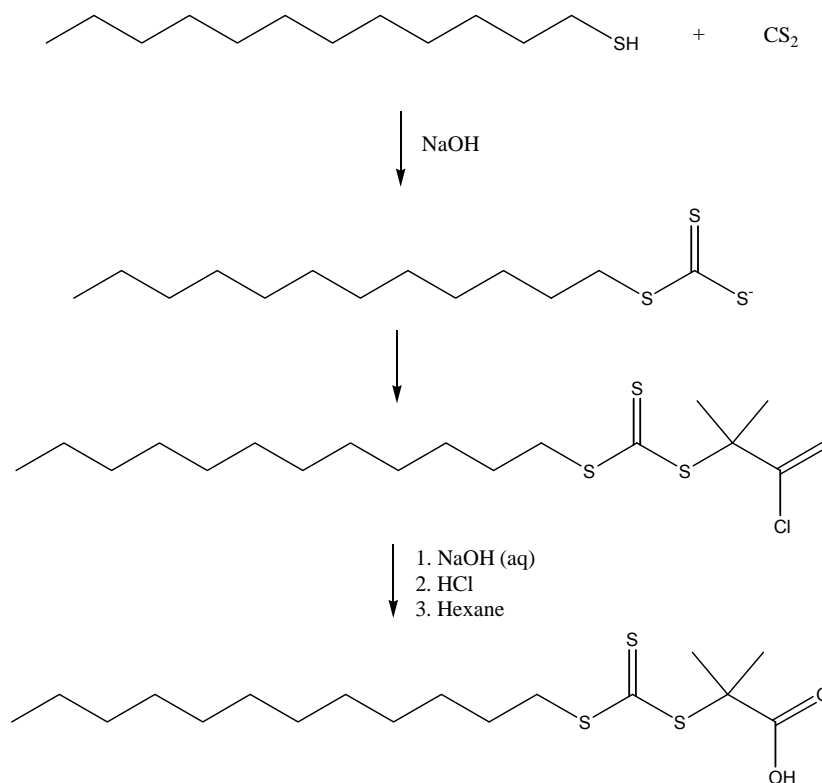


Figure 5.2: ^{13}C NMR spectrum of CVADTB.

5.3.3 Synthesis of S-1-dodecyl-S'- (α , α' dimethyl - α'' -acetic acid) trithiocarbonate

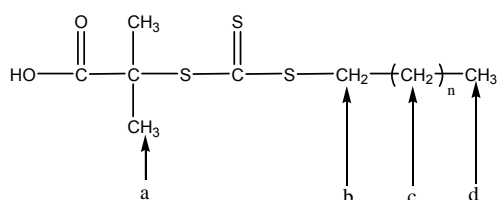
DIBTC was synthesised according to the method of Lai *et. al.*⁷ (Scheme 5.3). 1-Dodecanthiol (80 g, 0.4 mol), acetone (192 g, 3.3 mol) and Aliquot 336 (6.5 g, 0.016 mol) were mixed in a reactor and cooled in an ice bath. Sodium hydroxide (50%) (33.5 g, 0.4 mol) was first added dropwise, followed by a carbon disulfide solution (30 g, 0.4 mol) (40% in acetone), again dropwise. The reaction mixture turned yellow in colour and the viscosity increased. Chloroform (72 g, 0.6 mol) was added to the solution, followed by the addition of 50% sodium hydroxide (160 g, 2 mol). The reaction was stirred overnight. The

stirred solution was added to water (600 mL) and stirred vigorously to evaporate any remaining acetone, while adding hydrochloric acid. The solid product was collected after filtering, using a Buchner funnel, and stirring in isopropanol. The isopropanol solution was concentrated and the product was recrystallised from hexane to yield S-1-dodecyl-S'- (α , α' dimethyl - α'' -acetic acid) trithiocarbonate.



Scheme 5.3: Synthesis of DIBTC

Purity was estimated to be 99% by ^1H NMR. ^1H NMR (CDCl_3) δ : 0.99, 3H, $\text{H}_{\text{terminalmethyl}}$; 1.37-1.47, 20H, H_{alkyl} ; 1.75, 6H, H_{methyl} ; 3.42, 2H, $\text{H}_{\text{methylene}}$; 13.05, 1H, H_{acid} .



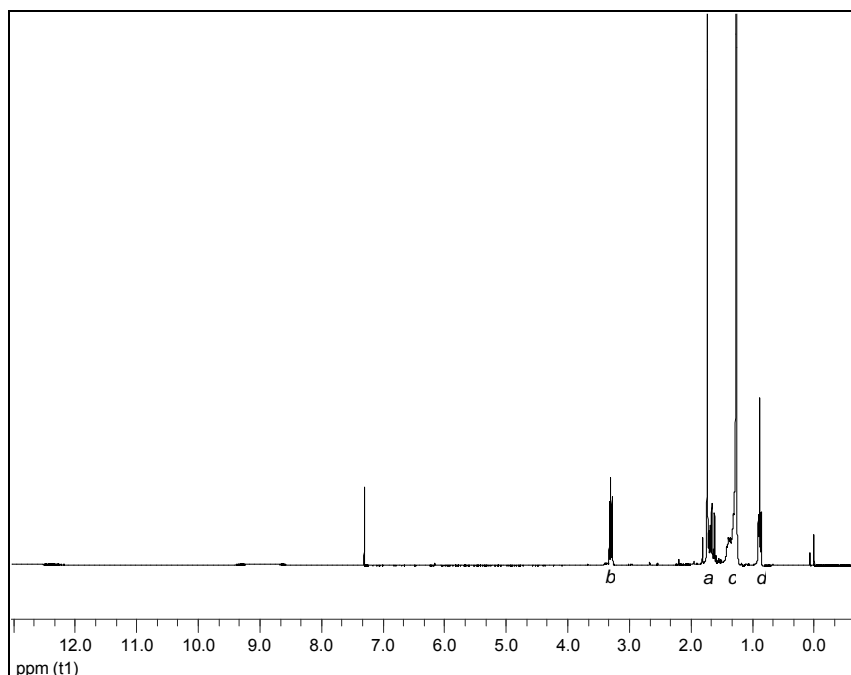


Figure 5.3: ¹H NMR spectrum of DIBTC.

5.3.4 Synthesis of MPEG dithiobenzoate macro RAFT agent

The MPEG dithiobenzoate macro RAFT agents were synthesised according to two different methods, that of De Brouwer *et al.*⁸ (Method 1) and Shi *et al.*⁹ (Method 2)

Typical quantities of the different reagents used in the two methods are shown in Table 5.1:

Table 5.1: Formulations for the synthesis of different MPEG-macro RAFT agents

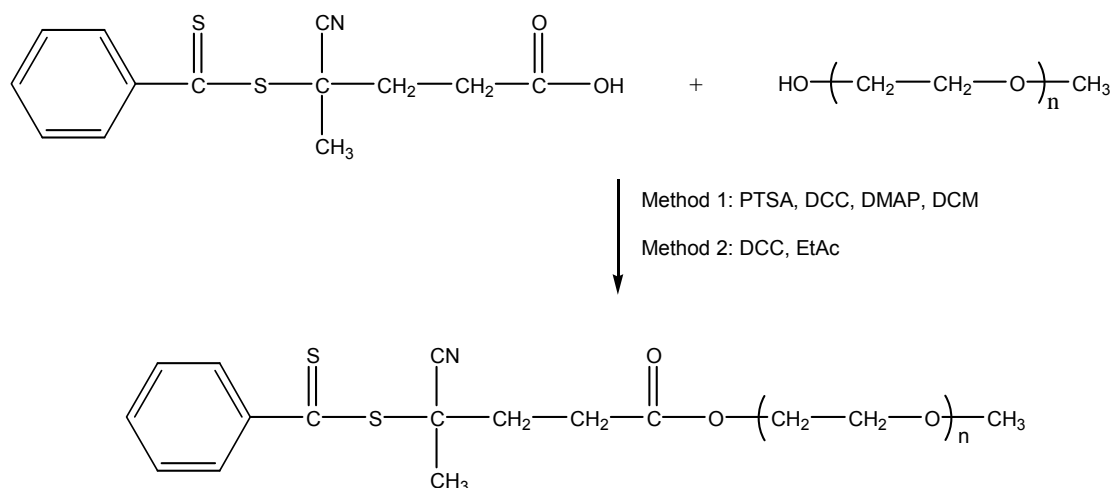
Reagent	Method 1		Method 2	
	Mass (g)	Millimoles	Mass (g)	Millimoles
MPEG*		8.0		7.5
CVADTB	2.23	8.0	2.79	10.0
<i>p</i> -Toluene sulphonic acid	0.30	1.6		
Dicyclo hexyl carbodiimide	3.90	19.0	3.90	19.0
Dimethyl amino pyridine	0.29	2.4		
Solvent				
Dichloromethane	200 mL			
Ethyl acetate			250 mL	
* The mass of MPEG varied according to the molar mass of the MPEG used.				

Method 1

The MPEG, *p*-toluene sulphonic acid (PTSA), 4-(dimethyl amino) pyridine (DMAP) and 1,3-dicyclohexylcarbodiimide (DCC) were dissolved in dichloromethane (DCM). The CVADTB was dissolved in DCM and slowly added to the reaction mixture. The temperature of the reaction was then raised to 30°C and the reaction was allowed to continue for 48 h. Upon completion, the product was filtered and washed with water. The product was dried over magnesium sulphate, filtered, and the excess DCM was removed under reduced pressure.⁸

Method 2

MPEG was dissolved in Ethyl Acetate (EtAc). CVABDTB and DCC were added. The reaction mixture was stirred for 24 h at 30°C where after the precipitated dicyclo hexyl urea was removed by filtering. The remaining solution was put in a refrigerator at 0°C for 24 h, whereby the product crystallised out of the solution. The product was removed by filtration.⁹



Scheme 5.4: MPEG-CVADTB macro RAFT agent synthesis.

Attempts to purify the MPEG macro RAFT agents using liquid chromatography were unsuccessful. Because the esterified product was not purified, it was not possible to determine the yield of the esterification reaction by ^1H NMR (Figure 5.4). Due to the nature of the macro RAFT agent, the crude product was used without further purification. De Brouwer *et al.*⁸ also reported the use of the crude esterification product in copolymer synthesis.

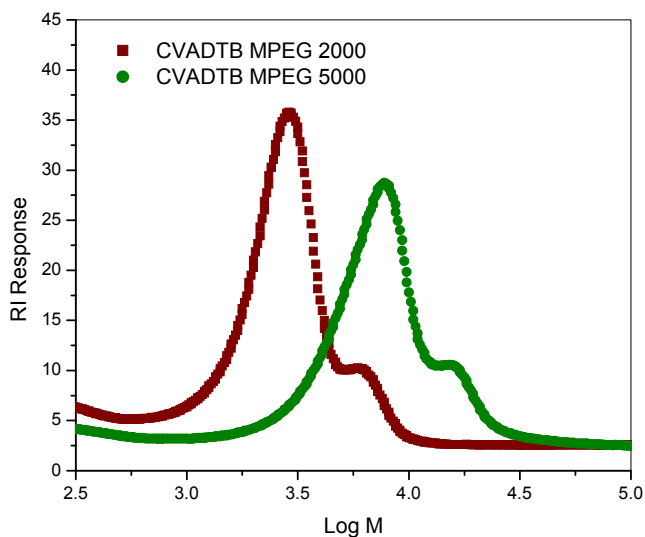


Figure 5.4: Graph of RI response vs. $\log M$ for SEC analysis of CVADTB MPEG macro RAFT agents.

SEC results show the existence of two different species obtained from RAFT macro initiator synthesis. Both products (CVADTB MPEG 2000 and CVADTB MPEG 5000) showed similar results: a large fraction of the esterified product, as well as a smaller fraction of a product with a molar mass double of the starting product. This second peak was attributed to a coupling reaction of two MPEG molecules during the esterification process.

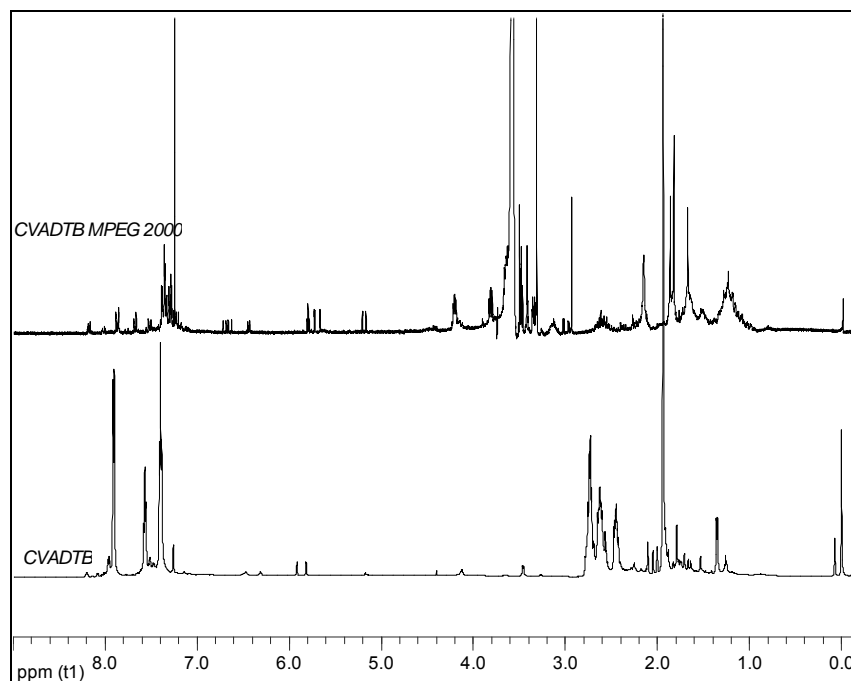


Figure 5.5: ^1H NMR spectrum of CVADTB MPEG 2000.

Due to the high intensity of the CH_2 peak of MPEG in the ^{13}C NMR spectrum of the MPEG macro RAFT agents, the low intensity and low number of $\text{C}=\text{S}$ carbons relative to the CH_2 carbons of MPEG, it was not possible to verify the structure of the products obtained in the esterification reactions (Figure 5.6).

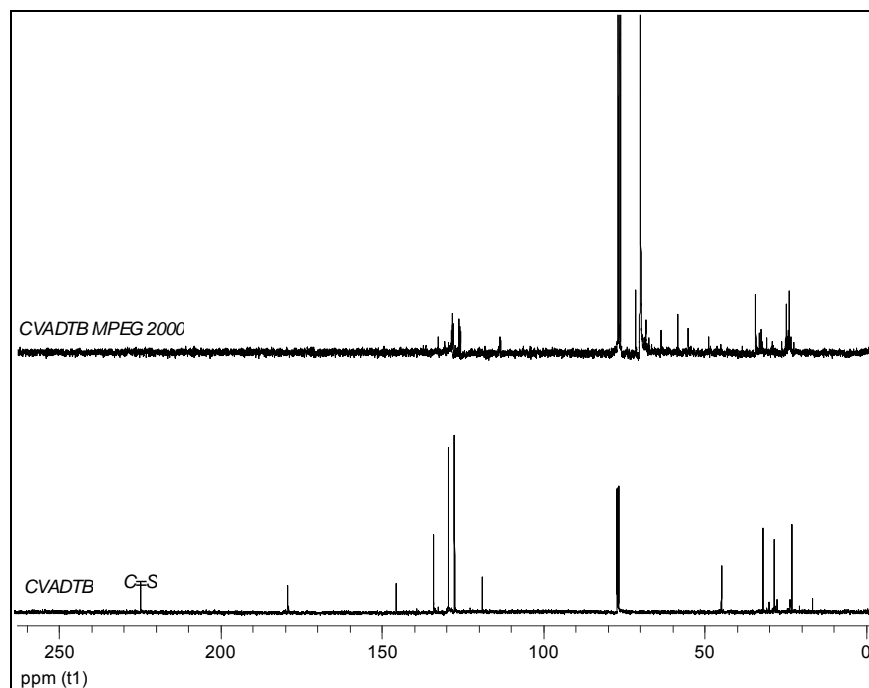
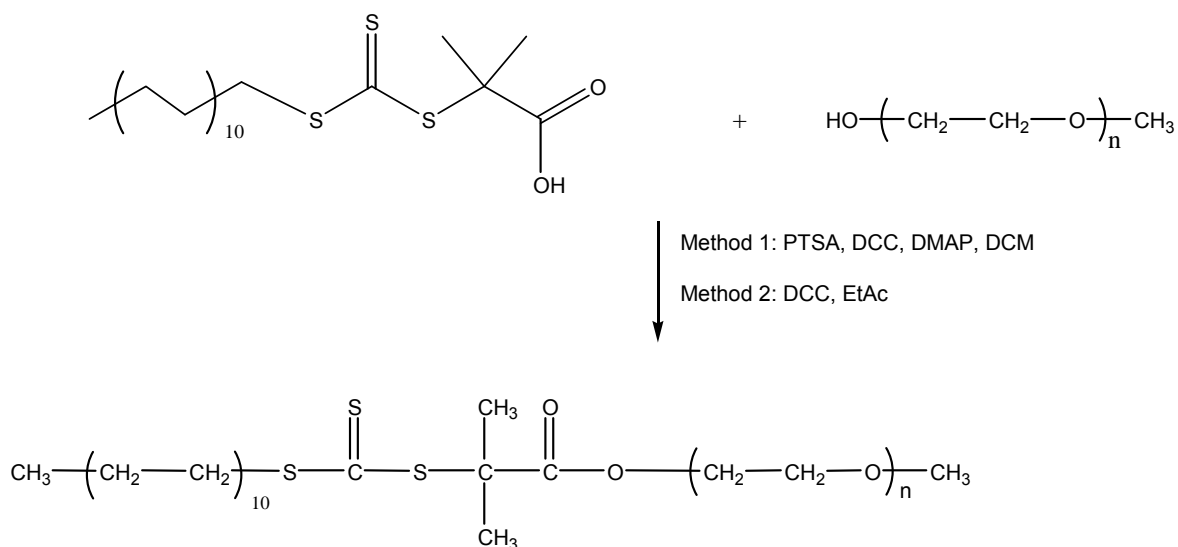


Figure 5.6: ^{13}C NMR of CVADTB MPEG 2000 macro RAFT agent.

For the purpose of this investigation, Method 1 was used in the synthesis of MPEG macro RAFT agents. In all cases where Method 2 was employed, it is specifically stated.

5.3.5. Synthesis of MPEG-tri-thiocarbonate macro RAFT agent.

The MPEG-tri-thiocarbonate macro RAFT agents were prepared under similar conditions as described in Section 5.3.4



Scheme 5.5: MPEG-DIBTC macro RAFT agent synthesis.

Figure 5.7 shows that the ^1H NMR spectrum of DIBTC MPEG 2000 macro RAFT agent is similar to that of DIBTC. As the esterified product was used without purification, it was expected that certain impurities would be detected in the ^1H NMR data (Figure 5.7).

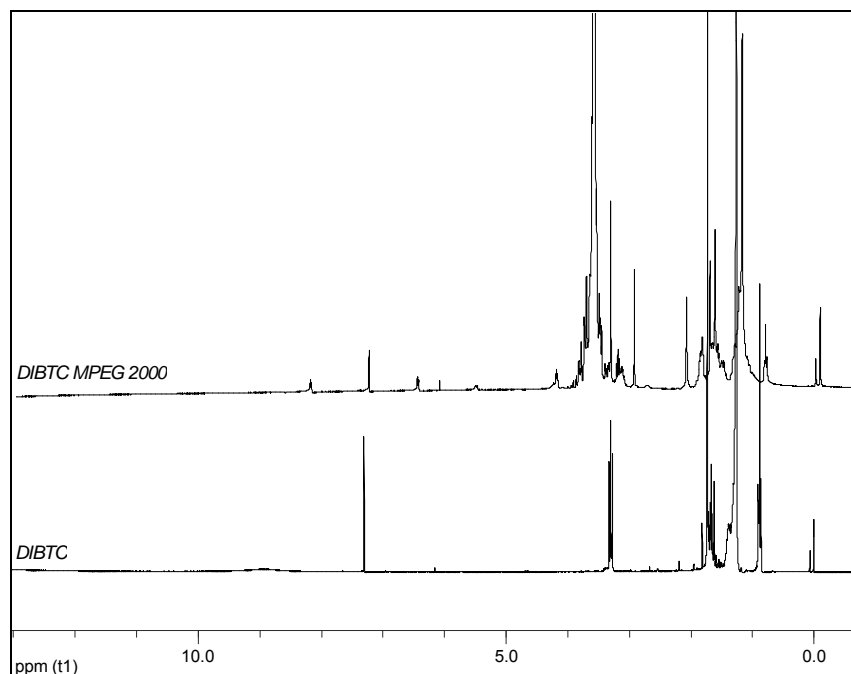


Figure 5.7: ^1H NMR spectrum of DIBTC MPEG 2000 macro RAFT agent.

As is shown in Figure 5.7, the corresponding signals of DIBTC were present in each of the spectra, as well as the signal of the protons in PEG ($\text{CH}_2\text{-CH}_2\text{-O}$) at $\delta = 3.6$.

5.4 Controlled free radical homopolymerisation of styrene

The focus of this investigation is the synthesis of copolymers with controlled structure in terms of the length of both the PEG block and the styrene block. It is therefore logic to synthesise homopolymers of styrene in the presence of the selected RAFT agents with the goal of a) verifying the effectiveness of the RAFT agents, and b) optimising reaction conditions for block copolymer synthesis.

5.4.1 Polymerisation conditions

Homopolymers of styrene were synthesised via controlled free radical polymerisation using the RAFT agents CVADTB and DIBTC, respectively. Table 5.2 shows the composition of reagents for the homopolymerisation of styrene.

Table 5.2: Composition of reagents for the RAFT assisted homopolymerisation of styrene

Reaction temperature (°C)	RAFT agent			AIBN		RAFT:AIBN
	Agent	Mass (g)	Millimoles	Mass (g)	Millimoles	
60	CVADTB	0.71	2.54	0.096	0.58	4.35
70	CVADTB	0.68	2.43	0.094	0.57	4.25
80	CVADTB	0.76	2.73	0.099	0.60	4.53
70	DIBTC	0.92	2.53	0.096	0.58	4.32

Polymerisations were carried out in the bulk as follows:

- 1 Styrene was distilled under vacuum at 60°C to remove inhibitor. The distilled styrene was stored at 0°C.
- 2 A 50 mL three-necked flask, equipped with a nitrogen purge, condenser and a septum, was charged with styrene (50 mL/45.45 g).
- 3 Styrene was purged with nitrogen for 30 minutes.
- 4 RAFT agent (about 2.5 milli moles) was added and the temperature increased to the required reaction temperature while maintaining the nitrogen purge.

- 5 AIBN (0.5 milli moles) was added as radical initiator when the reaction temperature was reached. The ratio of RAFT agent to AIBN remained constant at 5:1 for all polymerisations. According to Moad *et al.*¹⁰ it is important to use a system with a very low initiator concentration for block copolymer synthesis. This is due to the fact that termination might also result from the initiator-derived chains, therefore leading to the formation of a homopolymer of the second monomer to be formed. Although this is not important in the homopolymerisation of styrene, it will be of primary importance in Sections 5.5, 5.6 and 5.7, where copolymers of MPEG and styrene will be described.
- 6 Samples were taken at predetermined intervals during the reaction to determine gravimetric conversions. These samples were weighed before and after the remaining styrene monomer was evaporated off.

5.4.2 Experimental calculations

5.4.2.1 Molar mass predictions

Experiments by de Brouwer *et al.*⁸ with a hydroxy-terminated polyolefin and styrene showed a linear relationship between the number average molar mass and conversion, which corresponded closely to theoretical values. In Chapter 4 it was mentioned that one of the advantages of the RAFT process is the ability to predict the molar mass of the polymer formed. This can be accomplished by utilizing Equation 5.1¹¹:

$$\bar{M}_{theory} = \bar{M}_{RAFT} + \frac{[m]_0 M_0 x}{[RAFT]_0 + Cf[I]_0(1 - e^{-k_d t})} \quad (5.1)$$

where \bar{M}_{RAFT} is the molar mass of the RAFT agent as determined by SEC; $[m]_0$, $[RAFT]_0$ and $[I]_0$ are the starting concentrations of the monomer, RAFT agent and initiator respectively; M_0 is the molar mass of the monomer; x is the fractional conversion; f is the initiator efficiency; k_d is the initiator dissociation constant; and t is the time. C is a constant that describes the average number of chains per termination event, it has a value of between 1 and 2, and depends on whether termination is predominantly via combination or disproportionation. This equation makes it possible to predict the target molar mass by using specified concentrations of the reagents.

Although this formula assists in the experimental design, the fractional conversion also has to be taken into account. Reactions carried out in bulk have difficulty reaching high conversions due to the increased viscosity of the reaction mixture. The target molar mass is difficult to achieve due to viscosity effects, but the equation is sufficient to calculate theoretical \bar{M}_n values during the course of the reaction.

5.4.2.2 Fractional conversion

The fractional conversion (x) in Equation 5.1 is calculated as follows:

$$x = 1 - \left(\frac{m_{wet} - m_{dry}}{m_0} \right) \quad (5.2)$$

where m_{wet} is the mass of the sample taken, m_{dry} is the mass of the dried sample, and m_0 is the mass of the volatile fraction of the starting reagents (samples were weighed immediately after being taken, dried to a constant mass and weighed again, yielding a “wet” and “dry” mass for each sample). This was performed in accordance with the method of Haddleton *et al.*¹²

5.4.3 Homopolymerisation of styrene with CVADTB

Styrene was polymerised under controlled free radical conditions, using the RAFT process, with CVADTB as RAFT agent, as discussed in Section 5.4.1. Figures 5.8 to 5.10 show the SEC results (Refractive Index response vs. log M) of the synthesis of polystyrene homopolymers using CVADTB together with AIBN as radical initiator at 60°C, 70°C and 80°C respectively, while Figure 5.12 compares the polydispersities of the resulting polymers formed.

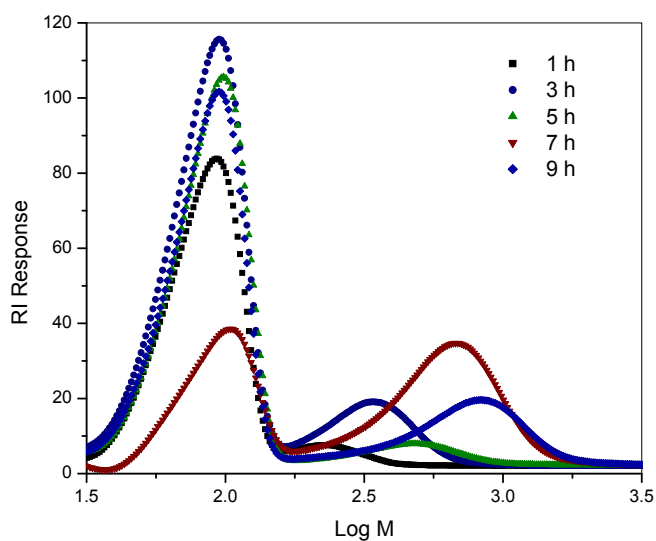


Figure 5.8: SEC graph of RI response vs. $\log M$ for the homopolymerisation of styrene with CVADTB at 60°C.

As can be seen for Figure 5.8 there are large peaks at $\log M \approx 2$. This was ascribed to styrene with a molar mass of 104 g/mol. The samples taken appeared to be “wet”, in the sense that some residual styrene is present in the samples.

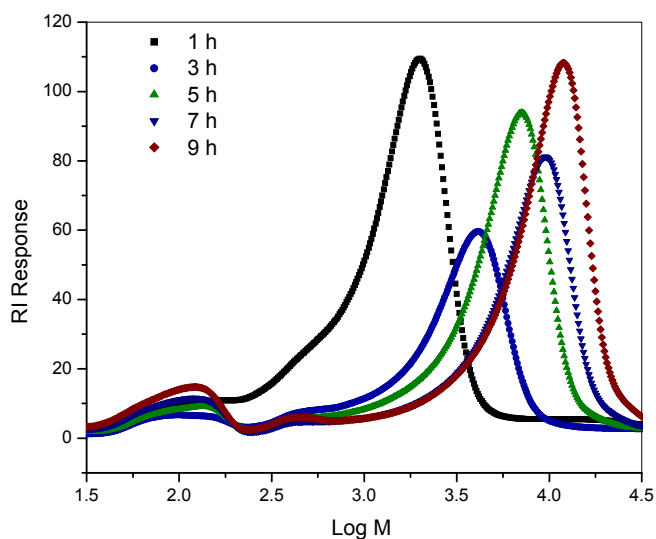


Figure 5.9: SEC graph of RI response vs. $\log M$ for the homopolymerisation of styrene with CVADTB at 70°C.

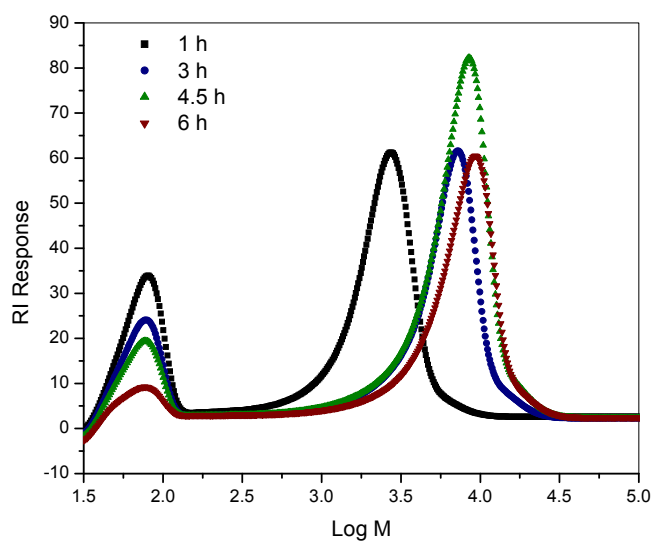


Figure 5.10: SEC graph of RI response vs. $\log M$ for the homopolymerisation of styrene with CVADTB at 80°C.

Each curve showed that there was a gradual increase in the $\log M$ for each reaction. For the reaction at 60°C, the $\log M$ values were much lower those of the reactions at 70°C and 80°C. It therefore seemed evident that therefore there was a greater rate of increase in \bar{M}_n with an increase in reaction temperature. In all three experiments there was a peak at $\log M \approx 2$, assigned to styrene monomer trapped within the product formed. For the experiment at 70°C a shoulder was found at the lower molar mass side of the curve. This would result in a lower output value for \bar{M}_n from SEC compared to a curve with an ideal normal distribution, i.e. without a shoulder. This is illustrated in Figure 5.11, where the \bar{M}_n values obtained via SEC are plotted against reaction time for the reactions at different temperatures.

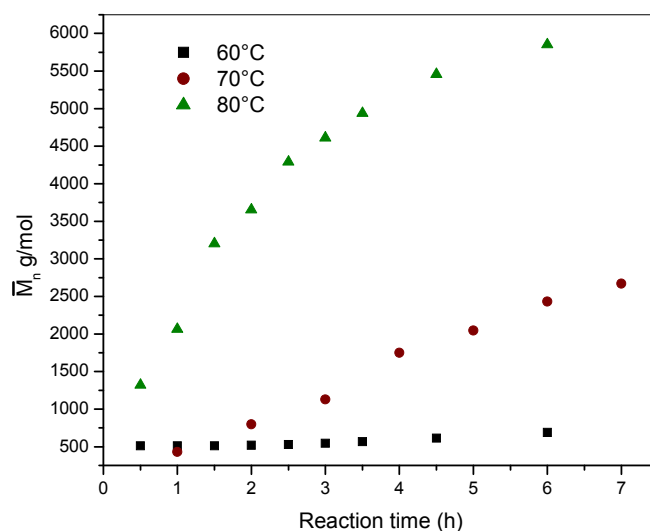


Figure 5.11: Graph of \bar{M}_n vs. time for homopolymerisation of styrene with CVADTB.

Figure 5.11 shows that the \bar{M}_n values for the reactions at 60°C and 70°C are low relative to the \bar{M}_n values obtained for the experiment at 80°C. The relationship between the individual rate constant (k) and temperature (T) for a polymerisation reaction is given by the Arrhenius expression.¹³

$$k_i = A_i \exp\left[-\frac{E_i}{RT}\right] \quad (5.3)$$

where A_i the frequency factor, and E_i is the activation energy. For equivalent systems it can be assumed that A_i and E_i are the same, and, with R being a constant, a direct relationship between k and T is obtained:

$$k \propto \exp\left[-\frac{1}{T}\right] \quad (5.4)$$

In addition to the relationship given in Equation 5.4, the decay of AIBN only commences at 60°C and only at higher temperatures have radical generation events for short spans.¹¹ This explains the phenomenon observed in Figure 5.11 where the growth of the polymer chain for the reactions at 60°C and 70°C are lower than that observed for the reaction at 80°C.

An increase in the reaction temperature resulted in an increase in the rate of both the controlled and uncontrolled reactions, leading to broader polydispersity at higher temperatures, as shown in Figure 5.12.

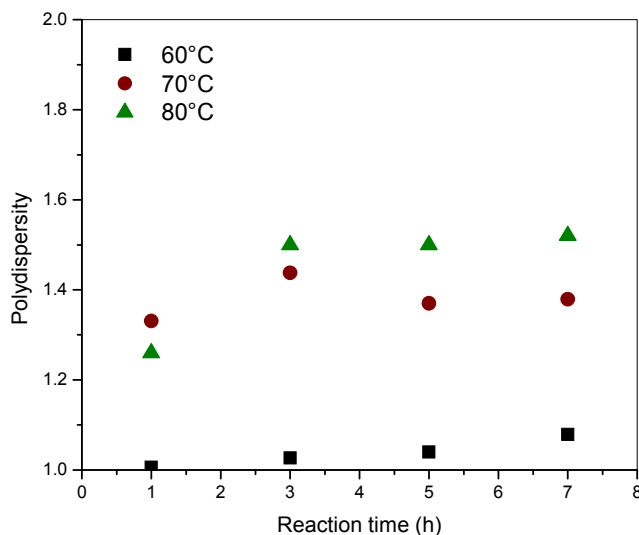


Figure 5.12: Graph of polydispersity vs. time for homopolymerisation of styrene with CVADTB.

Figure 5.11 shows that an increase in reaction temperature resulted in an increase in the rate of \bar{M}_n of the formed polymer, accompanied by an increase in the polydispersity with an increase in reaction temperature (Figure 5.12). This indicated less control over the MMD in the reaction compared to the reaction at lower temperature. Although the polydispersity increased with an increase in reaction temperature, the PDI values obtained were below or in the region of 1.5, which is the generally accepted benchmark PDI value for controlled free radical polymerisation.¹² It was therefore concluded that controlled growth of the polymer chains was achieved.

The polymerisation reaction at 60°C gave the greatest control in polydispersity (Figure 5.12). The rate of increase in \bar{M}_n , however, was very low. At 80°C the polymer chains grow much faster, but products with broader polydispersity were obtained. Theoretically lower temperatures are preferred because of the lower probability of side reactions. At higher temperatures, the reaction rate of polymerisation increases not only for the reversible transfer reaction, but thermal initiation and polymerisation also occur, leading to uncontrolled reactions. This thermal initiation and polymerisation has a negative effect on polydispersity in that products with broader polydispersity are obtained. The second

reason for the preferred lower temperatures is that the RAFT agent is thermally unstable. When degradation takes place, the ratio of RAFT agent versus AIBN generated radicals is decreased, leading to less control of the reaction, and to the formation of products with higher polydispersity. The data obtained for the reaction at 70°C offered an intermediate route in terms of lower polydispersity than for the reaction at 80°C, whilst offering faster reaction rates than those observed for the reaction at 60°C.

Conversion studies were performed on the RAFT (CVADTB) polymerisation of styrene at 70°C with AIBN as radical initiator. Figure 5.13 shows the fractional conversion vs. reaction time for the homopolymerisation of styrene with CVADTB. Indications were that the rate of monomer consumption was constant. The fractional conversion was calculated as a percentage of the volatile content of each sample compared to the volatile content at the onset of the reaction (Section 5.4.2.2).

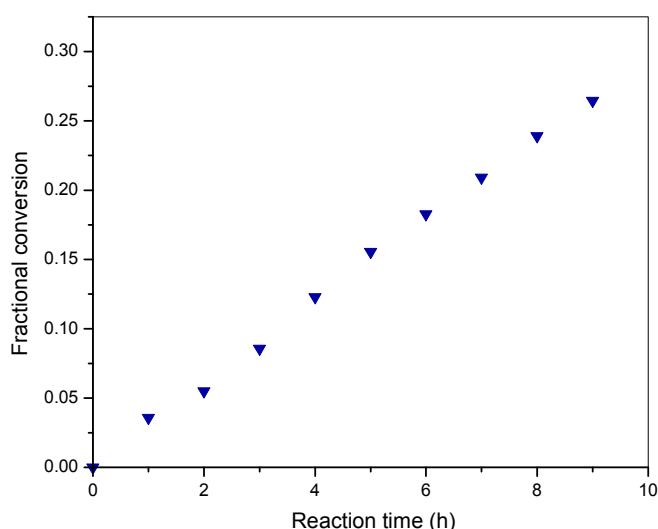


Figure 5.13: Graph of fractional conversion vs. reaction time for the homopolymerisation of styrene with CVADTB at 70°C.

The rate of the transfer reaction was low, and conversion of only 26.45% is reached after 9 h. Reaction times of 18 h and longer to reach 50% or higher conversion for the polymerisation of styrene using CVADTB have been reported in literature.

The results contained in Figures 5.12 and 5.13 again indicate controlled growth of the polymer chains. The polydispersity, as shown in Figure 5.12, remained below 1.5, again proving that good control was exercised throughout the reaction.

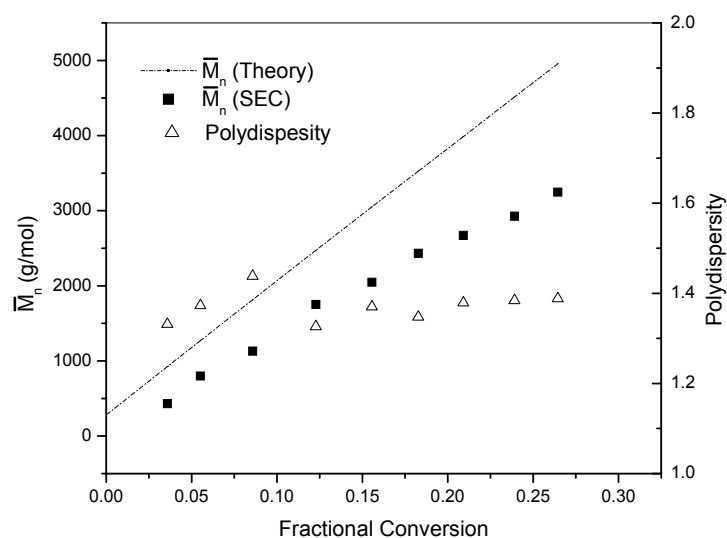


Figure 5.14: Graph of \bar{M}_n and polydispersity vs. fractional conversion for the homopolymerisation of styrene with CVADTB at 70°C.

$\bar{M}_{n(Theory)}$ in Figure 5.14 refers to the theoretically predicted \bar{M}_n (Equation 5.1). By comparing the theoretical values with experimental values, as determined by SEC, it appeared that the experimental \bar{M}_n values showed a similar trend to theoretical values, but were lower. As mentioned earlier, the SEC values are affected by shouldering in the SEC curve, which lead to lower \bar{M}_n values. Fractional conversions were calculated as described in Section 5.4.2.2. Any residual styrene monomer present in the samples after drying would therefore cause an increase in m_{dry} , which would lead to an increase in the fractional conversion, x . This could in turn lead to higher theoretical values for \bar{M}_n as illustrated in Figure 5.15, where the RI response is plotted against log M for a sample after 9 h reaction time.

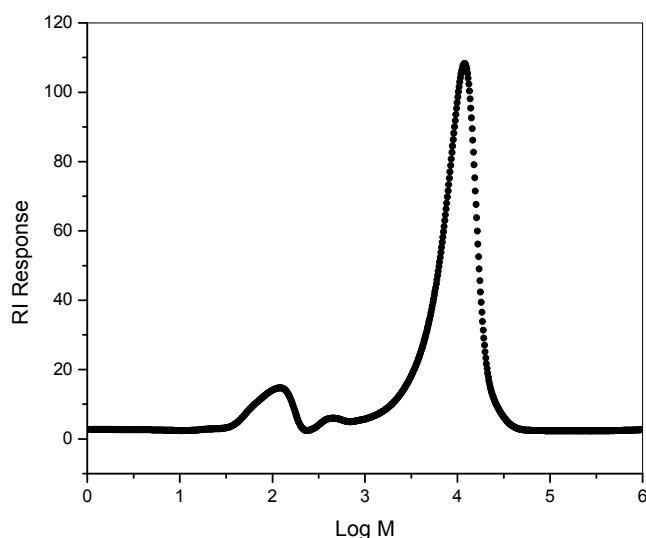


Figure 5.15: SEC graph of RI response vs. $\log M$ for sample taken at 9 hours in the polymerisation of styrene with CVADTB at 70°C.

The peak at $\log M \approx 2$ would represent species with molar masses in the region of 100 g/mol. As the molar mass of styrene being 104 g/mol, it was evident that there was a certain amount of styrene trapped in the sample, acting as a plasticizer. Re-evaluating the theoretical values would therefore lead to better correlation between the actual SEC values for \bar{M}_n and the theoretically calculated values. Yet, as the focus here is the determination of optimum conditions for controlled polymerisation, the effect of the “trapped” styrene can be ignored.

5.4.4 Homopolymerisation of styrene with DIBTC

In 2002, Lai *et al.*⁷ reported on the synthesis of DIBTC and its possible use as RAFT agent in controlled “living” free radical polymerisation. Results obtained with the polymerisation of styrene in the presence of CVADTB (Section 5.4.3) showed that CVADTB could be classified as a “slow” RAFT agent. Lai *et al.* reported that tri thiocarbonates offer certain advantages over other RAFT agents, especially in terms of the high chain-transfer efficiency. These compounds can also be prepared with greater ease than CVADTB.

The primary objective of introducing DIBTC was to evaluate its efficiency as a RAFT agent and compare the results with results obtained in the polymerisation of styrene with

CVADTB. Comparative experiments were conducted at 70°C. Similar conditions to those used for the RAFT polymerisation of styrene with CVADTB (Section 5.4.1) were used here, specifically in terms of the ratio of RAFT agent to AIBN, monomer concentration and reaction temperature.

Figure 5.16 shows the SEC results of the bulk homopolymerisation of styrene in the presence of DIBTC.

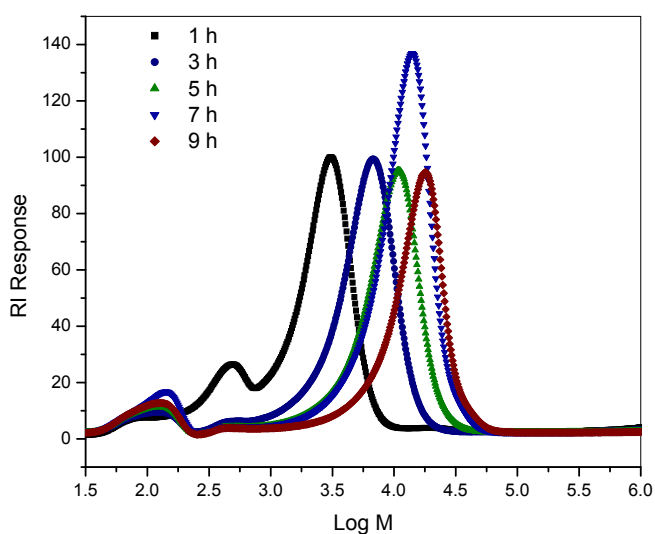


Figure 5.16: SEC graph of RI response vs. $\log M$ for the homopolymerisation of styrene with DIBTC at 70°C.

The shape of the SEC data showed that products with low MMD are obtained. Although the SEC curves showed a distribution with narrow polydispersity, there was a small amount of tailing at the low molar mass side of the curve. This would in turn lead to an increase in the observed polydispersity as well as lower \bar{M}_n values, as calculated by the GPC software.

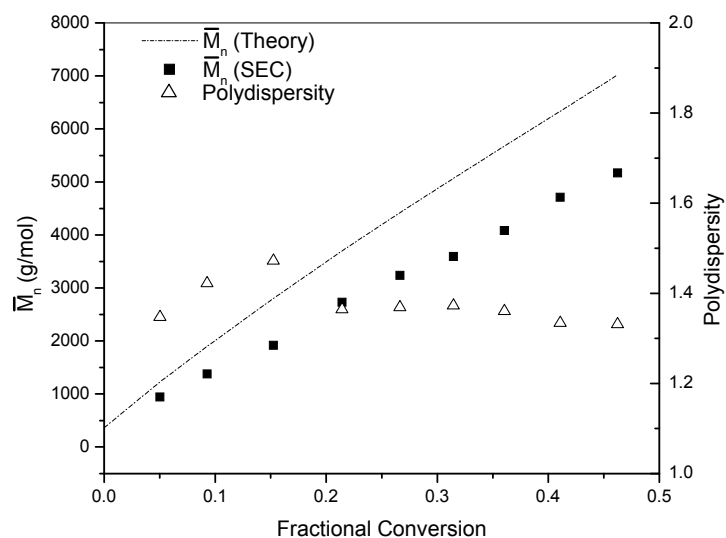


Figure 5.17: Graph of \bar{M}_n and polydispersity vs. fractional conversion for the homopolymerisation of Styrene with DIBTC at 70°C.

Figure 5.17 shows that \bar{M}_n increases linearly with conversion. This depicts the “living” character of the system. Again it was found that the SEC values were slightly lower than the theoretically predicted \bar{M}_n values. Due to tailing on the low molar mass side of the SEC curves, the \bar{M}_n values obtained were somewhat lower than for curves without low molar mass tailing. It may also be ascribed to the fact that some residual styrene monomer were trapped inside the polymer, acting as plasticizer, and therefore leading to higher values for fractional conversion. There was, however, a similarity in the trend of both the SEC and predicted values for \bar{M}_n . The polydispersity of the product formed was below 1.5, which is the benchmark for an efficient RAFT agent. It was therefore concluded that DIBTC was effective as a RAFT agent for the homopolymerisation of styrene.

Figure 5.18 shows a comparison between the efficiency of CVADTB and DIBTC:

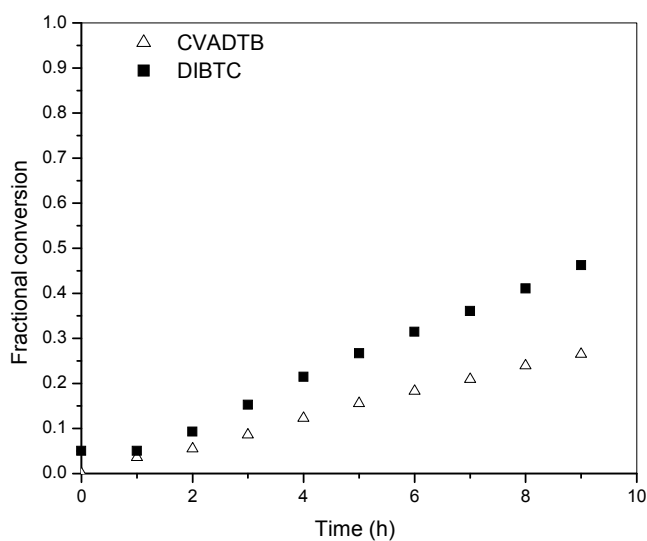


Figure 5.18: Graph of fractional conversion vs. reaction time for the homopolymerisation of styrene with CVADTB and DIBTC.

It can be seen from Figure 5.18 that the conversion is much higher for DIBTC than that for CVADTB. After 9 hours the reaction with DIBTC was at 46% conversion while a similar reaction with CVADTB was only at 26% conversion. The rate of addition and transfer was therefore much greater in the case of DIBTC compared to CVADTB.

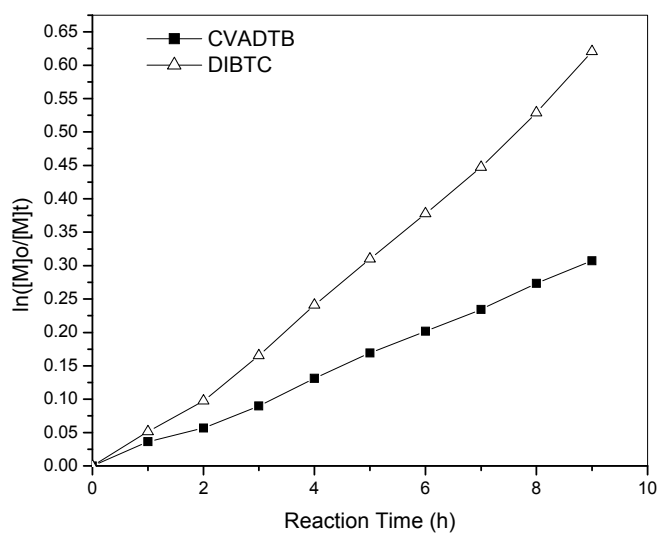


Figure 5.19: First-order kinetic plot for polymerisation of styrene with CVADTB and DIBTC.

Figure 5.19 shows the first-order kinetic plots of the controlled “living” polymerisation of styrene at 70°C by making use of CVADTB and DIBTC. These plots, together with the data in Figure 5.18 yielded proof that DIBTC was a “faster” RAFT agent, when compared to CVADTB, for the controlled “living” polymerisation of styrene. Both RAFT agents proved efficient in the controlled polymerisation of styrene, but the rate of transfer for CVADTB was lower than that of DIBTC, therefore resulting in the lower fractional conversion values observed in Figure 5.18.

5.4.5 Conclusions

From the results obtained in the controlled free radical polymerisation of styrene with CVADTB and DIBTC, the following conclusions can be drawn:

- 1 Both RAFT agents were effective in producing polystyrene homopolymers with narrow MMD (low polydispersity).
- 2 CVADTB was a relatively “slow” RAFT agent.
- 3 The rate of addition and fragmentation for DIBTC was higher than for CVADTB.
- 4 An increase in the reaction temperature caused an increase in the rate of the reaction as well as in the MMD of the formed polymers.
- 5 The molar mass of a polymer could be predicted in the RAFT process.

5.5 PS-b-MPEG 350 block copolymer synthesis

5.5.1 Introduction

The main aim of this investigation is the preparation of well-defined AB block copolymers with exact control of the hydrophilic:hydrophobic ratio (with A being the hydrophilic and B being the hydrophobic segment of the copolymer). Screening experiments on RAFT agent efficiency and reaction temperature for the homopolymerisation of styrene proved useful in determining the reaction conditions for the copolymerisation process. Results obtained in the controlled homopolymerisation of styrene showed that both CVADTB and DIBTC were effective RAFT agents for the controlled “living” free radical polymerisation of styrene. Suitable reaction conditions were also determined in the homopolymerisation of styrene with the aid of CVADTB and DIBTC, respectively. The next step in this investigation was the synthesis of macro RAFT agents for the formation of block copolymers.

Certain variables could prove to have an influence on the polymerisation product formed, namely:

- 1 method of macro RAFT agent formation (esterification reaction)
- 2 reaction temperature
- 3 length of the MPEG macro monomer used

The influence of each of the abovementioned variables was therefore to be investigated and evaluated in terms of the influence on the product formed. As was stated in Section 5.3.4, where the two methods of esterification are discussed, method 2 offers ease of removal of the by-products formed during esterification. It remained to be seen, however, whether this method would be the preferred method of esterification in terms of the yield of the reaction. Due to the fact that the esterified product of method 1 could not be purified, a comparative study in terms of the yield of the esterification product was not possible. Although Shi *et. al.*⁹ reported yields of 90% in their esterification experiments, the fact remained that both MPEG and the formed MPEG macro RAFT agent both precipitated out of solution in ethyl acetate at 0°C. The product obtained therefore also included a certain amount of unreacted MPEG. It is further important to ascertain what the influence of the esterification would be on the effectivity of the RAFT functionality of the macro RAFT agent obtained. Results of copolymerisation would have to be compared with that of the homopolymerisation of styrene in terms of the first-order kinetics and polydispersity of the products obtained.

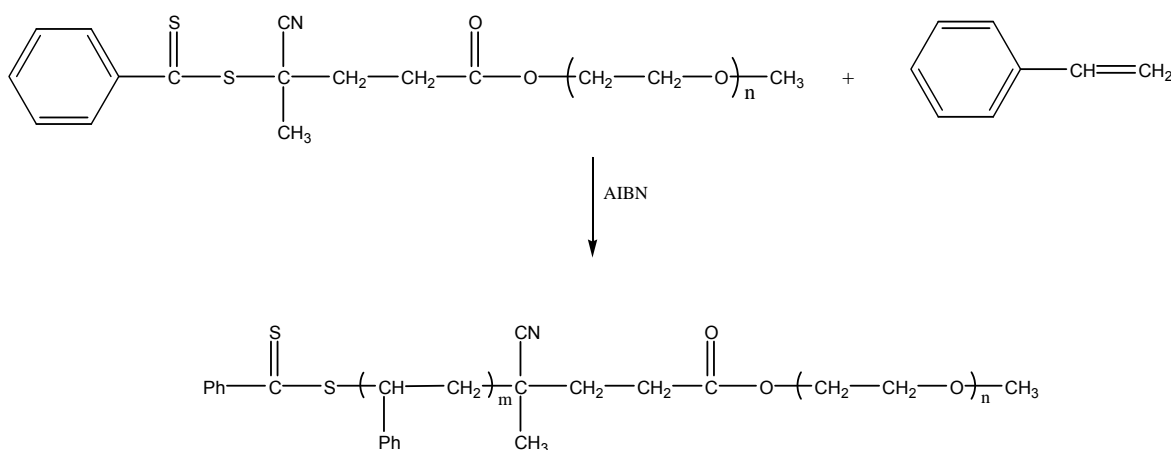
As was seen for the homopolymerisation of styrene, an increase in reaction temperature inevitably lead to an increase in the polydispersity of the product formed. Not only did the rate of addition and transfer from and to the RAFT agent increase, the rate of thermal initiation and propagation also increased. This in turn would lead to an increase in polydispersity due to an increase in uncontrolled reactions. Thermal initiation would further lead to the formation of homopolymer (polystyrene). The reaction product would therefore contain both homopolymer and block copolymer, which would in turn have to be purified.

As the reactions were conducted in bulk, diffusion of the active/dormant radicals were important in terms of the kinetics of the reaction; a larger macro RAFT agent would have less mobility within the system at higher conversions. At higher fractional conversion in bulk polymerisation less monomer is available to act as reaction medium (solvent), which

causes an increase in the viscosity of the reaction mixture. This affects the rate of the reaction as well as the composition of the copolymer formed.

5.5.2 Polymerisation conditions

A simplified scheme for the synthesis of a PEG-b-PS block copolymer is depicted in Scheme 5.5. Refer to Chapter 4 for a detailed description of the RAFT process.



Scheme 5.5: Synthesis of PEG-b-PS with a CVADTB MPEG macro RAFT agent.

Reaction conditions similar to those described in Section 5.4.1 were used for the copolymerisation reactions.

This investigation focuses on the type of RAFT agent used, the reaction temperature, as well as the size of the MPEG macro RAFT agent used in copolymer synthesis. The range of copolymers synthesized are summarised in Table 5.3.

Table 5.3: Composition of reagents for the RAFT assisted synthesis of PEG-b-PS block copolymers

Reaction temperature (°C)	RAFT agent			AIBN		RAFT:AIBN
	Agent	Mass (g)	Milli-moles	Mass (g)	Milli-moles	
60	CVADTB MPEG 350	1.63	2.59	0.097	0.59	4.38
70	CVADTB MPEG 350	1.67	2.65	0.095	0.58	4.59
80	CVADTB MPEG 350	1.63	2.59	0.095	0.58	4.48
60	CVADTB MPEG 2000	6.45	2.83	0.096	0.58	4.84
70	CVADTB MPEG 2000	6.35	2.79	0.094	0.57	4.87
80	CVADTB MPEG 2000	6.39	2.80	0.096	0.58	4.80
70	CVADTB MPEG 5000	13.04	2.47	0.098	0.60	4.14
70	DIBTC MPEG 350	1.80	2.52	0.095	0.58	4.36
70	DIBTC MPEG 2000	6.02	2.55	0.099	0.60	4.22

5.5.3 Copolymerisation of styrene using CVADTB MPEG 350 macro RAFT agent

Due to the relatively small size of the MPEG 350 macro monomer, the copolymers prepared with MPEG 350 macro RAFT agents would be worthless when analysing the hydrophilic:hydrophobic ratio within the copolymer. Any hydrophilic effect would be negligible compared to the hydrophobic effect of a large polystyrene block. The value of these model compounds lies in the ease of analysis of the copolymers formed as well as proof that copolymers of MPEG and styrene could be synthesised using this technique. With MPEG 350 being a smaller molecule than MPEG 2000 and MPEG 5000, it was assumed that chain mobility would have the least effect in both the esterification of MPEG 350 as well as the copolymerisation reaction of the MPEG 350 macro RAFT agent with styrene monomer.

Figures 5.20 to 5.22 show the SEC data obtained for copolymers prepared using a CVADTB MPEG 350 macro RAFT agent. The only variable for the three experiments was the variation in reaction temperature.

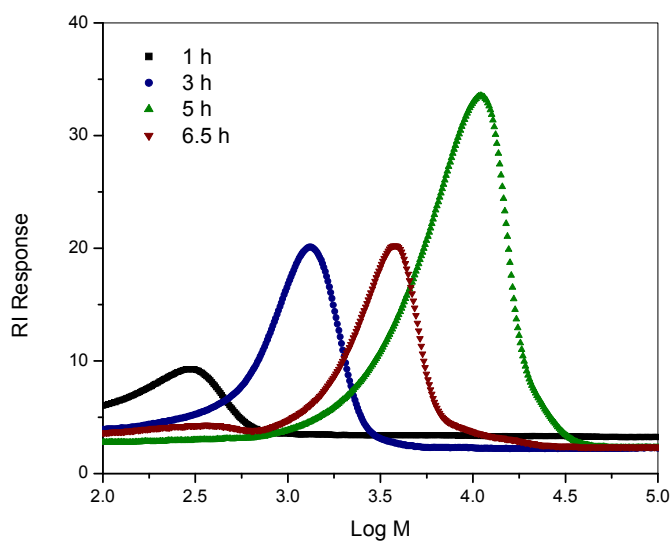


Figure 5.20: SEC graph of RI response vs. $\log M$ for the copolymerisation of styrene with CVADTB MPEG 350 at 60°C.

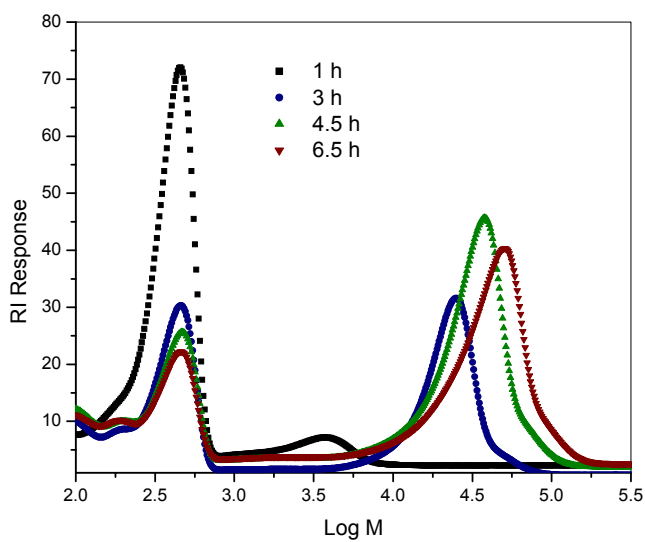


Figure 5.21: SEC graph of RI response vs. $\log M$ for the copolymerisation of styrene with CVADTB MPEG 350 at 70°C.

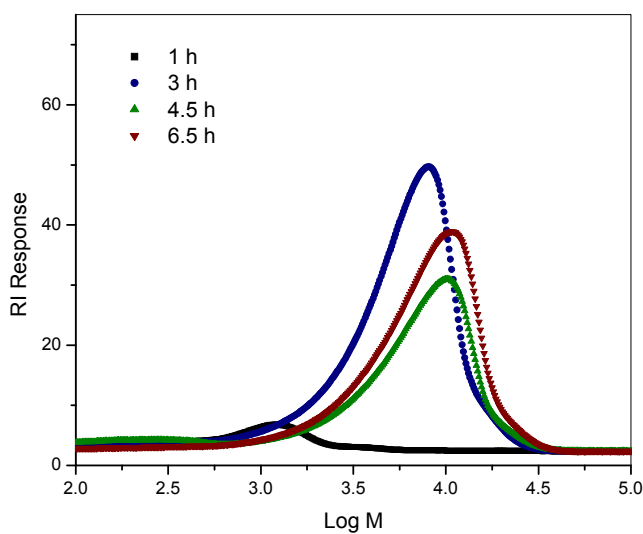


Figure 5.22: SEC graph of RI response vs. $\log M$ for the copolymerisation of styrene with CVADTB MPEG 350 at 80°C.

As was seen with the homopolymerisation of styrene in the presence of CVADTB, controlled growth occurred at all temperatures. The rate of growth of the polymer chains were slow at 60°C compared to the experiments conducted at 70°C and 80°C. SEC plots showed what appears to be a small amount of low molar mass tailing in the polymer products formed. It therefore seemed that a small amount of termination was inevitable for the reactions at higher temperatures. This is one of the disadvantages of bulk polymerisation, where active radicals can terminate reactions by either recombination or disproportionation. The RAFT process was developed to prevent unwanted termination reactions, but as the temperature is increased, thermal initiation occurs and a certain amount of “uncontrolled” PS homopolymer is formed. Theoretical calculations of the $[RAFT]:[AIBN]$ ratio (calculated at 5 for each experiment) does not take thermal initiation into account. This would result in a $[RAFT]:[R\cdot]$ ratio of 2.5:1, as two initiator molecules are generated from each AIBN molecule (Chapter 4, Section 4.2). Thermal initiation introduces more radicals into the system, effectively increasing the radical concentration, $[R\cdot]$, and therefore in effect lowering of $[RAFT]:[R\cdot]$ ratio, resulting in less control of the reaction. The possibility of the formation of PS homopolymer as well as the possibility of uncontrolled termination reactions occurring is therefore increased.

As one-dimensional SEC results only show the molar mass of the resulting polymerisation product, the amount of PS homopolymer formed could not be determined. Because the length of the MPEG 350 block was too short for 2D chromatography (as described in Section 5.2.2) it was not possible to analyse these products under critical conditions.

Figures 5.23 and 5.24 show the \bar{M}_n and polydispersity values of the polymerisation products from SEC graphs shown in Figures 5.20, 5.21 and 5.22 as a function of reaction time, respectively.

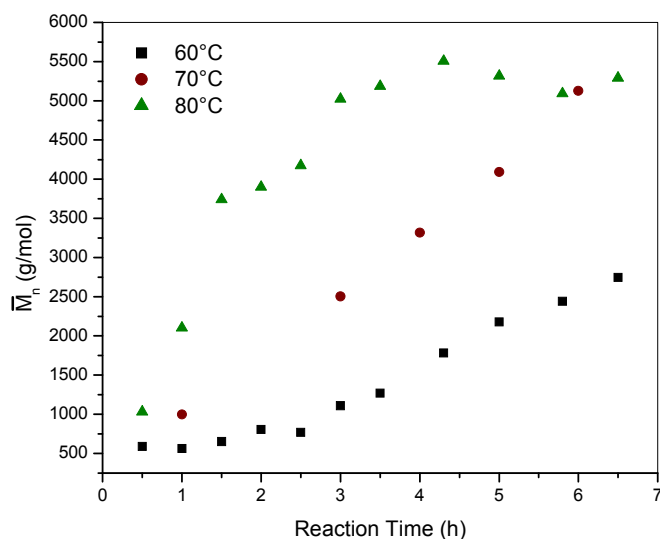


Figure 5.23: Graph of \bar{M}_n vs. reaction time for the copolymerisation of styrene with CVADTB MPEG 350.

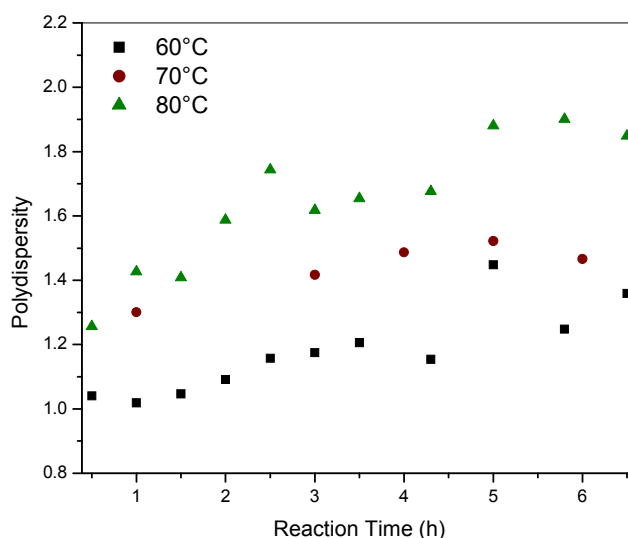


Figure 5.24: Graph of polydispersity vs. reaction time for the copolymerisation of styrene with CVADTB MPEG 350.

From Figures 5.23 and 5.24 it was seen that the best control in terms of polydispersity was obtained for the reaction at 60°C; however, the increase in \bar{M}_n was slow, leading to long reaction times for high conversions. Experiments at both 60°C and 70°C showed a gradual increase in \bar{M}_n with reaction time, which was expected of the RAFT process at lower conversions. The \bar{M}_n values for the experiment at 70°C showed a rather rapid increase to the extent that results of similar magnitude to those of the experiment at 80°C were observed. Thermal initiation and uncontrolled termination reactions taking place between lower molar mass species were more likely responsible for the increase in polydispersity caused by the low molar mass tailing observed. Termination could either lead to a dead polymer chain or a polymer chain with a double bond in the α position. The latter would be able to reinitiate and polymerise further, while the former would result in a lower molar mass product formed. On comparing Figure 5.22 and Figure 5.23 it seemed evident that the lower molar mass termination products were responsible for the shouldering observed in the SEC data. This also accounted for the rapid increase in \bar{M}_n , followed by a plateau during the later stages of the reaction.

The polydispersity data for Figure 5.24 showed acceptable values for the reactions at 60°C and 70°C, while values in the region between 1.5 and 2.0 were observed for the

reaction at 80°C. Values between 1.0 and 1.5 are the benchmark in polydispersity for controlled free radical polymerisation. The polydispersity values at 80°C were unacceptably high and showed a lack of control in the reaction. Here other influences came into affect, resulting in the formation of a polymer with a broader molar mass distribution.

Results showed that experiments performed at 60°C offered good control in terms of polydispersity, but were time consuming. Experiments performed at 80°C offered high reaction rates, but lack of control in terms of polydispersity. It was evident that experiments at 70°C offered a convenient compromise between the rate of the reaction and the control thereof.

5.5.4 Copolymerisation of styrene using DIBTC MPEG 350 macro RAFT agent

As stated in Section 5.4.4, Lai *et al.*⁷ reported the use of DIBTC as RAFT agent for the controlled “living” polymerisation of styrene. With results in Section 5.4.4 showing that DIBTC offered acceptable control of styrene polymerisation as well as an acid functionality for the synthesis of a MPEG-macro RAFT agent, it was decided to synthesize DIBTC MPEG 350 macro RAFT agents for the copolymerisation of styrene to form a PEG-b-PS diblock copolymer. Figure 5.25 shows the SEC results for the copolymerisation of styrene with DIBTC MPEG 350 macro RAFT agent.

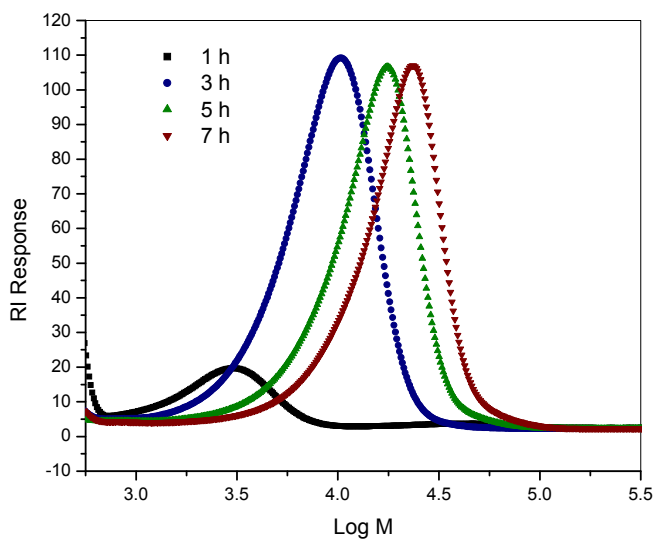


Figure 5.25: SEC graph of RI response vs. log M for the copolymerisation of styrene with DIBTC MPEG 350 at 70°C.

The results showed a narrow MMD in the curve of the RI response vs. log M (Figure 5.25). This showed that good control in terms of MMD. This was in agreement with what had been observed from results for the homopolymerisation of styrene in the presence of DIBTC, where similar trends in the SEC data were observed. This proved that DIBTC MPEG 350 macro RAFT agent was efficient in the controlled living polymerisation of styrene.

Figure 5.26 shows the polydispersity and \bar{M}_n values as determined by SEC for the copolymerisation of styrene with CVADTB- and DIBTC MPEG macro RAFT agents as a function of the reaction time.

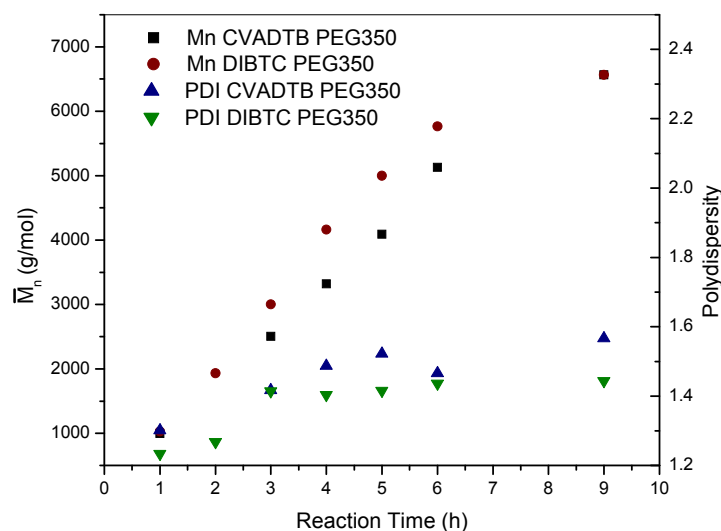


Figure 5.26: Comparative graph of copolymerisation of styrene with DIBTC MPEG 350 and CVADTB MPEG 350 at 70°C.

From homopolymerisation reactions it was found that DIBTC was a much “faster” RAFT agent than CVADTB, the former leads to a rapid increase in \bar{M}_n values. The results in Figure 5.26 show that \bar{M}_n for the CVADTB MPEG macro RAFT agent experiment grew at a similar rate to that observed for the DIBTC MPEG macro RAFT agent system. The polydispersity values obtained for the experiment with CVADTB MPEG 350 were also higher than the corresponding values for the experiment with DIBTC MPEG 350 macro RAFT agents. In Figure 5.23, where the effect of reaction temperature on the resulting polymer product was observed, the \bar{M}_n values of the reaction with CVADTB MPEG 350 at 70°C also showed values that were higher than expected. These higher than expected \bar{M}_n values and higher polydispersity values could be a result of the partial degradation of the CVADTB MPEG 350 macro RAFT agent. As the MPEG macro RAFT agents used without purification after the esterification process, degradation products could form part of the CVADTB-MPEG 350 esterification product. In the process of adding the predetermined mass of CVADTB MPEG 350 to the reaction mixture, the effective RAFT concentration might therefore have decreased. This would in turn lead to a shift in the [RAFT]:[R·] ratio towards [R·]. This would subsequently result in a higher reaction rate as well as uncontrolled reactions, leading to the formation of a polymerisation product with higher polydispersity.

5.5.5 Conclusions

Although fractional conversions were not determined and two-dimensional analysis of the copolymers formed in the copolymerisation of styrene with MPEG 350 macro RAFT agents was not possible, certain conclusions could be made from the results obtained:

- 1 Narrow molar mass polymers could be prepared in the copolymerisation of styrene with MPEG 350 macro RAFT agents.
- 2 Esterification appeared not to have an influence on the RAFT functionality in each of the RAFT agents used, as polymers of narrow polydispersity were obtained in each copolymerisation.

5.6 MPEG 2000-b-PS copolymer synthesis

5.6.1 Copolymerisation of styrene using CVADTB MPEG 2000 macro RAFT agent

Having results obtained for the copolymerisation of styrene with MPEG 350 macro RAFT agents, the next step was the synthesis of macro RAFT agents with MPEG of higher molar mass. Polymerisation conditions stated in Section 5.4.1 and Section 5.5.2 were used for the copolymerisation of styrene with the aid of MPEG 2000 macro RAFT agents.

MPEG 2000 macro RAFT agents of CVADTB were synthesized according to the conditions stated in Section 5.3.4. Initial experiments were conducted at 60°C, 70°C and 80°C. Figure 5.27 shows the SEC data of the polymerisation of styrene in the presence of a CVADTB MPEG 2000 macro RAFT agent, conducted at 60°C.

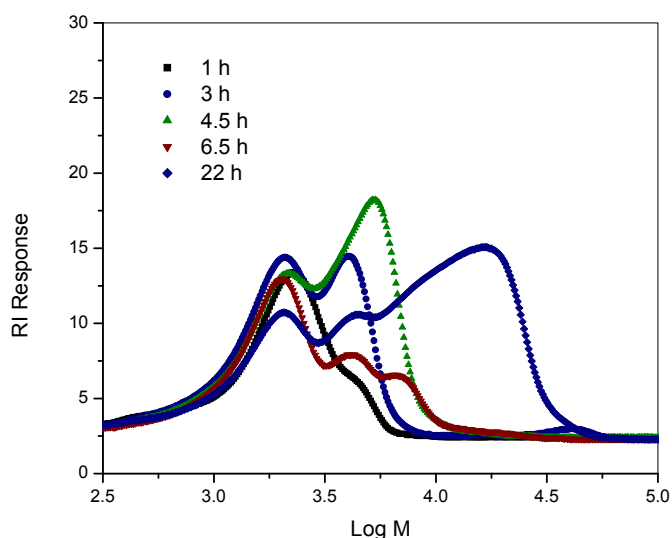


Figure 5.27: SEC graph of RI response vs. $\log M$ for the copolymerisation of styrene with CVADTB MPEG 2000 at 60°C.

Figure 5.27 shows a slow rate of growth in $\log M$, meaning that the rate of the reaction is presumably low. The polymerisation products from the start of the reaction right through to 22 hours showed a peak at $\log M \approx 3.3$ (a molar mass of approximately 2000 g/mol) and this peak remained present with increasing reaction time. This peak was therefore assigned to a dormant species present within the reaction mixture. The reaction flask was charged with the styrene, AIBN and the crude RAFT agent (Section 5.4.1). The only species present that both offered a molar mass in that range and dormant in terms of free radical polymerisation would be the MPEG 2000 macromolecule used in the synthesis of the CVADTB MPEG 2000 macro RAFT agent. MPEG 2000 could be present in the reaction mixture if the esterification reaction was incomplete, therefore introducing a dormant species into the system.

The reaction rate for this experiment was fairly low and even after 6.5 h no clear distinction could be made between the different peaks of the different species within the obtained polymeric product. With the CVADTB being classified as a “slow” RAFT agent, longer reaction times are needed for high conversions. With longer reaction times, more AIBN would have to be introduced into the reaction.

Figure 5.28 shows the SEC data of the polymerisation product obtained in the controlled free radical copolymerisation of styrene with CVADTB MPEG 2000 at 60°C, at a reaction time of 22 h.

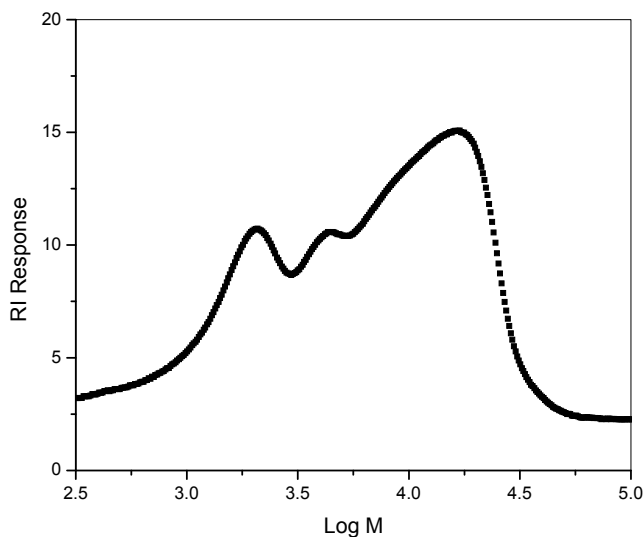


Figure 5.28: SEC graph of RI response vs. $\log M$ for the copolymerisation of styrene with CVADTB MPEG 2000 at 60°C (reaction time: 22 h).

SEC data showed a multi-component system, but because complete molar mass chemical composition distribution analysis is not possible with normal SEC, complete analysis of the product was not possible. Analysing SEC data would in this case lead to incorrect conclusions being drawn, as peak integration is subject to human interpretation.

This could lead to incorrect values for both \bar{M}_n and MMD of the polymer obtained. The main important deficiency in SEC is that no information regarding the chemical composition of the different species in the product is given. Conventional SEC was therefore insufficient for the successful analysis of copolymer blends (Section 5.2.2). The ^1H NMR spectrum of the resulting product is shown in Figure 5.29.

(^1H NMR spectra of all PEG-b-PS copolymerisation products discussed in the remainder of this Chapter show results similar to Figure 5.28, therefore showing that it was not possible to determine the chemical composition distribution by ^1H NMR spectra. To avoid tedious repetition of data, ^1H NMR spectra are given in Appendix 1.)

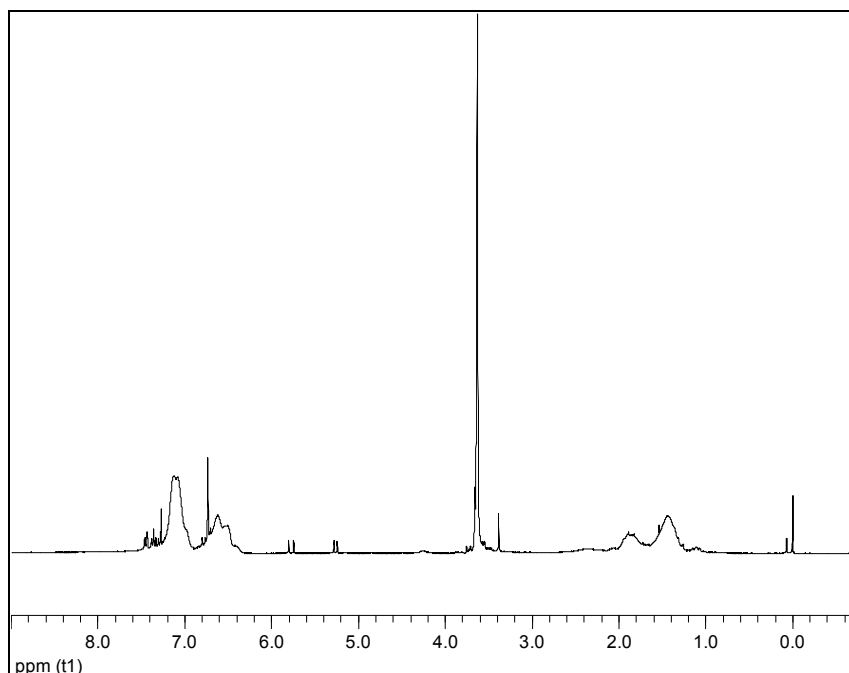


Figure 5.29: ^1H NMR spectrum for the copolymerisation of styrene with CVADTB MPEG 2000 at 60°C (reaction time: 22 h).

The PEG segment and the PS segment were identified at $\delta = 3.7$ and 7.2 respectively. It was not possible to ascertain whether the obtained product was indeed a pure block copolymer or a mixture of polymerisation products, namely: PEG- and PS homopolymers as well as PEG-b-PS block copolymers. NMR therefore showed evidence of the existence of both species within the copolymerisation product, but the exact chemical composition of the copolymerisation product could not be determined.

A two-dimensional chromatographic system, as described in Section 5.2.2, was used to analyse the copolymerisation products obtained. Figure 5.30 shows the three-dimensional (3D) representation of the data obtained from the 2D chromatographic analysis of the same polymeric product as shown in Figure 5.28.

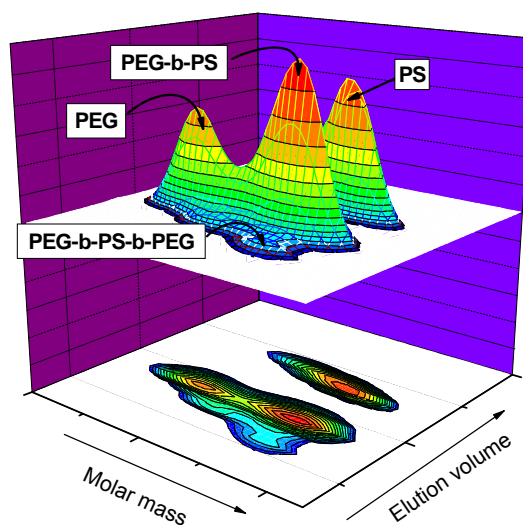


Figure 5.30: Three-dimensional plot of 2D chromatographic analysis for the copolymerisation of styrene with CVADTB MPEG 2000 at 60°C (reaction time: 22 h).

Figure 5.30 shows the existence of four different species in the product obtained. Distinction could be made in terms of the chemical composition distribution of the different species present within the polymer product. A detailed analysis (relative amount, \bar{M}_n , \bar{M}_w , and PDI) of the polymeric product represented in Figure 5.30 is given in Table 5.4.

Table 5.4: Composition of polymerisation product obtained from the copolymerisation of styrene with CVADTB MPEG 2000 at 60°C

	Relative amount %	\bar{M}_n g/mol	\bar{M}_w g/mol	PDI
PS	33	9800	15000	1.5
PEG-b-PS	40	13900	18300	1.3
PEG-PS-PEG	4	17200	21800	1.3
MPEG 2000	23			

The results of two-dimensional analysis of the polymerisation product (Table 5.4) show that the yield of the desired PEG-b-PS copolymer was 40%.

As mentioned earlier, conventional SEC showed a constant peak at $\log M \approx 3.3$. As was expected, Figure 5.30 clearly identified MPEG 2000 macromonomer in the system. The concentration of MPEG 2000 was relatively high at 23%, but with the reaction temperature being low, the rate of the reaction was low relative to reactions performed at higher temperatures. The MPEG 2000 that did not react with CVADTB to form the resulting CVADTB MPEG 2000 macro RAFT agent was present in the system from the onset of the reaction and, being a dormant species, the amount of MPEG 2000 remains constant in the reaction mixture. As the fractional conversion increased, the amount of PEG-b-PS copolymer as well as PS homopolymer would increase. This would therefore effectively decrease the relative amount of MPEG 2000 in terms of the polymer product. As seen later, the polymerisations performed at higher temperatures using the same RAFT agents, had a lower MPEG 2000 content at the end of the reaction.

The PEG-b-PS-b-PEG triblock copolymer was formed due to uncontrolled termination reactions, where the recombination of two growing chains occurred. Each growing chain had a diblock structure (PEG-b-PS \cdot), resulting in the formation of a triblock copolymer PEG-b-PS-b-PEG upon termination by recombination. The relative amount of these termination products was low, proving that the CVADTB MPEG 2000 macro RAFT agents were effective in preventing the formation of uncontrolled termination products. Similar types of termination products in RAFT copolymerisation were also reported by De Brouwer,¹⁴ where macro RAFT agents were employed in the synthesis of copolymers of styrene and PEB (polyethylene-butylene copolymer).

The PS homopolymer present in the polymerisation product could be attributed to thermal initiation. McLeary¹¹ reported that in the case of styrene, polymerisation due to thermal initiation occurred via a third-order mechanism, referred to as the Mayo Diels-Alder radical mechanism for styrene. The polydispersity of the PS homopolymer formed was 1.5, which was slightly higher than that of the PS-b-PEG block copolymer. This proves that there was CVADTB present in the crude MPEG 2000 macro RAFT agent, resulting in controlled growth of the PS chains. Two-dimensional chromatography was therefore effective for the analysis of copolymers formed during the copolymerisation of styrene in the presence of MPEG 2000 macro RAFT agents.

Xie *et al.*¹⁵ reported on the isolation of PEG-b-PS from a mixture containing PEG, PS and PEG-b-PS. They reported on a two-stage extraction process, where 1) the PS homopolymer was extracted with cyclohexane at elevated temperature, and 2) unreacted

MPEG was removed by extraction with H₂O. Normal extraction, as well as soxlet extractions, was found to be unsuccessful in the isolation of MPEG 2000-b-PS from the polymerisation products obtained. The products obtained in each of the extractions contained MPEG and PS homopolymers as well as MPEG-b-PS block copolymer.

Figures 5.31 and 5.32 represent SEC data obtained from reactions of CVADTB MPEG 2000 macro RAFT agents with styrene at 70°C. In Figure 5.31 the SEC data represents the products obtained for the copolymerisation of styrene in the presence of CVADTB MPEG 2000 macro RAFT agent which was synthesised by making use of Method 1 as described in Section 5.3.4, while Figure 5.32 represents the SEC data where the CVADTB MPEG 2000 macro RAFT agent had been prepared by making use of Method 2 as described in Section 5.3.4.

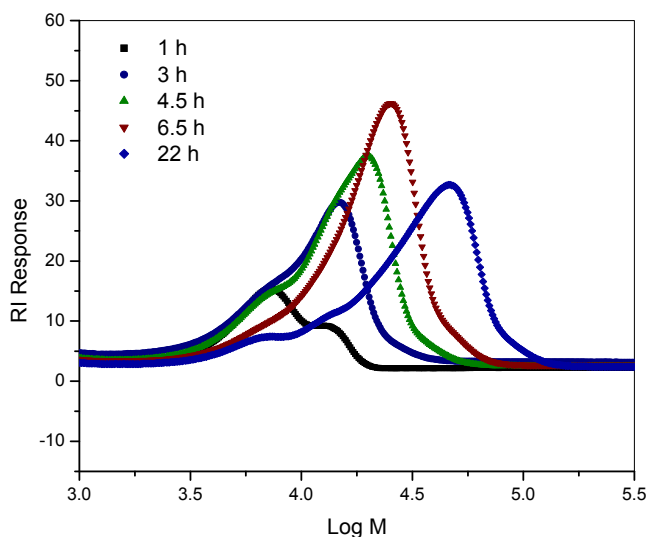


Figure 5.31: SEC graph of RI response vs. $\log M$ for the copolymerisation of styrene with CVADTB MPEG 2000 at 70°C. Macro initiator prepared by Method 1.

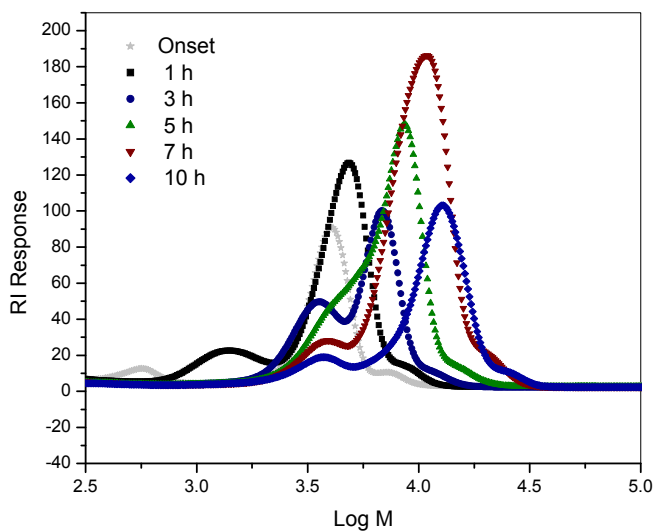


Figure 5.32: SEC graph of RI response vs. $\log M$ for the copolymerisation of styrene with CVADTB MPEG 2000 at 70°C. Macro initiator prepared by Method 2.

In both instances it was evident that controlled growth of the polymer took place. In both Figures 5.31 and 5.32 it could be seen that a certain amount of shouldering existed at the low molar mass end of the SEC curves. In both cases a peak at $\log M \approx 3.5$ indicated the presence of an amount of unreacted MPEG 2000 in the polymerisation product. This was similar to the reaction at 60°C. As stated in Section 5.3.4, where the esterification process to synthesize the CVADTB MPEG 2000 macro RAFT agent is described, the resulting product formed was used without purification.

Figures 5.33 and 5.34 show the 3D representation of the data obtained from the 2D chromatographic analysis of the respective polymer products shown in Figures 5.31 and 5.32. In Figure 5.33 the reaction time was 24 h, while the reaction time for the reaction represented in Figure 5.34 was 11 h. Tables 5.5 and 5.6 give the detailed data analysis of the respective polymerisation products.

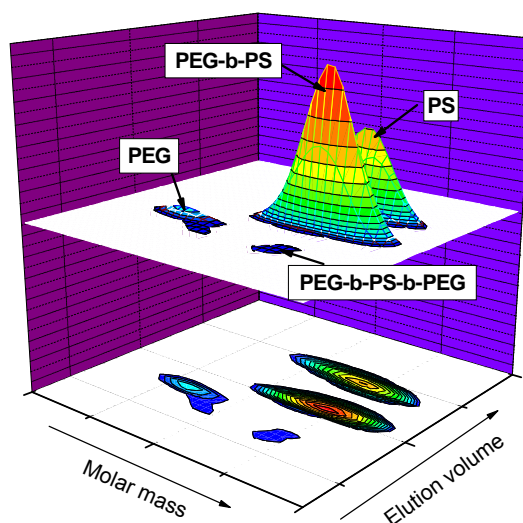


Figure 5.33: Three-dimensional plot of 2D chromatographic analysis for the copolymerisation of styrene with CVADTB MPEG 2000 at 70°C (Method 1).

Figure 5.33 shows the existence of four different species in the product formed. Similar to the case of the reaction at 60°C, the product contained PS and PEG homopolymers, PEG-b-PS diblock copolymer and a small amount of PEG-PS-PEG triblock copolymer. Table 5.5 gives a detailed compositional analysis of the products obtained from the data in Figure 5.33.

Table 5.5: Composition of polymerisation product obtained for the copolymerisation of styrene with CVADTB MPEG 2000 at 70°C (Method 1)

	Relative amount %	\bar{M}_n g/mol	\bar{M}_w g/mol	PDI
PS	37	11200	15400	1.4
PEG-b-PS	52	14600	18400	1.3
PEG-PS-PEG	5	14800	16200	1.2
PEG2000	6			

The amount of PEG-b-PS diblock copolymer formed at 70°C was higher than at 60°C, whilst the amount of MPEG 2000 homopolymer present in the system was less than that in the 60°C reaction. This was attributed to the higher reaction temperature (70°C), which

resulted in a higher fractional conversion of the polymerisation product. Similar to the experiment performed at 60°C, a small number of uncontrolled termination reactions occurred, but the percentage was low, at 6%.

Figure 5.34 and Table 5.6 represent the 3D data and compositional analysis of the 2D chromatographic analysis of the copolymer as shown in Figure 5.32. The reaction time for the copolymerisation product shown was 11 h.

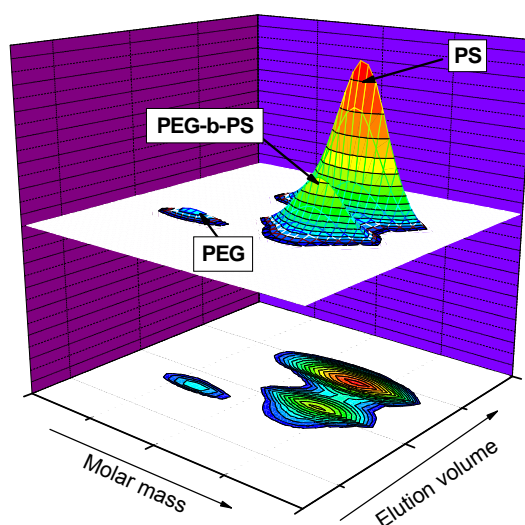


Figure 5.34: Three-dimensional plot of 2D chromatographic analysis for the copolymerisation of styrene with CVADTB MPEG 2000 at 70°C (Method 2).

SEC data from Figure 5.32 only showed bimodality in the SEC curve and, although a small amount of shouldering existed in the SEC curve, no evidence of the existence of a third species in the product was evident. Figure 5.34 shows that the polymer product comprised three different components: homopolymers of MPEG 2000 and PS, and PEG-b-PS diblock copolymer.

Table 5.6: Composition of polymerisation product obtained for the copolymerisation of styrene with CVADTB MPEG 2000 at 70°C (Method 2)

	Relative amount %	\bar{M}_n g/mol	\bar{M}_w g/mol	PDI
PS	70	7400	9900	1.3
PEG-b-PS	26	9500	11500	1.2
PEG2000	4			

In this experiment a large quantity of PS homopolymer was formed (70%), and only 26% PEG-b-PS diblock copolymer was formed. \bar{M}_n and \bar{M}_w values were lower than those shown in Table 5.5. This could be attributed to the shorter reaction time reported here. With the reaction time being shorter than for the experiment shown in Figure 5.33, it could be assumed that the fractional conversion was lower than the fractional conversion of the experiment in Figure 5.33. The contribution of the unreacted MPEG would therefore have an even smaller contribution towards the total polymeric product obtained at longer reaction times. The quantity of PS homopolymer formed, however, was much higher than that formed in the reaction where that CVADTB MPEG 2000 macro RAFT agent prepared via Method 1. In controlled free radical polymerisation, where all species should theoretically grow at equal rates, the rate of growth of the PS homopolymer should show a similar trend to the growth of the PEG-b-PS diblock copolymer. At higher conversions, the ratio of PS:PEG-b-PS should remain reasonably constant.

The PDI of the PS homopolymer formed was low at 1.3, therefore showing a controlled reaction. This could be ascribed to CVADTB present in the system. Method 2 utilises an excess of CVADTB (Section 5.3.4). This, together with the fact that unreacted PEG was being detected in 2D chromatography; indicated the possibility of unreacted CVADTB being present in the esterification product. Although the product was filtered and then washed with ethyl acetate, it was possible for a small percentage of CVADTB would be present in the “purified” esterification product. This CVADTB present in the system would then lead to the controlled homopolymerisation of styrene, parallel to the copolymerisation of styrene with a CVADTB MPEG 2000 macro RAFT agent.

No PEG-PS-PEG triblock copolymer products were detected by 2D chromatography. This could be ascribed to the shorter reaction time, which resulted in lower fractional conversions; there was less possibility of two growing polymer chains recombining. As the reactions were conducted in bulk, termination reactions were more likely to occur at

higher fractional conversions due to the increased viscosity of the reaction medium as well as the depletion of monomer. Longer reaction times could also lead to the degradation of CVADTB, therefore resulting in uncontrolled reactions.

SEC data for the polymerisation of styrene using CVADTB MPEG 2000 macro RAFT agent at 80°C are shown in Figure 5.35.

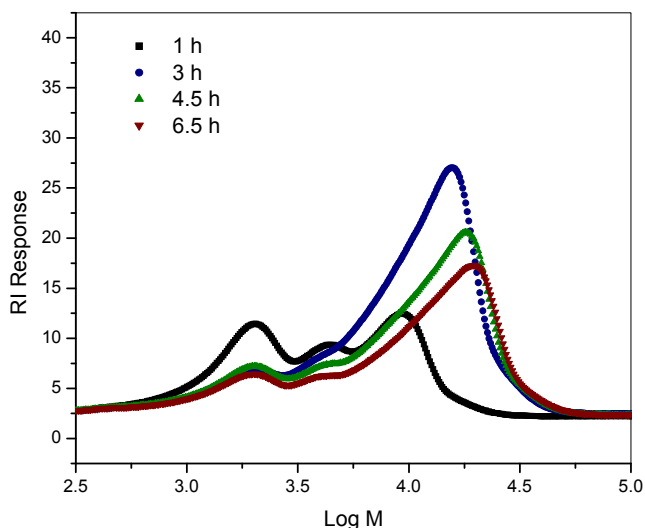


Figure 5.35: SEC graph of RI response vs. $\log M$ for the copolymerisation of styrene with CVADTB MPEG 2000 at 80°C.

The polydispersity of the product formed was much higher than that of the polymerisation products formed at lower temperatures. The shouldering observed at the lower molar mass end of the $\log M$ curves was more pronounced than was the case at the lower reaction temperatures. An increase in the $\log M$ was observed with an increase in reaction time.

Figure 5.36 shows a 3D representation of the 2D chromatographic analysis of the polymerisation product shown in Figure 5.35.

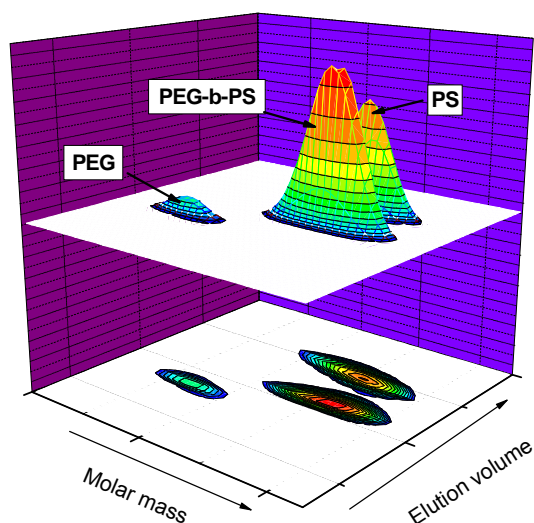


Figure 5.36: Three-dimensional plot of 2D chromatographic analysis for the copolymerisation of styrene with CVADTB MPEG 2000 at 80°C.

Results from Figure 5.36 and Table 5.7 showed that 50% PEG-b-PS diblock copolymer was formed, and unreacted PEG 2000 accounted for 8% of the total polymeric product.

Table 5.7: Composition of polymerisation product obtained for the copolymerisation of styrene with CVADTB MPEG 2000 at 80°C

	Relative amount %	\bar{M}_n g/mol	\bar{M}_w g/mol	PDI
PS	42	12100	16300	1.3
PEG-b-PS	50	16400	20700	1.3
PEG2000	8			

Conventional SEC data showed multimodality in the graph of RI vs. log M. It therefore seemed that control was lost in the reaction. Table 5.7 showed that the polydispersities of the different species in the polymer product were low, showing control in the reaction. No PEG-PS-PEG triblock copolymer is detected, similar to results given in Table 5.6, mainly due to the shorter reaction times.

Figure 5.37 and Figure 5.38 show comparative data of \bar{M}_n (SEC) and polydispersity vs. reaction time for the reactions at 60°C, 70°C and 80°C. At 70°C data of both esterification methods (as described earlier) are given.

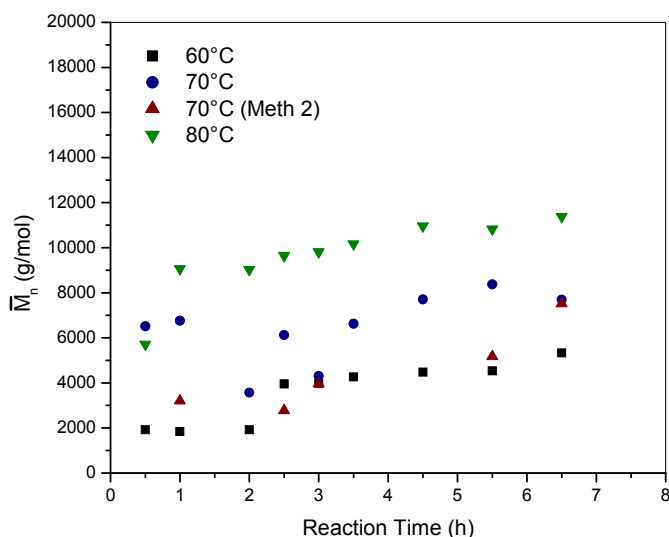


Figure 5.37: Graph of \bar{M}_n (SEC) vs. reaction time for the copolymerisation of styrene with CVADTB MPEG 2000.

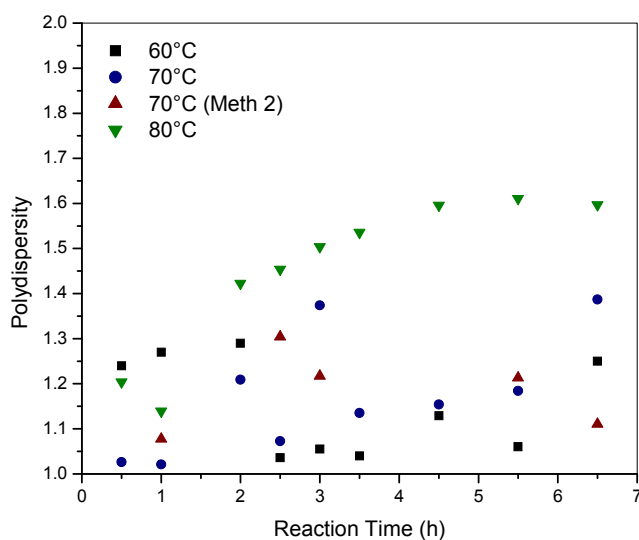


Figure 5.38: Graph of polydispersity vs. reaction time for the copolymerisation of styrene with CVADTB MPEG 2000.

Results with the CVADTB MPEG 2000 complied with the results of previous experiments with CVADTB and CVADTB MPEG 350, which showed that an increase in reaction temperature would result in higher \bar{M}_n values at corresponding reaction times as well as an increase in the polydispersities of the formed products. Higher \bar{M}_n values could either be due to a higher reaction rate, or to the occurrence of uncontrolled reactions due to thermal initiation. Uncontrolled reactions would lead to an increase in the polydispersity of the product formed, which could be observed for the reaction at 80°C. The shouldering that occurred at the low molar mass side of the curves was more pronounced at 80°C than for experiments at 60°C and 70°C. From the comparative results it could be concluded that a reaction temperature of 70°C would be preferred in terms of control of the reaction and the rate of polymerisation.

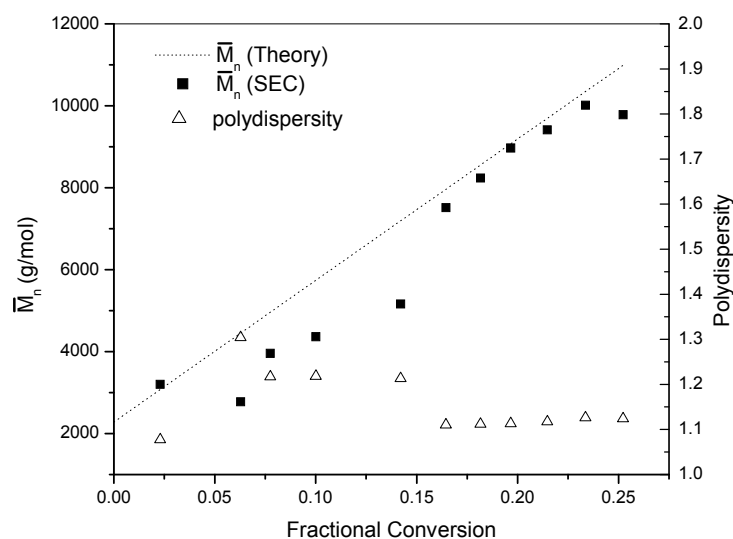


Figure 5.39: Graph of \bar{M}_n and polydispersity vs. fractional conversion for the copolymerisation of styrene with CVADTB MPEG 2000 macro RAFT agent at 70°C.

Figure 5.39 depicts the results of a more detailed investigation into the polymerisation of styrene with CVADTB MPEG 2000 macro RAFT agent at 70°C. It shows the \bar{M}_n and polydispersity values vs. fractional conversion. As can be seen from Figure 5.39, the polydispersity values were well within the benchmark value of 1.5 and the \bar{M}_n values, as determined by SEC, showed good similarity to the theoretically calculated values. With

the reactions occurring in bulk, high fractional conversions were unobtainable due to viscosity effects as a result of the consumption of monomer.

Figure 5.40 shows the first order kinetic plot for the polymerisation of styrene in the presence of CVADTB and a CVADTB MPEG 2000 macro RAFT agent.

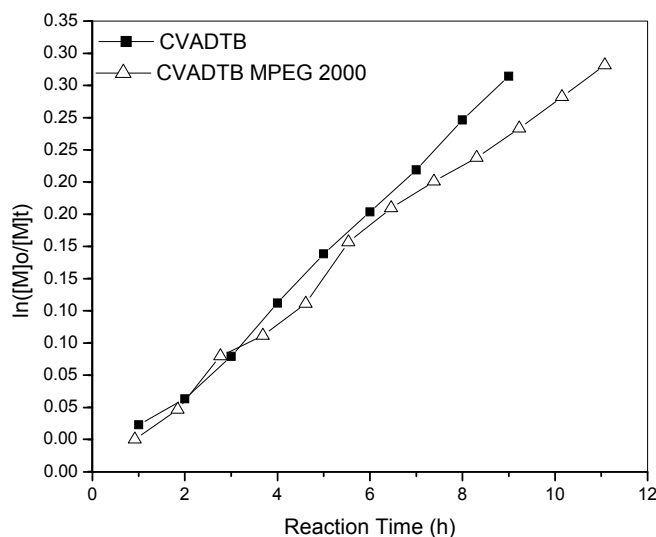


Figure 5.40: First-order kinetic plot for reactions of CVADTB and CVADTB MPEG 2000 with styrene at 70°C.

The first order kinetic plots showed that there was virtually no difference in the rate of the reaction for the different initiating species. The rate of a free radical reaction is normally determined by the diffusion rate of the growing chains within the reaction medium. It is therefore assumed that, according to molecular size, the diffusion of CVADTB MPEG 2000 through the reaction medium would be much slower than CVADTB and the rate of the reaction of the latter would be higher than the rate of the reaction with CVADTB MPEG 2000. This was however not the case.

In bulk polymerisation, the growing chain end is surrounded by monomer; it therefore does not have to diffuse through the reaction medium to collide with a monomer molecule. Furthermore, in bulk polymerisation, where the monomer is the reaction medium, all growing chains have equal probability to grow. The reactions of both CVADTB and CVADTB MPEG 2000 should therefore proceed at similar rate up to a stage where, at high conversions, the bulkiness of the higher molar mass chains will be less mobile in the reaction medium. At high conversions, with most of the reaction medium being depleted

and the growing chains relatively long, diffusion will have effects on the kinetics of the reaction. Bulk polymerisation; however, tends not to reach too high fractional conversion as gelling occurs in the reaction vessel.

It was therefore be concluded here that there was no difference in the rate of the reaction in the cases of CVADTB and CVADTB MPEG 2000, therefore the length of the MPEG block did not affect the rate of polymerisation at low fractional conversion.

5.6.2 Copolymerisation of styrene using DIBTC MPEG 2000 macro RAFT agent

With DIBTC being a “faster” RAFT agent than CVADTB and with the ease of synthesis thereof, DIBTC MPEG 2000 macro RAFT agents were prepared according to Method 1 as described in Section 5.3.5. Polymerisation conditions stated in Section 5.4.1 and Section 5.5.2 were adopted for the copolymerisation of styrene with the aid of DIBTC MPEG 2000 macro RAFT agents.

Figure 5.41 shows the SEC data for the copolymerisation of styrene with DIBTC MPEG 2000 macro RAFT agents at 70°C.

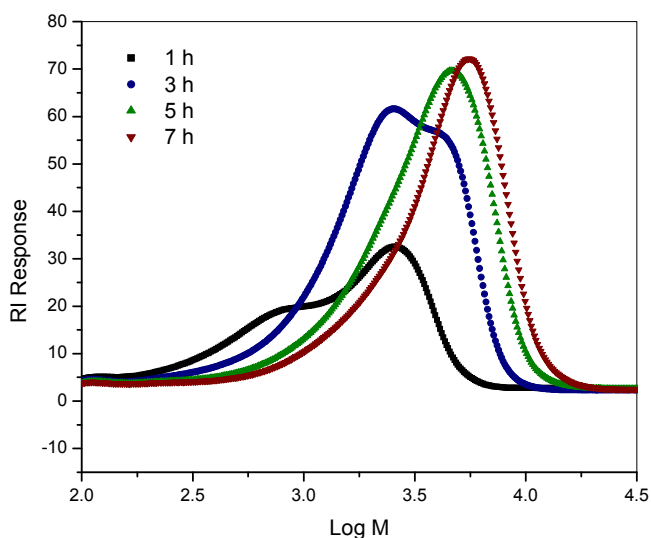


Figure 5.41 SEC graph of RI response vs. log M for the copolymerisation of styrene with DIBTC MPEG 2000 at 70°C.

SEC data showed bimodality in the early stages of the reaction, as could be seen at 1 h and 3 h into the reaction. With an increase in the reaction time, the peak at $\log M \approx 3.3$ diminished, but did not disappear. It therefore seemed that, similar to the reaction of CVADTB MPEG 2000, the esterification process was incomplete and that a percentage of MPEG 2000 remained present in the reaction product. With an increase in reaction time, there was an increase in the $\log M$ values, with the peak at $\log M \approx 3.5$ overlapping with the peak of the growing polymer chains, causing a broadening of the $\log M$ peak. SEC data can be misleading in that it appeared that there was no control in the reaction, as the polydispersity obtained was high (Figure 5.43).

Figure 5.42 gives a 3D representation of the 2D chromatographic analysis of the SEC data shown in Figure 5.41 (the reaction time was 7 h).

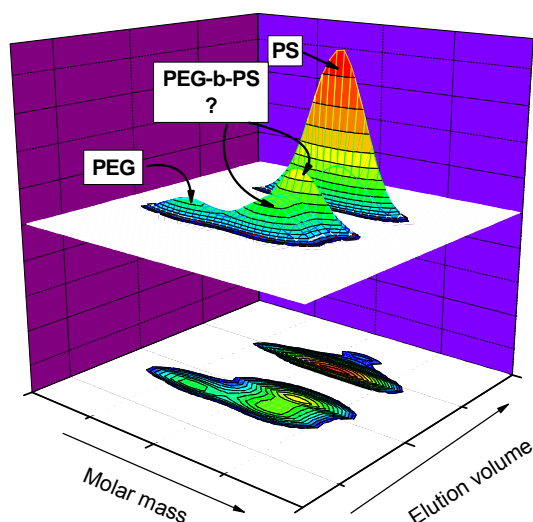


Figure 5.42: Three-dimensional plot of 2D chromatographic analysis for the copolymerisation of styrene with DIBTC MPEG 2000 at 70°C.

From Figure 5.42 it could be seen that three different species were present in the system, in contrast with SEC data in Figure 5.41 where only one broad peak is visible. The low polydispersity values in Table 5.8 showed that there was controlled growth of the polymer chains formed.

Table 5.8: Composition of polymerisation product obtained for the copolymerisation of styrene with DIBTC MPEG 2000 at 70°C

	Relative amount %	\bar{M}_n g/mol	\bar{M}_w g/mol	PDI
PS	54	4800	6300	1.3
PEG-b-PS	21	6300	7800	1.2
PEG-b-PS	16	5600	6700	1.2
PEG2000	9			

A relatively high quantity (54%) of PS homopolymer was formed. Two different peaks were assigned to the PEG-b-PS block copolymers formed with a difference in \bar{M}_n of 500 g/mol. With the molar mass of DIBTC being 364.16 g/mol, this could be due to the fact that some of the species were dormant (end-capped with DIBTC), while the other species were active growing chains. The fractional conversion is low at 30% (Figure 5.43) due to the relatively short reaction time.

Figure 5.43 shows the \bar{M}_n and polydispersity values (as determined by SEC) vs. fractional conversion for the product obtained in the copolymerisation of styrene at 70°C with the use of DIBTC MPEG 2000 macro RAFT agent.

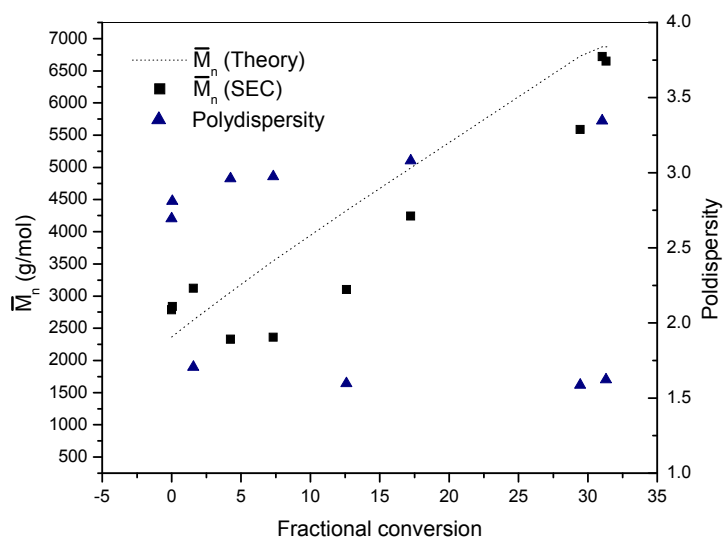


Figure 5.43: Graph of \bar{M}_n and polydispersity vs. fractional conversion for the copolymerisation of styrene with DIBTC MPEG 2000 macro RAFT agent at 70°C.

The observed \bar{M}_n values were in agreement with the theoretically predicted values. The theoretical values, calculated according to the actual fractional conversion, showed a linear trend, as would be expected for a controlled free radical process. The polydispersities of the formed products appeared to be high, but overlapping of the log M peaks for the different species within the product, as shown in Figure 5.41, led to inaccurate calculation of the polydispersity values as determined by SEC. The Millennium[®] software used to analyse the SEC does not take the overlapping of peaks into account and only integrates between the arbitrary selected values. These values are subject to human interpretation and are lower than the observed SEC data. 2D data from Table 5.8 showed a different trend in polydispersity values in that the polydispersity of the different species formed during the reaction were all below 1.3, therefore indicating controlled growth of the growing polymer chains in the reaction mixture.

5.7 PS-b-MPEG 5000 copolymer synthesis

5.7.1 Copolymerisation of styrene using CVADTB MPEG 5000 macro RAFT agent

Literature indicated a tendency towards the use of a PEG with a molar mass of 5000 g/mol for the purpose of membrane hydrophilization.^{16, 17} Following the success of the polymerisation of styrene by making use of RAFT agents containing either MPEG 350 or MPEG 2000, there was a shift in focus towards the synthesis of a diblock copolymer consisting of styrene and MPEG 5000. CVADTB MPEG 5000 macro RAFT agents were synthesized according to the procedure described in Section 5.3.4. Polymerisations were conducted under conditions stated in Section 5.4.1 and Section 5.5.2. Conventional SEC analysis of the polymerisation products obtained was not possible due to the insolubility of these products in THF. MPEG 5000 is insoluble in THF, even at elevated temperatures. Products containing MPEG 5000, i.e. MPEG 5000 macro RAFT agents, as well as MPEG 5000-b-PS block copolymers, were also found to be insoluble in THF and SEC analysis of the formed block copolymers was not possible. MPEG 5000-b-PS block copolymers were, however, found to be soluble in a 90:10 THF:H₂O mixture. This was used as solvent in the 2D analysis of these copolymers. Figure 5.44 gives a 3D representation of the 2D chromatographic analysis of the copolymerisation product obtained, the reaction time being 7 h.

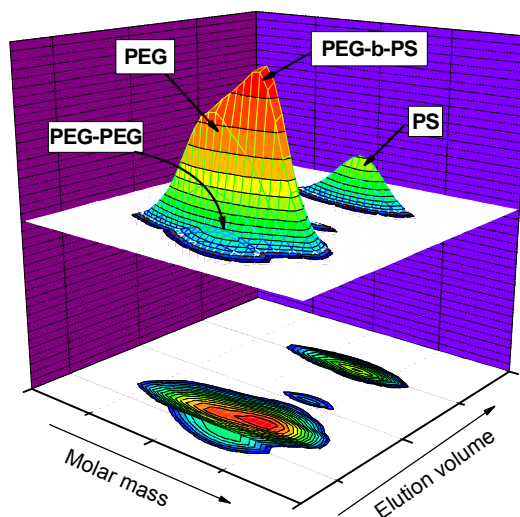


Figure 5.44: Three-dimensional plot of 2D chromatographic analysis for the copolymerisation of styrene with CVADTB MPEG 5000 at 70°C.

Figure 5.44 and Table 5.9 show that 25% unreacted PEG 5000 was present in the polymerisation product and that the PEG-*b*-PS diblock copolymer content was 56%. Very low PS content was found. This was mainly due to the low fractional conversion at 22% (Figure 5.45). As only 22% of the styrene monomer had been converted to polymer, and with the MPEG 5000 RAFT agent being added in terms of molar ratio to styrene, the mass of CVADTB MPEG 5000 represented a large fraction of the total mass of the polymeric product. The rate of addition of monomer is low, as in starting with CVADTB MPEG 5000 (\bar{M}_n of 5278 g/mol), the \bar{M}_n of the PEG-*b*-PS copolymer formed after 7 h in the reaction was 7 900 g/mol.

Table 5.9: Composition of polymerisation product obtained for the copolymerisation of styrene with CVADTB MPEG 5000 at 70°C

	Relative amount %	\bar{M}_n g/mol	\bar{M}_w g/mol	PDI
PS	14	6200	8200	1.3
PEG-b-PS	56	7900	9200	1.2
PEG5000	25			
PEG-PEG	4			

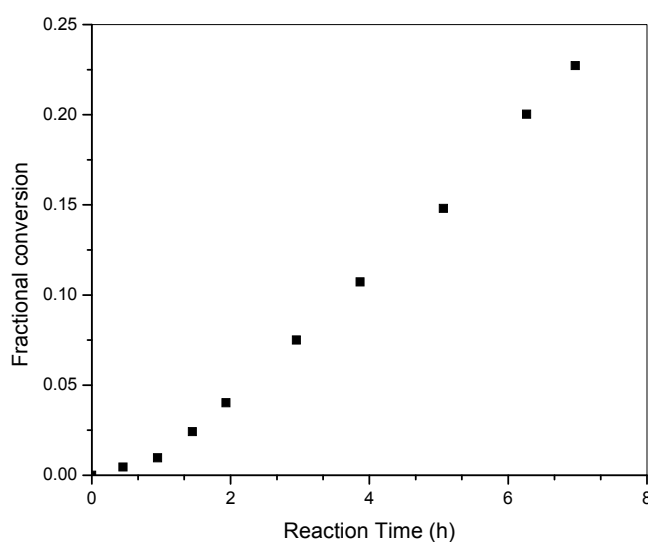


Figure 5.45: Graph of fractional conversion vs. reaction time for the copolymerisation of styrene with CVADTB MPEG 5000 macro RAFT agent.

Figure 5.46 show comparative fractional conversions of the CVADTB- and DIBTC RAFT agents and their respective MPEG counterparts. Results showed that the size of the MPEG coupled to the RAFT agent did not have a major effect on the fractional conversion. CVADTB, MPEG 2000, and MPEG 5000 derivatives all showed similar fractional conversions at similar reaction times. The same phenomenon was found to be true for DIBTC and DIBTC MPEG 2000 RAFT initiators.

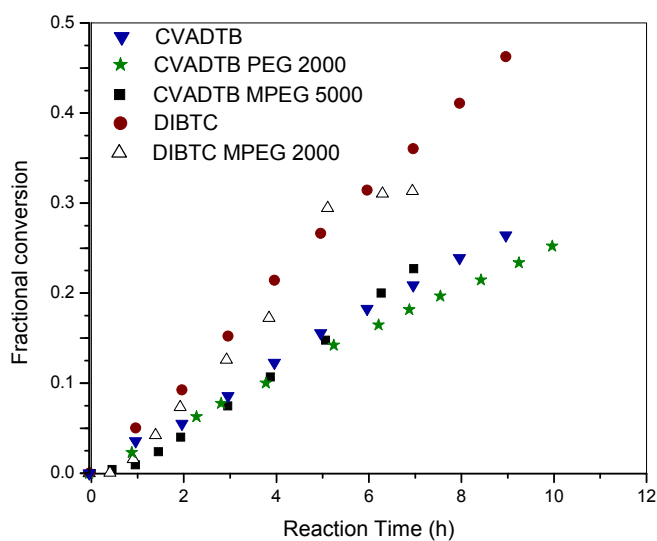


Figure 5.46: Comparative graph of fractional conversion vs. time for polymerisation of styrene with CVADTB- and DIBTC based RAFT initiators.

By comparing the first-order kinetic plots (Figure 5.47), it was concluded that the size of the RAFT agent did not have a significant influence on the rate of the reactions as the CVADTB-based macro RAFT agents showed kinetic data in agreement with the homopolymerisation of styrene with CVADTB. This was also found to be true for the DIBTC based macro RAFT agents. This data was in agreement with the fractional conversion data.

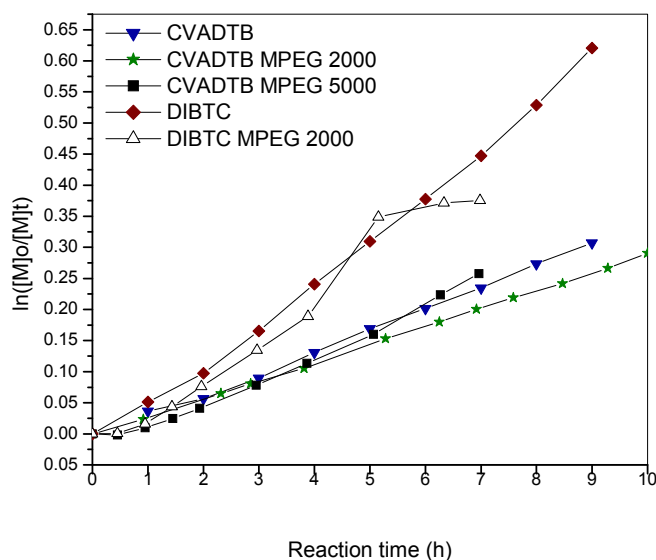


Figure 5.47: Comparative first-order kinetic plot for the polymerisation of styrene with CVADTB- and DIBTC based RAFT initiators.

5.8 Conclusions

From the RAFT assisted homopolymerisation of styrene and copolymerisation of styrene in the presence MPEG macro RAFT agents, the following conclusions were drawn:

1. In the controlled free radical homopolymerisation of styrene with the aid of CVADTB and DIBTC as RAFT agents it was found that both RAFT agents were effective in producing homopolymers with narrow MMD. CVADTB was found to be what is termed a “slow” RAFT agent, in that the rate of transfer from and to RAFT agent was low. The rate of transfer for DIBTC, on the other hand, was faster than that of CVADTB. In the homopolymerisation of styrene with CVADTB, an increase in reaction temperature resulted in an increase in the rate of the reaction, however, as the reaction temperature was increased, control over the growth of the polymer was compromised in that there was an accompanying increase in the MMD of the polymer. With RAFT assisted homopolymerisation of styrene it was possible to predict the molar mass of the PS homopolymer formed, therefore offering the possibility of synthesizing tailored polymers with narrow MMD.

2. Copolymers were successfully prepared via the RAFT assisted copolymerisation of styrene with PEG-based macro RAFT agents. Conventional SEC was found to be insufficient in the characterisation of these polymers. A 2D chromatographic system revealed the chemical composition distribution of the formed polymer products. Overlapping of peaks in conventional SEC resulted in incorrect conclusions being drawn. In all cases studied, the polymerisation products obtained contained at least three components, PS and PEG homopolymers, as well as PEG-b-PS block copolymer. In certain instances, especially at longer reaction times, and therefore higher fractional conversions, uncontrolled termination reactions led to the formation of PEG-PS-PEG triblock copolymers.
3. Certain factors proved to have an influence on the products formed. The most important factor was the method of formation of the MPEG macro RAFT agents (two methods were employed). Method 1 as described in Section 5.3.4 yielded MPEG macro RAFT agents that produced less PS homopolymers. PTSA and DMAP were essential in increasing the yield of the MPEG macro RAFT agents. Parallel with homopolymerisation, an increase in the reaction temperature resulted in an increase in the polydispersity of the formed polymers. The PS homopolymer fraction formed in the reaction with the DIBTC macro RAFT agents was higher compared with the CVADTB counterparts. It therefore appears that higher yields were obtained in producing CVADTB MPEG macro RAFT agents as opposed to DIBTC MPEG macro RAFT agents.
4. 2D chromatography proved to be instrumental in analysing the polymer products formed.
5. In accordance with homopolymerisation, CVADTB MPEG macro RAFT agents were termed as “slow” RAFT agents, while DIBTC MPEG macro RAFT agents offered faster rates of transfer and the reactions with DIBTC macro RAFT agents therefore reached higher fractional conversion at corresponding reaction times compared to CVADTB macro RAFT agents (Figure 5.46).

5.9 References

1. Baran, K., Laugier, S. and Cramail, H., Fractionation of functional poly(styrenes), poly(ethylene oxide)s and poly(styrene)-b-(poly(ethylene oxide)) by liquid chromatography at the exclusion-adsorption transition point, *Journal of Chromatography B*, **2001**, 139-149.
2. Pasch, H. and Trathnigg, B., HPLC of polymers, *Springer-Verlag, Berlin*, **1998**.
3. Nguyen, S. H., Berek, D., Capek, I. and Chiantore, O., Polystyrene-graft-poly(ethylene oxide) copolymers prepared by macromonomer technique in dispersion. I. Liquid chromatographic separation of product mixtures, *Journal of Polymer Science: Part A: Polymer Chemistry*, **2000**, 38, 2284-2291.
4. Pasch, H., Hyphenated techniques in liquid chromatography of polymers, *Advances in Polymer Science*, **2000**, 150, 1-66.
5. Le, T., Moad, G., Rizzardo, E. and Thang, S., Polymerisation with living characteristics, *WO 98/01478*, **1998**.
6. Thang, S., Chong, Y. K., Mayadunne, R. T. A., Moad, G. and Rizzardo, E., A novel synthesis of functional dithioesters, dithiocarbamates, xanthates and trithiocarbonates, *Tetrahedron Letters*, **1999**, 40, 2435-2438.
7. Lai, J. T., Filla, D. and Shea, R., Functional polymers from novel carboxy-terminated trithiocarbonates as highly efficient RAFT agents, *Macromolecules*, **2002**, 35, 6754-6756.
8. De Brouwer, H., Schellekens, M. A. J., Klumperman, B., Monteiro, M. J. and German, A. L., Controlled radical copolymerisation of styrene and maleic anhydride and the synthesis of novel polyolefin-based block copolymers by reversible addition-fragmentation chain transfer polymerisation, *Journal of Polymer Science: Part A: Polymer Chemistry*, **2000**, 38, 3596-3603.
9. Shi, L., Chapman, T. M. and Beckman, E. J., Poly(ethylene glycol)-block-poly(N-vinylformamide) copolymers synthesised by the RAFT methodology, *Macromolecules*, **2003**, 36, 2563-2567.

10. Moad, G., Chiefari, J., Chong, Y.-K., Krstina, J., Mayadunne, R. T. A., Postma, A., Rizzardo, E. and Thang, S., Living free radical polymerisation with reversible addition-fragmentation chain transfer (the life of RAFT), *Polymer International*, **2000**, 993-1001.
11. McLeary, J. B., Reversible addition-fragmentation transfer polymerisation in heterogeneous aqueous media, *PhD dissertation, University of Stellenbosch*, **2004**.
12. Haddleton, D. M., Kukulj, D., Duncalf, D. J., Heming, A. M. and Shooter, A. J., Low-temperature living "radical" polymerisation (atom transfer polymerisation) of methyl methacrylate mediated by copper (I) N-alkyl-2-pyridylmethanimine complexes, *Macromolecules*, **1998**, 31, 5201-5205.
13. Rosen, S. L., Fundamental principles of polymeric materials, *Wiley Interscience, United States of America*, **1993**.
14. De Brouwer, H., RAFT memorabilia: living radical polymerisation in homogeneous and heterogeneous media, *PhD dissertation, Eindhoven*, **2001**.
15. Xie, H.-Q. and Xie, D., Molecular design, synthesis and properties of block and graft copolymers containing polyoxyethylene segments, *Progress in Polymer Science*, **1999**, 24, 275-313.
16. Hancock, L. F. and Ting, Y.-P. R., Preparation of polysulfone/poly(ethylene oxide) block copolymers, *Macromolecules*, **1996**, 29, 7619-7621.
17. Hancock, L. F., Fagan, S. M. and Ziolo, M. S., Hydrophilic, semipermeable membranes fabricated with poly(ethylene oxide)-polysulfone block copolymer, *Biomaterials*, **2000**, 21, 725-733.

Chapter 6

Polysulphone-b-poly (ethylene glycol) triblock copolymer synthesis and characterisation

6.1 Introduction

The objective of this investigation was the synthesis of well-defined amphiphilic block copolymers for the improvement of the properties of polysulphone membranes. As stated in Chapter 5, where the rationale behind the choice of monomers and macromonomers was discussed, it is important that the hydrophilic block of the amphiphilic block copolymer is compatible (miscible) with polysulphone (PSU), as this is the substrate to be treated. In this study, the main aim was to determine the influence of the hydrophilic:hydrophobic ratio (A:B, where A refers to the hydrophilic segment and B refers to the hydrophobic segment of the copolymer) on the physical properties of the polymerisation products. It was therefore important that good control be exercised in the synthesis of these polymers. In order to minimize the amount of variables regarding the A:B ratio of the block copolymer, the following general method of synthesis was proposed:

- use a known poly (ethylene glycol) mono methyl ether (MPEG) as starting material (hydrophilic segment, A),
- select suitable functional monomers for the polycondensation of these monomers with MPEG to form the resulting ABA triblock copolymer.

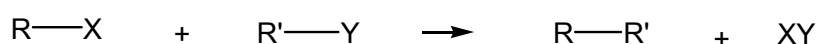
The groups of Hancock¹⁻⁴ and Klein⁵ have reported on the synthesis and characterisation of PSU-b-PEG block copolymers as well as their use in the improvement of the properties of membrane substrates in biomedical applications.

All chemical reactions are divided into different classes according to the mechanism (chemistry) of these reactions. In Chapter 4 and Chapter 5 free radical chemistry and specifically controlled free radical chemistry was discussed. Free radical chemistry is an *addition (chain growth) polymerisation* process, where unsaturated monomers can add to any growing chain. The synthesis of PSU is classified in the group of chemical reactions referred to as *condensation (step-growth) polymerisations*. Before the synthesis of PSU-b-PEG block copolymers is discussed, it is important to have an understanding of

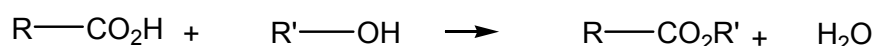
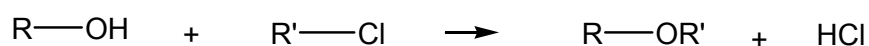
polycondensation reactions in general, as well as the polyetherification reaction for the synthesis of PSU.

6.2 Polycondensation reactions

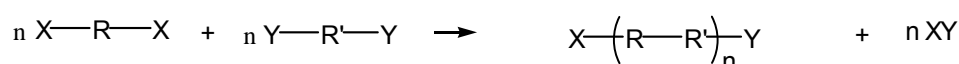
Condensation reactions differ from addition polymerisation (Section 4.2), where unsaturated molecules add on to a growing chain, in that monomers with different reactive functional end groups react to form new products. During the course of condensation reactions two monomers with different functionality react (combine) to form a new product, usually with the evolution of a small molecule as by-product.⁶



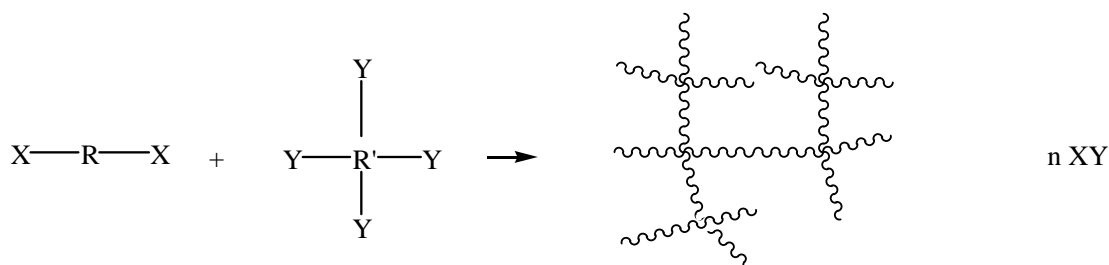
Depending on the nature of the functional groups, the small molecule evolved could be H₂O, CO₂, HCl, etc., for example:



In polycondensation reactions, where each monomer is di-functional, a linear polymer will be formed:



Using monomers with functionality greater than two results in the formation of branched polymers.

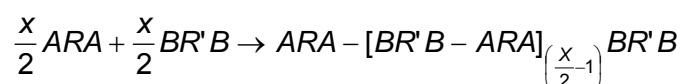


Regardless of the type of polymerisation reaction, quantitative treatments are normally based on the assumption that the reactivity of the functional group at a chain end is

independent of the length of the chain. In practice, this is an excellent assumption for n greater than five or six.

The statistics of polycondensation reactions are of importance in terms of the experimental design of reactions. It is important that certain key aspects be addressed in order to fully understand the basis of polycondensation reactions.

Consider the case where both reacting molecules are difunctional:⁶



where A and B represent the complementary functional groups, and R and R' the unreactive parts of the molecule. It is important to note that x is used to denote the number of monomer residues or structural units in the chain, rather than the repeating units.

Each of the polymer molecules contains a total of x A groups (1 unreacted A end group and $x-1$ reacted groups).

Let p = probability of finding a reacted A group
 = mol fractions of reacted A groups present
 = conversion of reaction of A groups

$\Rightarrow (1-p)$ = probability of finding an unreacted A group

N = total number of molecules present in the reaction

n_x = number of molecules containing x A groups, both reacted and unreacted

$\Rightarrow \frac{n_x}{N}$ = total probability of finding a molecule with x A groups

= total probability of finding $x-1$ reacted A groups and 1 unreacted A group

= $p^{(x-1)}(1-p)$

= mol fraction x -mer

This is the so-called most probable distribution.

In polycondensation reactions it will always be found that there are more shorter chains than longer chains. At higher conversions, however, shorter chains recombine to form longer chains, therefore increasing the number of longer chains and resulting in a decrease in the number of shorter chains. The number average chain lengths of polymers formed by polycondensation can be derived as follows:

Each molecule in the reaction has one unreacted A group. If N_0 is the original number of molecules present in the reaction, there will be N_0 unreacted A groups present at the onset of the reaction. At a certain stage in the reaction, there are N unreacted A groups present, therefore $N_0 - N$ of the A groups have reacted. Therefore,

$$p = \frac{N_0 - N}{N_0} = \text{fraction of reacted A groups} \quad (6.1)$$

Further, with N_0 the original number of molecules present at the onset of the reaction and N the number of molecules present at time t in the reaction, the average number of monomer residues per molecule, \bar{x}_n is given by

$$\bar{x}_n = \frac{N_0}{N} = \text{average number of monomer residues per molecule} \quad (6.2)$$

This gives:

$$\bar{x}_n = \frac{1}{1 - p} \quad (\text{Carothers' equation}) \quad (6.3)$$

If the restrictions of stoichiometric equivalence are removed, then

$$\bar{x}_n = \frac{1 + r}{1 + r - 2rp} \quad (6.4)$$

where $r = \frac{N_{A0}}{N_{B0}}$ (stoichiometric ratio of functional groups present), with component A taken as the limiting reactant, therefore $r < 1$ and p represents the fraction of reacted A groups.

By taking $p=1$, therefore having reacted all of the molecules of A , the limiting reactant, reduces \bar{x}_n to

$$\bar{x}_n = \frac{1+r}{1-r} \quad (6.5)$$

By therefore controlling r , the extent of the reaction can be manipulated. With $r=1$, theoretically one molecule of infinite length will result. By changing r , the value of \bar{x}_n can be changed, as can be seen in Table 6.1

Table 6.1: Effect of variation in r on \bar{x}_n

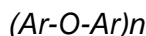
r	\bar{x}_n
0.99	199
0.975	79
0.95	39
0.9	19
0.5	3

It is therefore important to have conditions as close as possible to stoichiometric equivalence to reach high conversion.

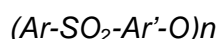
6.3 Polysulphone homopolymer synthesis

6.3.1 Introduction

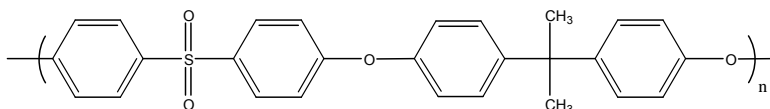
PSU is classified under the general classification as an aromatic polyether,⁷ with the following structure:



More precisely the general classification of polysulphone is represented by the following structure:



Specifically, PSU is characterised by the following repeat unit structure:



PSUs are chemically stable, main chain arylene polymers with broad applications as basis materials for both porous and dense polymeric membranes.⁸ One of the main advantages is that PSU can be modified by both electrophilic and nucleophilic reactions to yield polymers with specific properties.⁸ Electrophilic reactions take place in the electron-rich Bisphenol A part of PSU, whereas the nucleophilic reactions occur in the electron deficient diaryl sulphone segment of the polymer.⁸

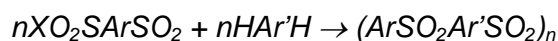
6.3.2 Possible synthetic routes

Polycondensation reactions producing polysulphone are of two general types:

- 1 polycondensation via sulphonyl linkage formations, and
- 2 polycondensation of reactants containing sulphonyl groups.

In terms of polycondensation via sulphonyl linkages, three different routes are possible, namely:

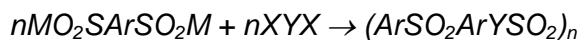
- Friedel-Crafts polycondensation of arenedisulphonyl halides with compounds bearing at least two aromatic hydrogens (here X represents a halogen),



- polycondensation of arenedisulphonic acids with compounds having at least two aromatic hydrogen atoms, and



- polycondensation of alkali metal arenedisulphinates with dihalides.

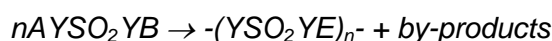


In terms of the polycondensation of reactants bearing sulphonyl groups the following are essential:

- the molecules must have functional groups that are able to react with each other



- or in the case of self-polycondensation, where the molecule has two different functional groups, must be able to react with a similar molecule.

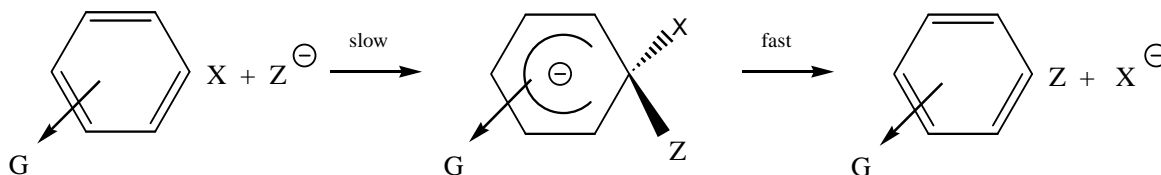


This study will focus on the polycondensation products formed from monomers bearing sulphonyl groups.

6.3.3 Polycondensation of monomers bearing sulphonyl groups

Polycondensation, as compared to sulphonylation reactions, are generally feasible under mild conditions and give little or no structural irregularity, branching, or crosslinking, which are common with sulphonylation reactions.⁹ Polycondensation often represents the best synthetic route to polymers containing sulphonyl groups. Polymers containing sulphonyl groups can also be prepared by polysulphonylation, as in the case of polyetherification to produce poly (aryl ether sulphone).

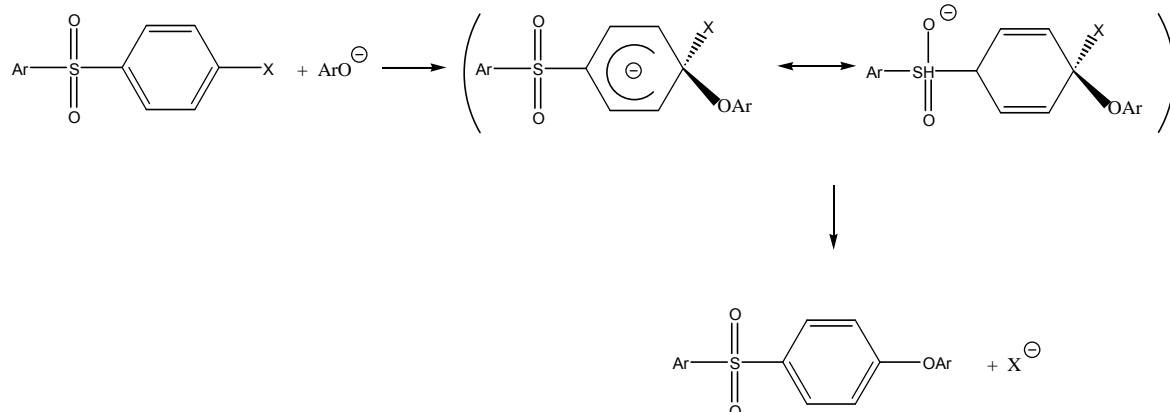
Aryl halides activated by electron-withdrawing substituents ($-\text{NO}_2$, $-\text{CN}$, $-\text{SO}_2\text{Ar}$, $-\text{SO}_2\text{R}$, $-\text{COAr}$, $-\text{COR}$, etc.) *ortho* or *para* to the halogen on the aromatic nucleus can undergo halogen substitution by nucleophilic reagents in highly dipolar solvents. Aromatic nucleophilic substitutions operated by reagents of weak to medium basicity (such as ArO^- , RO^- , HO^- , ArSO_2^- , and CN^-) follow a bimolecular elimination-addition mechanism,¹⁰ through intermediate complexes with highly delocalized negative charges:



Scheme 6.1: Bimolecular elimination-addition mechanism.

Here G, X and Z represent the electron-withdrawing substituent, the halogen, and the anion of the nucleophilic agent. The intermediate adducts are often called Meisenheimer complexes. Electron-withdrawing substituents cause strong stabilization of the intermediate complex by conjugation with the negative charge when they are *ortho* or *para* to the halogen. These substituents therefore promote the slowest (rate determining) initial step in the reaction and therefore the overall rate of the reaction.

In the following situation, the sulphonyl moiety powerfully activates halogen displacement by stabilization of the intermediate adduct resulting from attack of the phenoxide anion.



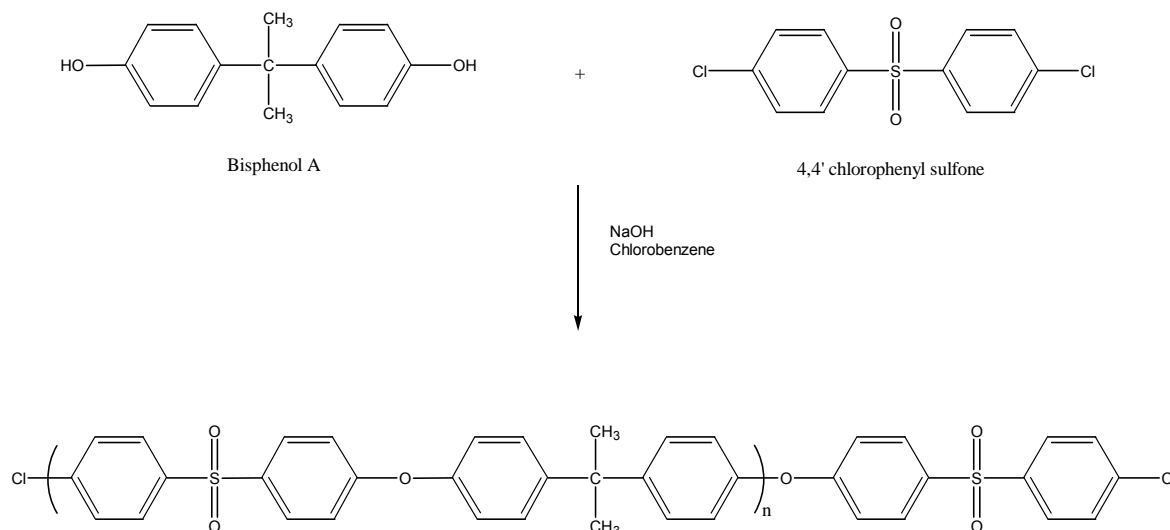
Scheme 6.2: Etherification by nucleophilic substitution.

With the replacement of Ar with ArX , and ArO^- with $-OArO^-$, polyetherification reactions take place.

6.3.4 Bis (4-chlorophenyl) sulphone-bisphenol A polysulphone

6.3.4.1 Background

PSU has been produced by Union Carbide Corporation since 1965 by the reaction of Bisphenol A (BPA) with 4,4'-dichlorophenyl sulphone (CPS) under basic conditions:¹¹



Scheme 6.3: Bis (4-chlorophenyl) sulphone-bisphenol A polysulphone synthesis.

The whole process is carried out under an inert atmosphere to avoid phenoxide oxidation, which cause polymer discoloration.

Kerres *et al.*⁸ and Guiver *et al.*¹² have reported on the modification of PSU by the introduction of functional groups on the backbone structure. Both authors reported to the introduction of aldehyde groups into the structure.

6.3.4.2 Reaction mechanism

The mechanism of the reaction has been studied in detail, including the influence of temperature, cations and solvent. Polyetherification reactions such as the synthesis of polysulphone occur by the bimolecular addition-elimination path of aromatic nucleophilic substitution.^{11, 13, 14} The influence of the different halogens on the increase in the rate of polycondensation follows an expected trend ($F \gg Cl \geq Br \geq I$) in aromatic nucleophilic substitutions, with the condensation of the fluorides being extremely fast.

Aromatic halide reactivity and phenoxide basicity are strongly influenced, in opposite senses, by both electron affinity and the position of aromatic ring substituents, and by their conjugative, inductive, and steric effects. Electron withdrawing groups enhance halide reactivity and vice versa depress the phenoxide basicity by delocalization of the negative charge of the phenoxide anion. The activating effect of the sulphonyl group on the halogen in one ring can further be enhanced by electron withdrawing or electron-releasing substituents in a sulphonyl-linked adjacent nucleus, mainly by conjugation when the groups are in the *ortho* or *para* positions. In a certain sense, the sulphonyl group can play a "bridge effect", in that it transmits the influence of the substituents to an adjacent ring.

6.3.4.3 Possible side reactions

Even in some of the earliest polyetherification reactions to form polysulphones, several side reactions were reported.¹¹ In two-component polycondensation reactions, even under anhydrous starting conditions, an excess of base (alkali metal hydroxide) over Bisphenol A implies irreversible halogen displacement from part of the bis (halo phenyl) sulphone and yields a certain amount of alkali metal phenoxide. Although still able to self-polycondensate under more drastic conditions, the required 1:1 halide:phenoxide stoichiometry is altered, an excess of free alkali metal phenoxide is left present and low molar mass product results.¹³

On the other hand, residual water or moisture present during the polymerisation, though unable to react with the halide, reversibly hydrolyzes the alkali metal hydroxides to form free alkali metal hydroxide, the equilibrium concentration of which depends mainly on the

phenol acidity. The hydroxide produced, in turn, leads again to irreversible halogen displacement of the dihalide.

Free alkali metal hydroxides, accidentally present in excess or coming from alkali metal phenoxide hydrolysis, cause a reduction in the molar mass. Under proper anhydrous conditions, the phenoxide end groups of the growing polymer chain can attack ether linkages similar to ester interchange in polyesterification. This ether interchange does not have an influence on the molar mass of the product formed, but does lead to the formation of polymers with irregular repeat structures.

6.3.4.4 Synthesis of bis (4-chlorophenyl) sulphone-bisphenol A polysulphone

Hancock *et al.*¹ reported on the synthesis of PEG-PSU-PEG triblock copolymers via polycondensation of bis(4-chlorophenyl) sulphone, Bisphenol A and MPEG. In order to gain insight into the polycondensation reaction, conditions used by Hancock were modified for the synthesis of PSU homopolymer.

The following chemicals were used in the synthesis of PSU homopolymer.

Chemicals:

Bisphenol A [80-05-7] (Aldrich), bis (4-chlorophenyl) sulphone [80-07-9] (Aldrich), potassium carbonate [584-08-7] (Unilab), N-methylpyrrolidinone (NMP) [5075-92-3] (BASF, USA), toluene [108-88-3] (Sigma).

NMP and Toluene were redistilled prior to use.

A typical composition of a polycondensation reaction to form PSU is as shown in Table 6.2.

Table 6.2: Typical quantities of reagents used for PSU preparation

Bisphenol A	5.70g	0.0250 mol
Bis (4-chlorophenyl) sulphone	7.54g	0.0263 mol
K ₂ CO ₃	8.20g	0.0602 mol
NMP	40mL	
Toluene	60mL	
r	0.95	
\bar{x}_n	39	

Procedure:

- Bisphenol A, bis (4-chlorophenyl) sulphone, K₂CO₃ were charged to a 250 mL round bottom flask equipped with a stirrer, Dean-Starke trap, nitrogen purge and a thermometer.
- NMP and toluene were added under a nitrogen purge.
- The Dean Starke trap was filled with toluene.
- The reaction vessel was heated to a point where the toluene refluxed (130°C to 150°C).
- Water was removed in the Dean Starke trap as a toluene/water azeotrope over a period of 4 h.
- The toluene was distilled from the system, whereafter the temperature was increased to 190°C to effect polymerisation.
- The polymerisation was allowed to continue for 6 h, whereafter the polymer solution was precipitated in an excess of water containing sufficient HCl to neutralize the K₂CO₃.
- The polymer was washed with water and dried in an oven under reduced pressure.

6.3.4.5 SEC characterisation of bis (4-chlorophenyl) sulphone-bisphenol A polysulphone

Sample preparation and SEC analysis were performed according to methods described in Chapter 5, Section 5.2.2 for the PEG-b-PS copolymers. Figure 6.1 shows the SEC data of the bis (4-chlorophenyl) sulphone Bisphenol A polysulphone.

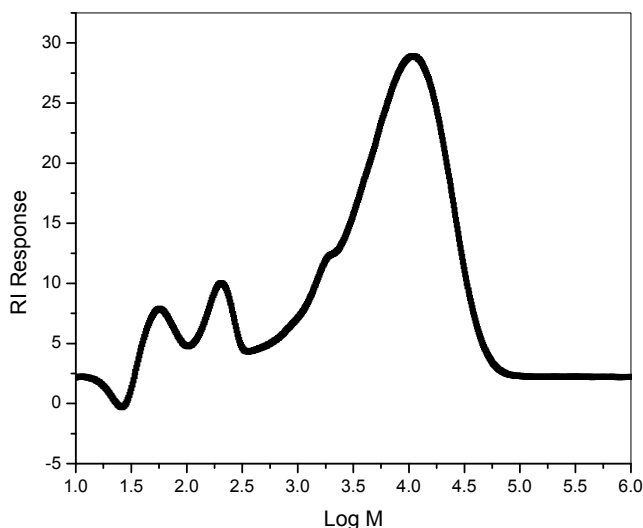


Figure 6.1: Graph of RI response vs. log M for the polycondensation of bis (4-chlorophenyl) sulphone and Bisphenol A.

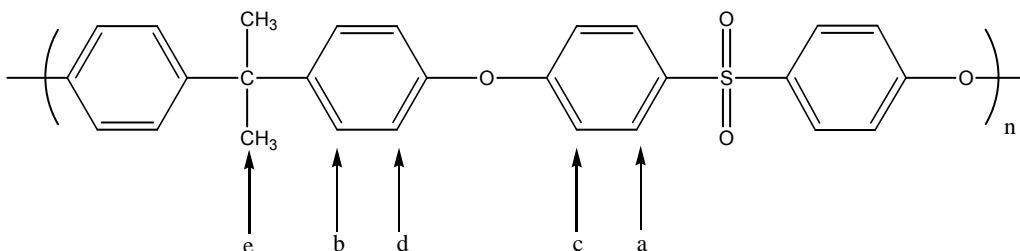
The SEC calibration curve used in this experiment was similar to the curve used in Chapter 5, a calibration curve based on narrow distribution PS. Although conventional SEC would be insufficient in the characterisation of the formed polycondensate, relative values could be useful in comparing the different PEG-b-PSU copolymers synthesized. In Chapter 5 it is shown that SEC gave separation based on the hydrodynamic volume of a sample in a given solvent system and not on the chemical composition of a sample. It was also shown that functional groups and copolymers of different chemical structure, molar mass, and MMD might exhibit similar SEC character. Unfortunately, the 2D chromatographic system employed in Chapter 5 for the analysis of the different PEG-b-PS block copolymers could not be employed for the analysis of the PSU-PEG block copolymers. 2D chromatography is unique to each copolymer system, as it is based on separation of blends or copolymers in terms of the “critical conditions” of one polymer, as discussed in Chapter 5.

The peaks at $\log M \approx 1.75$ and 2.25 (Figure 6.1) were either unreacted monomer species or solvents in the product. The main peak at $\log M \approx 4.0$ showed a rather narrow distribution for polycondensation reactions at 1.64. It should be noted that the reaction time was relatively short and conversion low, therefore there would be a higher distribution of shorter chain polymer molecules at this stage in the reaction. This is typical of what is expected in polycondensation reactions (Section 6.2). It is expected that the polydispersity of the formed polymer would increase at higher conversions.

6.3.4.6 NMR analysis of bis (4-chlorophenyl) sulphone-bisphenol A polysulphone

NMR is a powerful analytical technique; it provides chemical composition analysis of the formed PSU polymer. Where ^{13}C NMR gives a detailed description of the carbon backbone and side chains, ^1H NMR provides the relative quantities of different protons within the polymer. The NMR analysis was performed as described in Chapter 5.

The proposed structure of the repeat unit of the synthesized PSU homopolymer is given as follows:



^1H NMR and ^{13}C NMR spectra of the synthesized PSU polymer are shown in Figures 6.2 and 6.3

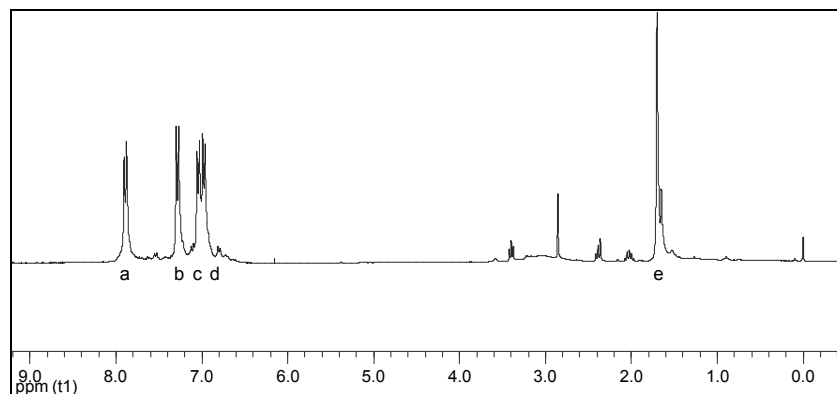
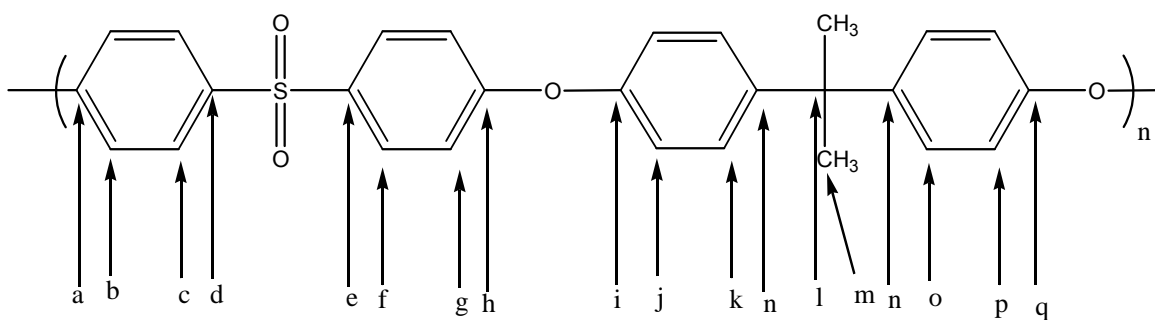


Figure 6.2: ^1H NMR spectrum of PSU homopolymer.

^1H NMR data in Figure .2 were in good agreement with the predicted ^1H NMR shifts as well as with the published data of Hancock *et al.*¹ Note the assignment of the chemical shift of the different protons in the polymer as this will be of relevance in the determination of the PEG content of the block copolymer as discussed in Section 6.4

The ^{13}C NMR shifts for the backbone structure of the bis (4-chlorophenyl) sulphone Bisphenol A polysulphone polycondensate are given in Figure 6.3:



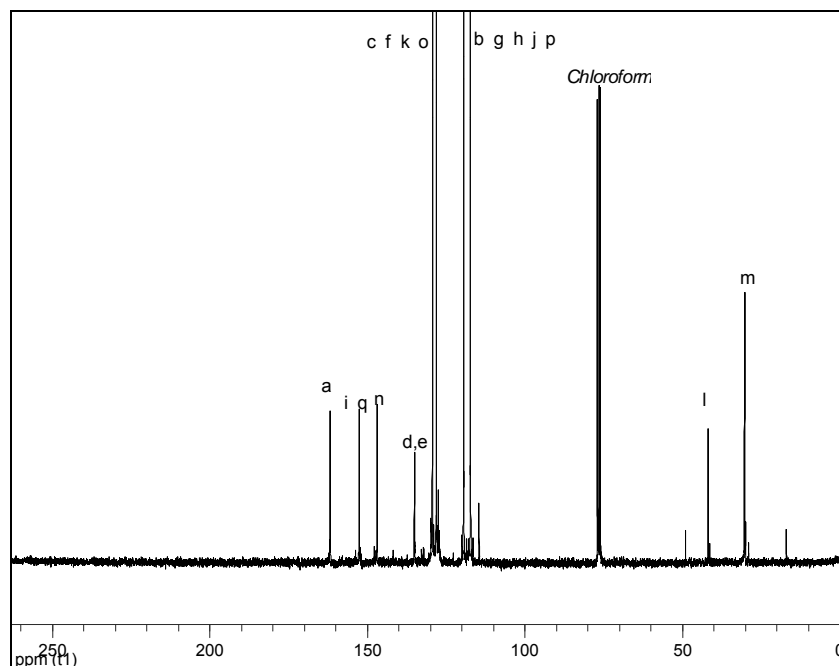


Figure 6.3: ^{13}C NMR spectrum of PSU homopolymer.

From Figure 6.3 it was concluded that the desired PSU polymer had been formed by the polycondensation of bis (4-chlorophenyl) sulphone and Bisphenol A.

6.4 PSU-PEG block copolymers

PEG-PSU linear block copolymers have been reported by several authors.^{1, 5, 15, 16} There have also been investigations into the synthesis of branched or crosslinked PSU homopolymers and PEG-PSU block copolymers.^{4, 8, 12, 17} Methods to produce branched PEG-PSU structures mainly focus on the incorporation of functional groups (mainly aldehyde) into the benzene ring of the dihalides used in the synthesis of the block copolymer. It is, however, important to note that the substituents on the benzene ring have an effect on the stabilization of the molecule and that careful consideration is needed to ensure that the polycondensation reaction will not be inhibited by substituents that introduce branching. In some instances bis (4-fluorophenyl) sulphone was introduced into the reaction in order to ensure higher reaction rates (refer to Section 6.3.4.2 for relative reactivities of different halogens). Hancock *et al.*⁴ patented the use of a tetra functional *Tetronic*[®] to introduce branch points into the block copolymers formed. *Tetronic*[®] is a tetra functional macromonomer consisting of an ethylene diamine branching point attached to low molar mass *Pluronic*[®]. In most instances more than one step is required in the synthesis of the branched copolymers.

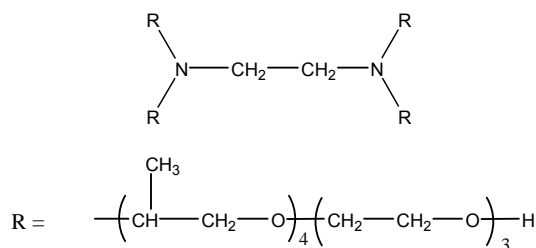


Figure 6.4: Tetronic 304.

The main goal of this investigation was to perform a model study on the influence of the hydrophilic:hydrophobic ratio on the surface properties of the formed copolymers. In order to perform a basic study on the surface properties of these polymers, the precise characterisation of the block copolymers would be necessary. Including branched copolymers and even multi block copolymers in this investigation, would bring additional variables into the equation and it would be more complicated to do draw conclusions on the effect of the hydrophilic:hydrophobic ratio on the properties of the formed copolymers.

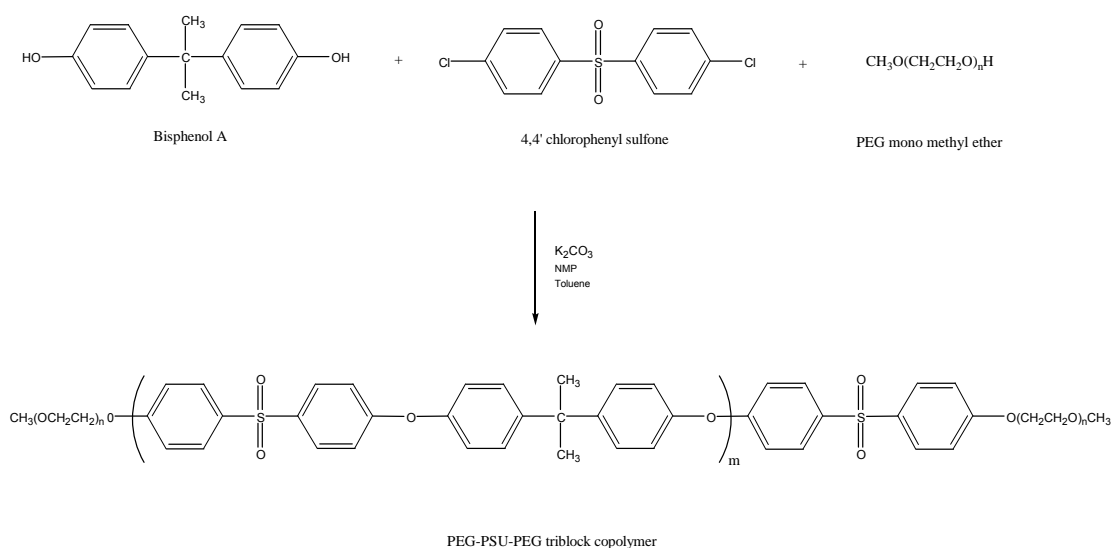
Butuc *et al.*¹⁶ reported on the polycondensation of α -hydroxy- ω -allyl PEO with a bis (4-chlorophenyl) sulphone terminated PSU homopolymer to form copolymers of PSU and PEO in a two step process. Aksenov *et al.*¹⁵ employed di-isocyanate chemistry in the preparation of PEO-b-PSU copolymers. They reported on the use of hydroxy-terminated PSU oligomers and PEG to form the PEG-b-PSU copolymers.

Klein *et al.*⁵ reported on a two-step process where a PSU homopolymer was formed by the polycondensation of bis (4-chlorophenyl) sulphone with Bisphenol A in the first step. Simultaneously, MPEG was reacted with methanesulphonyl chloride to form the mesylate of MPEG. In the second step the two different products were combined and the resulting copolymer is formed.

Hancock *et al.*¹ reported on a one step process for the polycondensation of bis (4-chlorophenyl) sulphone, Bisphenol A, and MPEG to synthesize the resulting PEG-b-PSU block copolymer. They reported that MPEG 5000 was fully compatible with a polycondensation system for the synthesis of bis (4-chlorophenyl) sulphone Bisphenol A polysulphone. The MPEG could therefore be directly charged into the polycondensation system to yield a one step process for the formation of a PEG-b-PSU block copolymer.

They concluded that reaction temperature, fraction of MPEG, and/or the polymerisation stoichiometry controlled the composition and the molar mass of the block copolymer formed.

As bis (4-chlorophenyl) sulphone Bisphenol A polysulphone is produced by polycondensation of a dihalogen and a diol (Section 6.3.4.4), the introduction of MPEG into the reaction will result in the formation of a block copolymer, with fixed length of the PEG block. Unlike the RAFT assisted PEG-b-PS diblock copolymer synthesis, where the growing polymer chains are only active (growing) at one end, with the other being dormant, there will be less control over the length of the PSU hydrophobic segment (B) of the triblock copolymer, as the growing polymer chains are capable of growing at both chain ends. MPEG and Bisphenol A both contain similar reactive groups, namely –OH, and therefore compete with each other for the available active halogen atoms. MPEG is monofunctional and will therefore terminate the chain growth at one end upon reacting with the halogen end group of a growing polymer chain or a dihalogen monomer. The other growing chain end will continue to grow until the monomers are depleted, or in the case where the halogen end group reacts with another monofunctional MPEG macro monomer to form a dormant species. This will result in the formation of a tri block copolymer with the following structure:



Scheme 6.4: (Bis (4-chlorophenyl) sulphone-bisphenol A polysulphone)-b-PEG block copolymer synthesis.

By therefore starting with PEG of known molar mass it is possible to control the molar mass of the hydrophilic segment of the polymer. By using MPEG it is therefore possible to limit the amount of variables in the system.

6.4.1 PSU-b-PEG copolymer synthesis

Copolymers of PSU and MPEG were synthesized using conditions stated in Section 6.3.4.4. Typical contents of the systems for the syntheses of both copolymer with MPEG 2000 and MPEG 5000 are given in Table 6.3

6.3: Typical composition of reagents for PEG-b-PSU preparation

	MPEG 2000		MPEG 5000	
Bisphenol A	23.2 g	0.102 mol	12.5 g	0.058 mol
Bis (4 chlorophenyl) sulphone	28.0 g	0.096 mol	17.1 g	0.060 mol
MPEG	7.5 g	0.004 mol	12.5 g	0.003 mol
K ₂ CO ₃	40.0 g	0.294 mol	23.0 g	0.169 mol
NMP	100.0 mL		50.0 mL	
Toluene	70.0 mL		60.0 mL	
R	0.96		0.85	
\bar{X}_n (theory)	49		12	

With the addition of MPEG to the reaction mixture, r is calculated as follows:

$$r = \frac{N_A}{N_B + 2N_{B'}}$$

where N_A , N_B and $N_{B'}$ represent the mol fractions of bis (4-chlorophenyl) sulphone, Bisphenol A, and MPEG.

6.4.2 PSU-PEG-PSU triblock copolymer characterisation

6.4.2.1 SEC analysis of PEG-b-PSU block copolymers

Figure 6.5 shows the SEC data of the PEG 2000-b-PSU copolymer.

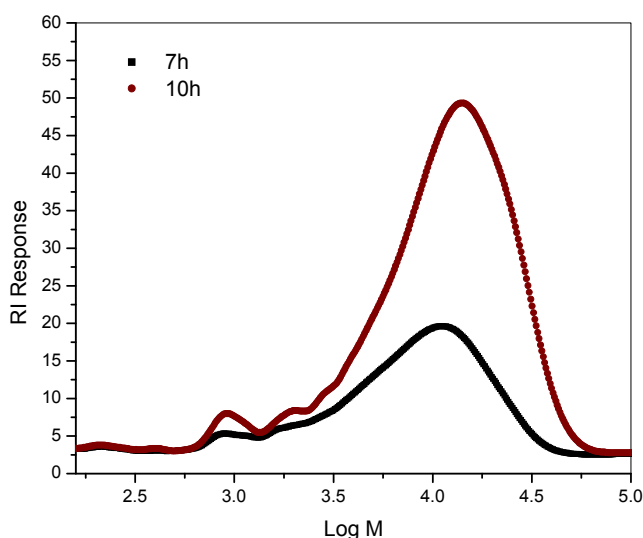


Figure 6.5: Graph of RI response vs. log M for the polycondensation of bis (4-chlorophenyl) sulphone with Bisphenol A and MPEG 2000.

There was no significant growth in the polymer from a reaction time of 7 h to 10 h. The polydispersity of the copolymer ranged from 1.5 to 2.0, depending on the reaction time. This is low for polycondensation reactions. As the reaction time increased, there would be an increase in the polydispersity of the copolymer, as the recombination of longer chains would tend to increase the polydispersity as longer chains were formed. The low polydispersity was a result of the low molar mass of the samples.

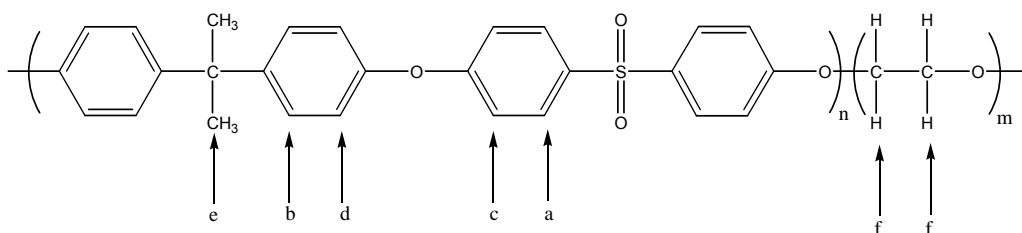
The observed low molar mass of the polymer products was ascribed to several factors, namely:

- The reaction time could have been too short
- The value of \bar{X}_n (49) could have been too low
- The $[K_2CO_3]$ might have been too high, resulting in the formation of low molar mass products
- The solvent concentration could have been too high, resulting in a solution that was too dilute for effective polymerisation.

Similar to what was reported for the SEC characterisation of the PEG 5000-b-PS copolymers in Section 5.7 (Chapter 5), copolymers of PEG 5000 with PSU were insoluble in THF and conventional SEC was not possible. 1H NMR was used to gather information regarding the molar mass of the resulting copolymer.

6.4.2.2 NMR characterisation

Similar to the characterisation of the PSU homopolymer (Section 6.3.4.6), the chemical composition analysis of the formed block PEG-b-PSU block copolymers were determined by ^1H NMR and ^{13}C NMR. The proposed structure of the repeat unit of the formed copolymer is given as:



The different protons experience different chemical environments and different chemical shifts will result. The ^1H NMR spectrum of the formed PEG-b-PSU block copolymer is given in Figure 6.6.

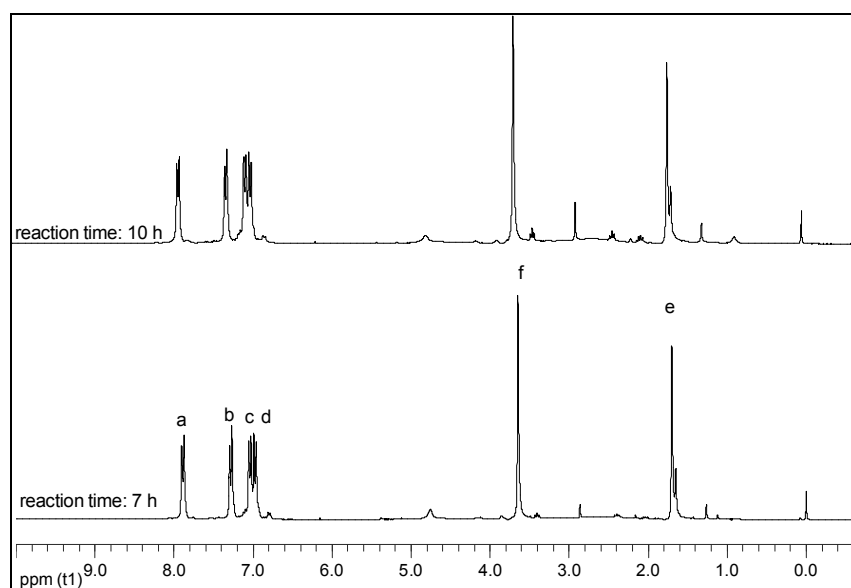


Figure 6.6: ^1H NMR spectrum of MPEG 2000-b-PSU block copolymer.

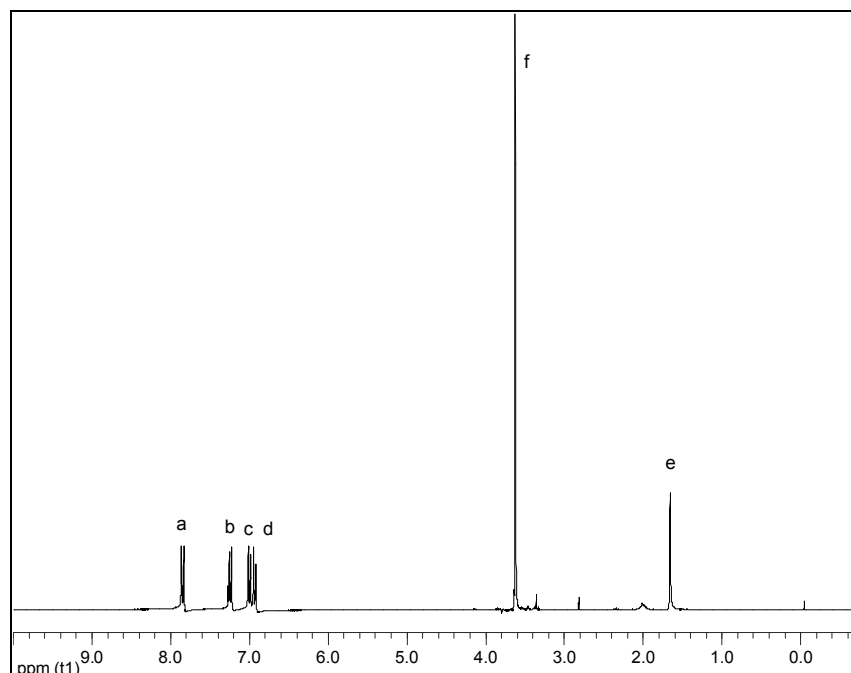


Figure 6.7: ^1H NMR spectrum of MPEG 5000-b-PSU block copolymer.

When comparing ^1H spectra of the PEG-b-PSU block copolymers with those of the PSU homopolymer, the main difference is the peak at $\delta = 3.6$ ppm (refer to Figures 6.6 and 6.7 for ^1H NMR of PEG-b-PSU block copolymers with MPEG 2000 and MPEG 5000, respectively). This is as a result of the MPEG protons (f) as shown in the proposed structure of the copolymer.

In ^1H NMR the relevant peaks were integrated and the intensity of each of the different peaks for each group of identical protons in the copolymer could be compared to analyze the chemical composition of the copolymer. The PEG:PSU ratio of the PEG-b-PSU copolymer was calculated by comparing the methylene protons (4 protons, $\delta = 3.6$) arising from the PEG fraction with the aryl protons (2 protons, $\delta = 7.8$; 4 protons, $\delta = 6.9$) associated with the PSU fraction. The relative compositions of the PEG-b-PSU block copolymers are given in Table 6.3.

Table 6.3 PEG-b-PSU compositions

Copolymer	Reaction time (h)	PEG segment (%)
PEG 2000-b-PSU	7	45.0
PEG 2000-b-PSU	10	44.1
PEG 5000-b-PSU	11	68.5

From Table 6.3 it could be seen that the PEG fraction in the MPEG 2000-b-PSU copolymer remained almost constant in the 7 h to 10 h period in the reaction. Factors as described in Section 6.4.2.1 could be responsible for the low molar mass, resulting in the formation of a copolymer with a high PEG fraction. The ^{13}C NMR spectrum in Figure 6.8 showed that the only difference between the spectrum of the MPEG 2000-b-PSU and the spectrum of PSU homopolymer, was the peak at 71 ppm. This peak was assigned to the methylene carbons of PEG ($\text{CH}_2\text{CH}_2\text{O}$)_n at 71 ppm in the MPEG 2000-b-PSU block copolymer, again proving that the MPEG 2000-b-PSU block copolymer had been synthesized.

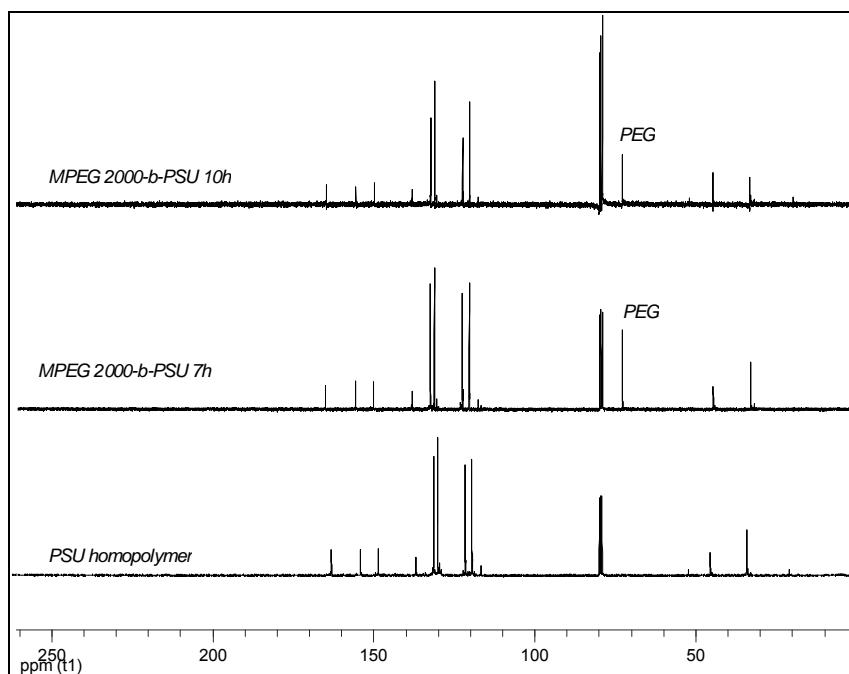


Figure 6.8: ^{13}C NMR spectrum of MPEG 2000-b-PSU block copolymer.

In the case of the PEG 5000-b-PSU copolymer similar factors could have caused the low molar mass of the formed copolymer (Figure 6.9).

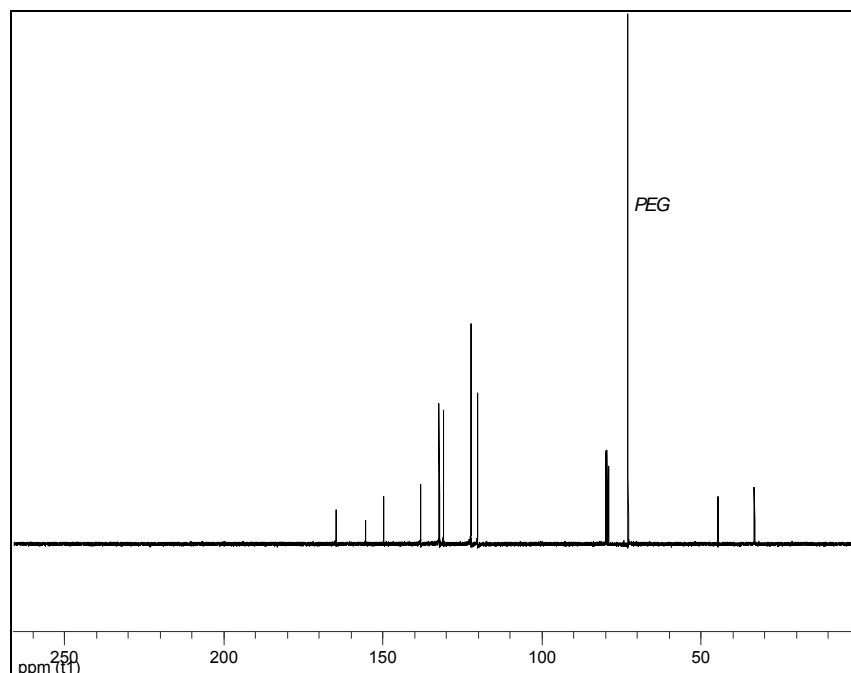


Figure 6.9: ^{13}C NMR spectrum of MPEG 5000-b-PSU block copolymer.

6.5 Summary of results

From the experiments conducted on the copolymerisation of PEG with PSU to form PEG-b-PSU block copolymers, the results were summarised as follows:

1. Bis (4-chlorophenyl) sulphone-bisphenol A polysulphone was synthesized according to the conditions described in Section 6.4.2.
2. The PSU polymer was successfully characterised by making use of both ^1H NMR and ^{13}C NMR.
3. Copolymers of bis (4-chlorophenyl) sulphone-bisphenol A and MPEG, both MPEG 2000 and MPEG 5000, were successfully synthesized and characterised by both ^1H NMR and ^{13}C NMR.
4. The molar masses of both the Bis (4-chlorophenyl) sulphone-bisphenol A polysulphone and the bis (4-chlorophenyl) sulphone-bisphenol A-MPEG copolymers that were obtained were low, as determined by SEC (relative to narrow MMD polystyrene standards). Longer reactions times and more careful consideration of the stoichiometric imbalance is necessary to optimize the synthetic procedure to produce bis (4-chlorophenyl) sulphone-bisphenol A and MPEG copolymers of higher molar mass.

6.6 References

1. Hancock, L. F. and Ting, Y.-P. R., Preparation of polysulfone/poly(ethylene oxide) block copolymers, *Macromolecules*, **1996**, 29, 7619-7621.
2. Hancock, L. F., Phase inversion membranes with an organised surface structure from mixtures of polysulfone and polysulfone-poly(ethylene oxide) block copolymers, *Journal of Applied Polymer Science*, **1997**, 66, 1353-1358.
3. Hancock, L. F., Fagan, S. M. and Ziolo, M. S., Hydrophilic, semipermeable membranes fabricated with poly(ethylene oxide)-polysulfone block copolymer, *Biomaterials*, **2000**, 21, 725-733.
4. Hancock, L. F., Fagan, S. M. and Mullon, C. J.-P., Highly branched block copolymers, *US Patent 6,172,180 B1*, **2001**.
5. Klein, E. and Balachander, N., Self-wetting membranes from engineering plastics, *US Patent 5911880*, **1995**.
6. Rosen, S. L., Fundamental principles of polymeric materials, *Wiley Interscience, United States of America*, **1993**.
7. Hay, A. S., Aromatic polyethers, *Advances in Polymer Science*, **1967**, 4, 496-527.
8. Kerres, J., Ullrich, A. and Hein, M., Preparation and characterisation of novel basic polysulfone polymers, *Journal of Polymer Science: Part A: Polymer Chemistry*, **2001**, 39, 2874-2888.
9. Rose, J. B., Preparation and properties of poly (arylene ether sulphones), *Polymer*, **1974**, 15, 456-465.
10. Morrison, R. T. and Boyd, R. N., Organic Chemistry, *Allan and Bacon, Boston*, **1983**.
11. Johnson, R. N., Farnham, A. G., Clendinning, R. A., Hale, W. F. and Merriam, C. N., Poly (aryl ethers) by nucleophilic aromatic substitution I. Synthesis and properties, *Chemical Abstracts*, **1967**, 68: 40159u.

12. Guiver, M. D., Zhang, H., Robertson, G. P. and Dai, Y., Modified polysulfones. III. Synthesis and characterisation of polysulfone aldehydes for reactive membrane materials, *Journal of Polymer Science: Part A: Polymer Chemistry*, **2001**, 39, 675-682.
13. Johnson, R. N. and Farnham, A. G., Poly (aryl ethers) by nucleophilic aromatic substitution III. Hydrolytic side reactions, *Chemical Abstracts*, **1967**, 68: 40161p.
14. Schulze, S. R. and Baron, A. L., Kinetics of solution polycondensation of aromatic polyethers., *Chemical Abstracts*, **1969**, 72: 21993z.
15. Aksenov, A. I., Storozhuk, I. P., Aksenova, T. S. and Korshak, V. V., Synthesis and some properties of poly (arylene sulfone oxide)- poly (ethylene oxide) block copolymers., *Chemical Abstracts*, **1984**, 100: 122520y.
16. Butuc, E., Cozan, V., Giurgiu, D., Migalache, I., Ni, Y. and Ding, M., Modified polysulphones I: Synthesis and characterisation of polysulphones with unsaturated groups., *Journal of Macromolecular Science: Pure and Applied Chemistry*, **1994**, A31, 219-230.
17. Kricheldorf, H. R., Fritsch, D., Vakhtangishvili, L. and Schwarz, G., Multicyclic poly(ethersulphone)s of phloroglucinol forming branched and cross-linked architectures, *Macromolecules*, **2003**, 36, 4337-4344.

Chapter 7

Surface analysis of amphiphilic block copolymers

7.1 Introduction

The main focus of this study was to investigate the influence of the hydrophilic:hydrophobic ratio within an amphiphilic block copolymer and the influence thereof on the surface properties of polysulphone ultrafiltration membranes. Knowledge of film preparation (membrane preparation) and surface analysis techniques is important to perform this study.

Different methods are available for the determination of the wettability/hydrophilicity of a surface. These methods include:

- 1 contact angle measurement;
- 2 atomic force microscopy (AFM); and
- 3 Fourier Transform Infrared (FTIR).

7.2 Contact angle

7.2.1 Introduction

Probably the easiest method by which to determine the hydrophilicity of a surface is the determination of the contact angle of a sessile drop on that particular surface. Surface hydrophilicity is measured in terms of the wettability of the surface of that said sample with a liquid; in this case that liquid would be water. It is formed by the tangent of the liquid at the air/liquid solid line of contact and the line through the base of the liquid drop where it contacts the solid. The lines of force acting along the line of intersection are the surface tensions of the liquid in equilibrium with the surrounding vapor (γ_{LV}), the solid/vapor surface tension (γ_{SV}), and the solid/liquid surface tension (γ_{SL}). Simple geometric considerations lead to the Young's Equation:¹

$$\cos \theta = \frac{\gamma_{SV} - \gamma_{SL}}{\gamma_{LV}} \quad (7.1)$$

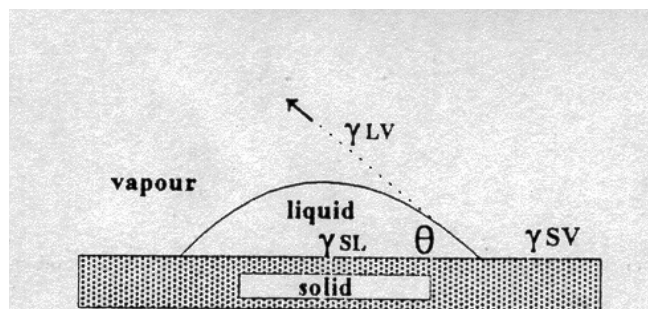


Figure 7.1. Hydrophilicity calculation of water droplet on a surface.

Certain conditions apply to this equation, mainly relating to the sessile drop being in equilibrium. Other conditions relate to equilibriums with respect to the capillary, gravitational and mechanical forces.¹ The requirement for measuring the equilibrium contact angle are most often violated by surface uniformity; both in terms of roughness of the surface and chemical heterogeneity. A major requirement for any analysis that attempts to account for the effect of surface roughness or chemical heterogeneity must account for the strong contact angle hysteresis that is invariably observed between the advancing angle, θ_A , and the receding angle, θ_R .

The Wenzel equation was derived by assuming that the roughness increases the solid/liquid and the solid/vapour interfacial tensions by a factor r , the surface roughness coefficient, so the effective interfacial tensions become $r\gamma_{SL}$ and $r\gamma_{SV}$ and by direct substitution into the Young's equation yields:¹

$$r(\gamma_{SV} - \gamma_{SL}) = \gamma_{LV} \cos \theta_A \quad (7.2)$$

Johnson² in 2002 reviewed Young's Equation and stated that for equilibrium to exist, the force vectors should sum to zero and if the forces are resolved in any direction, they should balance.

$$\gamma_{LV \rightarrow} + \gamma_{SV \rightarrow} + \gamma_{SL \rightarrow} = 0 \quad (7.3)$$

Vertical resolution of the vectors in Young's equation produces a resultant. The equation to complete the vector equilibrium can be written down, but that alone does not imply physical significance.

7.2.2 Sample preparation

7.2.2.1 PEG-b-PS sample preparation

PEG-b-PS films were prepared as follows:

- 1 A 30% (300 mg/mL) polymer solution in THF was prepared.
- 2 A drop of the solution was placed on a glass plate and the THF was allowed to evaporate off at room temperature resulting in film formation.

7.2.2.2 Modified PSU membrane preparation

A similar method to the method used in Section 7.2.2.1 was introduced for the preparation of PEG-b-PSU films. However, the samples prepared were brittle and could not be analyzed due to their low molar mass. Hancock³ and Hancock *et al.*⁴ reported on the surface properties of PSU membranes prepared by making use of a mixture of PSU and PEG-b-PSU casting solution. They prepared a range of different mixtures of PSU and PEG-b-PSU, cast membranes and analyzed the surfaces of these membranes. A typical formula contained 20% polymer in NMP, with the PSU:PEG-b-PSU ranging from 7:1 to 1:1.

The following procedure was used to prepare membranes from PSU (Udel, USA) and PEG-b-PSU:

- 1 A PSU (12 g) solution in NMP (35 g) was prepared and placed in an oven at 45°C for 72 h.
- 2 PEG-b-PSU (3 g) was added to the PSU solution and the sample was replaced in the oven for 48 h.
- 3 The resulting solution was then placed on a roller for 48 h.
- 4 Membrane films were cast on a glass plate (using a casting knife) and the films was then placed in water.
- 5 The membranes were then washed with water to remove the remaining NMP.
- 6 Membranes were stored in water.

7.2.3 Results and discussion

The surface tension or the repulsion of water was determined by means of the water droplet method and subsequent measurement of the contact angle of the water to the substrate.

Representative samples were cut from the films and membranes, dried for 30 minutes in air and analyzed. A 1 μL droplet of distilled water was placed on the surface of the substrate to be measured. A photograph was then taken with a stereomicroscope that was connected to a computer. The contact angle of the water droplet with the surface of the substrate was therefore measured and reported as angle theta (θ) (Figure 7.1) Ten different readings were taken of each sample, whereafter the average value as well as the standard deviation were determined, as reported in Table 7.1 and Table 7.2.

7.2.3.1 PEG-*b*-PS films

Table 7.1 and Figure 7.2 show the results of static contact angle measurements of films made from different PEG-*b*-PS block copolymers (refer to Chapter 5 for copolymer synthesis and analysis). The composition of the different copolymers, as well as the molar mass and MMD of the different films are shown in Table 7.1.

Chapter 7: Surface analysis of amphiphilic block copolymers

Table 7.1: Contact angle measurements of PEG-b-PS block copolymer films

Sample	Components	Relative amount (%)	\bar{M}_n g/mol	PDI	Contact angle (θ)
1	PS	37	11200	1.4	83.2 \pm 1.4
	PEG-b-PS	52	14600	1.3	
	PEG-PS-PEG	5	14800	1.2	
	PEG2000	6			
2	PS	42	12100	1.3	73.9 \pm 2.7
	PEG-b-PS	50	16400	1.3	
	PEG2000	8			
3	PS	70	7400	1.3	79.1 \pm 1.9
	PEG-b-PS	26	9500	1.2	
	PEG2000	4			
4	PS	54	4800	1.3	66.2 \pm 4.0
	PEG-b-PS	21	6300	1.2	
	PEG-b-PS	16	5600	1.2	
	PEG2000	9			
5	PS	14	6200	1.3	82.1 \pm 1.6
	PEG-b-PS	56	7900	1.2	
	PEG5000	25			
	PEG-PEG	4			
6	PS	33	9800	1.5	76.9 \pm 2.3
	PEG-b-PS	40	13900	1.3	
	PEG-PS-PEG	4	17200	1.3	
	PEG2000	23			

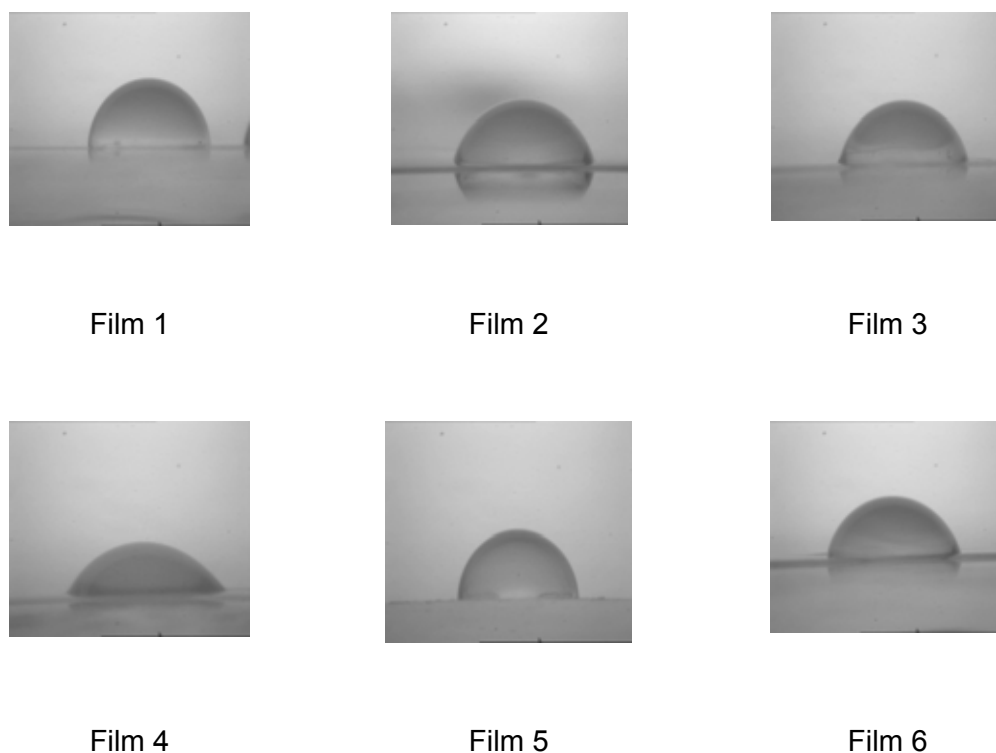


Figure 7.2: Static contact angle measurements of PEG-b-PS films.

Due to the chemical composition of each sample, direct comparison of the films was not possible. Efforts to separate the different components in each sample proved to be unsuccessful, as stated in Chapter 5. Taking the chemical composition of each of the films into account, an explanation of the measured contact angles is possible. In each sample, not only does the copolymer content have a large influence on the hydrophilicity of the film, but also the molar mass of the compound. The lowest static contact angle (θ) was found for Film 4, which is confirmed by the pictures in Figure 7.2. Here the copolymer content in the sample was only 24%, which is relatively low compared to that of Film 1 and Film 2, where the copolymer content is 50%.

The major difference in these samples, however, was the low molar mass of Film 4. In each of the polymerization processes, MPEG macro RAFT agent was used in copolymer synthesis. The size of the hydrophilic block therefore remains constant in the reaction. The molar mass of the PEG-b-PS copolymers in Film 4 were 6300 g/mol and 5600 g/mol and, with the molar mass of the PEG block being 2000 g/mol, the hydrophilic:hydrophobic ratio (A:B ratio) in the copolymer was 1:2. Adding the contributions of the different

Chapter 7: Surface analysis of amphiphilic block copolymers

homopolymers to the A:B ratio, resulted in a compound in which 46% of the components in the product contained A with an A:B ratio of 1:2. The total contribution of PEG in Film 4 was therefore large, compared to Films 1, 2 and 6, where the molar masses of the products are much higher. The higher the molar mass of the PEG-b-PS block copolymer, the lower the A:B ratio, as only the hydrophobic segments increase in size with an increase in molar mass. In Film 6, for example, where the molar mass of the PEG-b-PS block copolymer is 13 900 g/mol, the A:B ratio was 1:6, therefore resulting a much more hydrophobic product.

In Film 3, consisting of polymers with molar masses comparable to those in Film 4, the PS homopolymer content was high at 70%, therefore shifting the A:B ratio towards the hydrophobic side. Here only 30% of the compound contained hydrophilic polymers or polymers with hydrophilic segments.

In Film 5 a MPEG 5000 RAFT macro initiator was used in the polymerisation reaction. Due to the molar mass of the PEG segment, together with the relatively low molar mass of the compounds in the product, it was expected that Film 5 would have the lowest θ . However, results showed a relatively high θ at 82°. In Chapter 5 it was stated that the use of conventional SEC was not suitable for the MPEG 5000-b-PS block copolymers due to the insolubility of MPEG 5000 in THF. MPEG 5000 and its low molar mass copolymers with styrene was only miscible in 100% THF, resulting in the presence of an insoluble fraction in the solution for film preparation. Upon placing the solution droplet on a glass plate (Section 7.2.2.1), the insoluble MPEG 5000 segments precipitated on the glass plate, leaving the PS segments dissolved in THF. As the THF evaporated off, the PS segments in the product formed a film over the MPEG segments, resulting in the hydrophobic surface of the films.

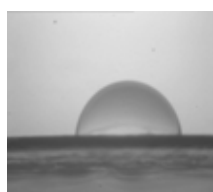
7.2.3.2 Modified PSU membranes

Results from static contact angle measurements of unmodified and modified PSU membranes are given in Table 7.2. Sample 1 was a reference PSU membrane: the casting solution was prepared without the addition of PEG-b-PSU block copolymer. Membranes 2 and 3 were both hydrophilized by the addition of a MPEG 2000-b-PSU block copolymer to the casting solution, while a MPEG 5000-b-PSU block copolymer was added to the casting solution of membrane 4.

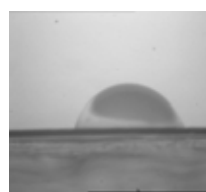
Chapter 7: Surface analysis of amphiphilic block copolymers

Table 7.2: Contact angle measurement of PSU membranes modified with MPEG-b-PSU block copolymers

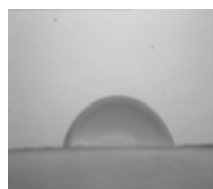
Membrane	\bar{M}_n MPEG (g/mol)	PEG content in PEG-b-PSU (%)	PEG-b-PSU molar mass (g/mol)	Contact angle (θ)
1	-	-	-	81.1 ± 2.3
2	2000	45	9171	78.1 ± 2.9
3	2000	44	11 691	78.3 ± 2.0
4	5000	68	Not determined	71.5 ± 2.2



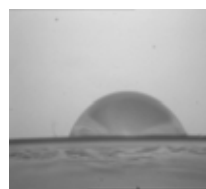
Membrane 1



Membrane 2



Membrane 3



Membrane 4

Figure 7.3: Static contact angle measurements of modified PSU membranes.

Results in Table 7.2 as well as the images of the water droplet in Figure 7.3 show that the modified membranes showed an increase in hydrophilicity when compared to the reference membrane (Membrane 1). The highest improvement in hydrophilicity was found in Membrane 4, where a MPEG 5000-b-PSU block copolymer was added to the casting solution. Membranes 2 and 3 showed similar improvements in hydrophilicity with regards to the reference Membrane 1, irrespective of the size of the PSU block (hydrophobic segment). From contact angle measurements it therefore concluded that the governing

factor with regards to the hydrophilization of the PSU membranes was the size of the PEG block (hydrophilic segment).

The influence of the hydrophobic segment will, however, have to be investigated during membrane operation to determine what influence cross flow separation will have on the modified surfaces. With the hydrophobic segments being of low molar mass, it might be possible that the hydrophilizing agents might be stripped off the surface of the membrane due to the lack of entanglements of polymer chains between the PSU membrane substrate and the PSU segment of the PEG-b-PSU block copolymer.

7.3 Atomic force microscopy

7.3.1 Introduction

Recent advances in AFM have opened the door for this method to be used for the determination of hydrophilicity of a polymer surface.⁵⁻⁷ AFM was first applied to polymer surfaces in 1998, shortly after its invention.⁸ Initially, AFM studies were aimed at visualization of polymer morphology, nanostructure, and molecular order. More recently, due to the discovery of new AFM capabilities, the range of AFM applications to polymers has been broadened substantially from relatively simple visualizations of morphology to more advanced examinations of polymer structures and properties on a nanoscale. AFM offers the advantage over other microscopic techniques in that it allows observations of changes of the surface properties of polymers under water, for example, and the change of surface energy under water.

7.3.2 Force-distance analysis

Atomic force microscopy is based on the detection of atomic interaction forces between a sharp tip and the sample. A topographic image with (sub) nanometer resolution is generated by sampling the interaction force over a two-dimensional array. To prevent the interaction between the tip and the surface from destroying or modifying the sample, the interaction forces are often determined by force modulation techniques. In this intermittent contact, or tapping mode, the tip touches the surface only briefly during each cycle, and no lateral forces are present. Force spectroscopy can be performed by determining a force–distance curve⁷ at a particular point on the sample. From this curve physical properties such as the adhesion or stiffness of the sample can be determined. Kim and Kim⁷ reported the use of AFM to measure the effect of hydrophilic PEO pendent

Chapter 7: Surface analysis of amphiphilic block copolymers

chains on the local elasticity and surface energy of a polymer surface by using the “force-distance” analysis of AFM. The effect of the pendent PEO chains on the surface properties of a polymeric surface, for example, surface elasticity (hardness) and adhesion force, is easily investigated by using “force-distance analysis” of the SPM technique. Figure 7.4 shows the principle of the experiment.

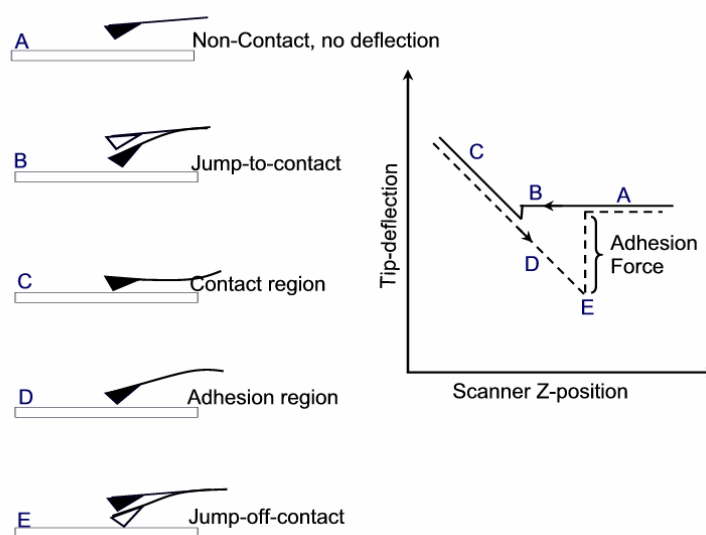


Figure 7.4: AFM “force-distance” analysis.

In force-distance analysis, the distance between sample and tip (Z-position) was gradually decreased and then increased without changing the horizontal position (XY-position). When there exists tip-sample interaction, the cantilever with the tip deflects until the elastic force of the cantilever equals the tip-sample force, and the system is in equilibrium. At point A, there is no interaction, and tip deflection does not occur. At point B, the tip jumps to contact the sample surface because a thin layer of water covers most sample surfaces. The “jump to contact” disappears when the force-distance analysis is carried out in water. Once the tip is in contact with the surface, cantilever deflection will increase (C). If the force-distance analysis is carried out in water, the probe tip may indent the soft surface of a polymer, and the slope or shape of the contact part of the force-distance curve can provide information about the elasticity of the sample surface. After loading the tip to a desired force value, the process is reversed. As the cantilever is withdrawn, adhesion formed during contact with the surface causes the tip to adhere to the sample (D) some distance past the initial contact point on the approach curve (B). A key measurement of the AFM force curve is point E, at which the adhesion is broken and the

cantilever comes free from the surfaces. This can be used to measure the rupture required to break the adhesion, that is, the tip-sample adhesion force. If the tip is very hydrophilic, for example, a Si₃N₄ tip, the adhesion force indicates the surface hydrophilicity.

7.3.3 Digital pulsed force mode

The digital pulsed force mode (DPFM) combines both force-distance analysis and topographic analysis and generates a topographic image simultaneously with an image of, for example, the adhesion of the scanned area. The tip makes contact with the sample periodically and measures a force-distance curve at every point in the image. In this way a spatial map of the adhesion characteristics is determined.

Okabe *et al.*⁹ used the same technique to discriminate the functional groups of self-assembled sample surfaces, by using chemically modified tips.

A silicon tip was used to scan the surface of the membranes investigated in this study. Untreated silicon has a native oxide layer with hydroxyl bonds. These hydroxyl groups are adsorption sites for water molecules and silicon with a natural oxide surface layer is therefore hydrophilic. A conventional silicon tip with SiO₂ groups at the surface will show a higher adhesive force with a hydrophilic surface than with a hydrophobic surface.¹⁰⁻¹² The image of the adhesion force therefore represents the hydrophilicity of the sample. Lighter parts represent more hydrophilic compounds and darker parts represent more hydrophobic compounds.

Quantitative values of the adhesive force (F_{adh}) are given by the following equation:¹³

$$F_{adh} = V_{adh} C k S / g_A \quad (7.4)$$

where V_{adh} is the average voltage value of the adhesion image, C is a machine dependant amplification factor (here $C = 1$), k is the spring constant of the cantilever, S the sensitivity of the photodiode, and g_A is a constant of the instrument. The spring constant k of the force modulation cantilever was 2.8 N/m¹⁴ and the sensitivity S is determined to be 85.5 nm/V. This then reduces the relationship between the adhesive force (F_{adh}) and average voltage value of the adhesion image (V_{adh}) to

$$F_{adh} = Y V_{adh} \quad (7.5)$$

where Y is a constant for the instrument.

7.3.4 Experimental

All AFM measurements were made using a Veeco Multimode instrument with a Witec digital pulsed force mode controller.

In the digital pulsed force mode (DPFM)^{10-12, 15} the AFM is operated in contact mode with a sinusoidal modulation applied to its z-piezo. The modulation frequency is typically between 1 and 10 kHz, which is well below the resonance frequency (f_r) of the cantilever (force modulation cantilever with $f_r \approx 70\text{kHz}$). This makes it possible to measure force-distance curves at every scan point, by continuously bringing the tip into contact with the surface and retracting it. Therefore, topography and physical surface properties, such as stiffness or adhesion can be measured simultaneously and with the same spatial resolution.

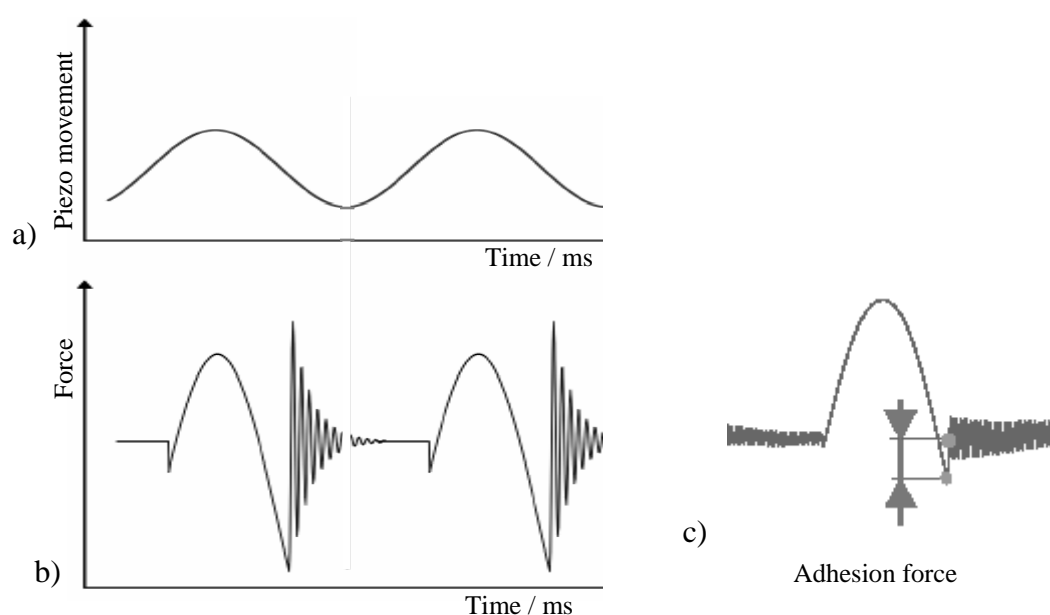


Figure 7.5 a) z modulation of the piezo, b) force signal as a function of time and c) adhesion force measured for each sinus cycle.¹⁶

The peak force shown in Figure 7.5b serves as the input for the control loop of the AFM to maintain a “constant” force mode. This force signal is used to obtain a topographical image of the sample. The adhesion force is determined by measuring the difference between the negative force peak and the baseline (Figure 7.5c) and is represented as an

Chapter 7: Surface analysis of amphiphilic block copolymers

adhesion image of the sample. Each voltage value is allocated a colour value, which results in an adhesion image. Lighter colours represent higher adhesive forces.

To aid the interpretation of the results, each adhesion image was displayed as a histogram, as displayed in Figure 7.6. This shows the relative frequency with which each voltage value occurs within the scanned area. The average value represents the average adhesive force value, which corresponds to the average hydrophilicity of the sample. The standard deviation is a measure of the range of these values and serves as an error bar in our presentation of the data.

A similar technique was applied by Sato *et al.*¹⁷ to determine the distribution of observed values of the adhesive forces on self-assembled sample surfaces.

Every image was recorded with a scan size of $5\ \mu\text{m} \times 5\ \mu\text{m}$ and with a resolution of 256×256 pixels. The value of the adhesive force was therefore determined by averaging over 65536 measurements. This presented a good statistic distribution, compared to the few individual force-distance measurements customarily used to describe adhesive forces.

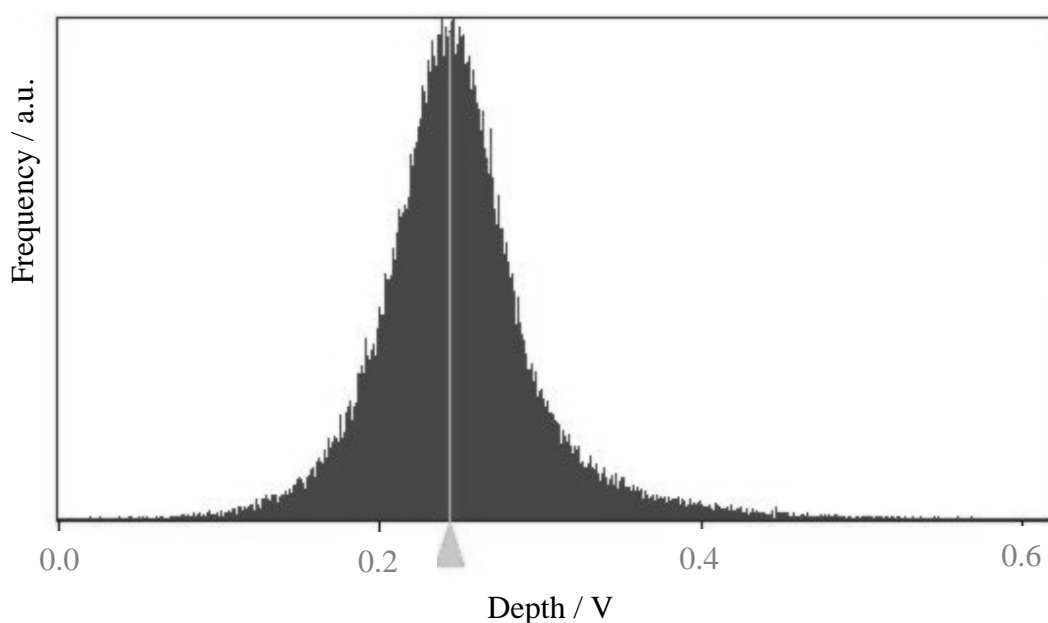


Figure 7.6: Histogram of the voltage distribution in an adhesion image.

7.3.5 Sample preparation

Samples were prepared according to the method described in Section 7.2.2.

Chapter 7: Surface analysis of amphiphilic block copolymers

PEG-b-PS films and modified PSU membranes were stored in water prior to analysis. Prior to analysis, representative samples were cut from the films, dried for 30 minutes and analyzed.

7.3.6 Results and discussion

7.3.6.1 PEG-b-PS films

Representative samples were taken from the different films prepared according to the method described in Section 7.2.2.1. Table 7.3 shows the composition of the copolymers analyzed as well as the measured AFM hydrophilicity.

Table 7.3: AFM analysis of PEG-b-PS block copolymers

Sample	Components	Relative amount %	\bar{M}_n g/mol	PDI	Adhesion force (nN)
1	PS	37	11200	1.4	263 ± 37.3
	PEG-b-PS	52	14600	1.3	
	PEG-PS-PEG	5	14800	1.2	
	PEG2000	6			
2	PS	42	12100	1.3	218.9 ± 30.5
	PEG-b-PS	50	16400	1.3	
	PEG2000	8			
3	PS	70	7400	1.3	114.3 ± 24.9
	PEG-b-PS	26	9500	1.2	
	PEG2000	4			
4	PS	54	4800	1.3	289.7 ± 11.8
	PEG-b-PS	21	6300	1.2	
	PEG-b-PS	16	5600	1.2	
	PEG2000	9			
5	PS	14	6200	1.3	288.48 ± 20.1
	PEG-b-PS	56	7900	1.2	
	PEG5000	25			
	PEG-PEG	4			
6	PS	33	9800	1.5	Not determined
	PEG-b-PS	40	13900	1.3	
	PEG-PS-PEG	4	17200	1.3	
	PEG2000	23			

Chapter 7: Surface analysis of amphiphilic block copolymers

Table 7.3 shows that the different samples all had different compositions in terms of PS homopolymer and PEG-b-PS block copolymer content as well as different \bar{M}_n values. Of importance is the PEG content of the samples, as this influences the hydrophilicity of the film sample. In Section 7.2.3.1 the influence of molar mass on the A:B ratio was discussed. The higher the molar mass, the lower the A:B ratio. Samples 1 and 2 almost had similar fractions in terms of the PS and PEG homopolymers and the PEG-b-PS block copolymer. The only difference in these two samples was the molar mass of the PS homopolymer and PEG-b-PS block copolymer. The block copolymer was synthesized via the macro RAFT agent method, therefore starting with a fixed PEG block and therefore adding a PS block. Higher molar masses of these polymers therefore imply larger polystyrene content in the PEG-b-PS block copolymer. It was therefore expected that the film prepared from sample 2 would be more hydrophobic than the film prepared from sample 1. It was expected that sample 3, with the highest PS homopolymer content (70%), would be the most hydrophobic as shown in Table 7.3. The total PEG content was therefore lower than in the other films. The molar mass of the different fractions in sample 4 is low and the fraction of PEG homopolymer was higher than in the other samples. It was therefore expected that the total contribution of all PEG fractions would have a greater influence on the hydrophilicity of this sample compared to samples 1, 2 and 3. The adhesion force value obtained for sample 5, where the block copolymer comprised of PEG 5000 as compared to PEG 2000 in the other samples, was lower than would be expected. With the \bar{M}_n of film 5 being low and the PEG having a $\bar{M}_n \approx 5000$ g/mol, it would be expected that the contribution of the MPEG block towards the total hydrophilicity of the sample would have a larger effect than what was observed. The problem in film formation, as explained in Section 7.2.3.1, could have resulted in the deviation of the adhesion force from the expected trend.

The chemical composition of each film represents the bulk of the sample, and with the films being stored in H₂O prior to analysis, it was expected that the pendent PEG segments of the block copolymers would migrate to the surface of the films, therefore creating increased hydrophilicity in the sample.

7.3.6.2 Modified PSU membranes

Table 7.4 shows the results of the AFM force-distance analysis of PSU membrane samples prepared as described in Section 7.2.2. Membrane 1 was an unmodified PSU

Chapter 7: Surface analysis of amphiphilic block copolymers

membrane. Membranes 2 and 3 were hydrophilized by adding MPEG 2000-b-PSU block copolymers to the membrane casting solution, while in Membrane 4 a MPEG 5000-b-PSU block copolymer was added to the casting solution.

Table 7.4: AFM analysis of PSU membranes modified with PEG-b-PSU block copolymers

Sample ID	\bar{M}_n MPEG (g/mol)	PEG content in PEG-b-PSU (%)	PEG-b-PSU molar mass (g/mol)	Adhesion force (nN)
1	-	-	-	55.1 ± 5.6
2	2000	45	9 171	59.7 ± 6.8
3	2000	44	11 691	66.2 ± 13.6
4	5000	68	ND*	60.5 ± 9.3

ND*: not determined

Table 7.4 shows that all the membranes (Membranes 2, 3 and 4) made from casting solutions that contain PEG-b-PSU block copolymer had a more hydrophilic surface when compared to Membrane 1 (the unmodified PSU membrane). The influence the PEG-b-PSU block copolymer on the hydrophilicity of the membrane was rather small. This could be due to the PSU:PEG-b-PSU ratio of 4:1 that will have an influence on the hydrophilicity of the membrane sample. The adhesion force for Membrane 3 was higher than expected, as it would be expected that the values for Membrane 2 would be in accordance with Membrane 3, as both these membranes were made from casting solutions that contain similar amounts of PEG-b-PSU block copolymer of comparable hydrophilic:hydrophobic ratio. With AFM measurements being conducted on a small segment of a sample (5 μm x 5 μm), it might be possible that the sample had been scanned at a hydrophilic segment of that sample and that the value might be distorted. It would be expected that Membrane 4 would have the highest adhesion force value due to both the size of the PEG segment as well as the fraction of PEG in the PEG-b-PSU copolymer added to the casting solution. Chain mobility could, however, have prevented the PEG chains from migrate to the surface of the membrane resulting in lower adhesion forces measured for Membrane 4.

7.4 FTIR-PAS

7.4.1 Introduction

While contact angle and AFM measurements rely on the physical properties of the surface analyzed, FTIR provides information on the chemical properties of these surfaces. With

Chapter 7: Surface analysis of amphiphilic block copolymers

FTIR it is possible to determine the fraction of the hydrophilic segment of the polymer at the surface thereof.

The desired result with all FTIR sampling techniques is to obtain the absorbance spectrum as quickly and easily as possible. In many cases, however, direct analysis of the sample by transmission or reflection methods is not practical because the sample either transmits inadequate light to measure or it lacks suitable surface or particle size conditions for reflectance spectroscopies.¹⁸ In other cases, reflectance spectroscopy may not probe deeply enough into the sample to yield the desired information.

Photo acoustic spectroscopy (PAS) is a unique sampling technique, because it does not require that the sample be transmitting, has low sensitivity to surface condition, and can probe over a range of selectable sample depths ranging from several micrometers to more than 100 μm .¹⁸ PAS has these capabilities because it directly measures IR absorption by sensing absorption induced heating of the sample within the experimentally controllable sampling depth below the sample's surface. Heat deposited within this depth transfers to the surrounding gas at the sample surface, producing a thermal-expansion-driven pressurization in the gas, known as the PAS signal, which is detected by a microphone. The magnitude of the PAS signal varies linearly with increasing absorptivity, concentration or sample depth until at high values of their product gradual roll off in sensitivity occurs. The phase of the PAS signal corresponds to the time delay associated with heat transfer within the sample.

PAS signal generation is initiated when the FTIR beam, which oscillates in intensity, is absorbed by the sample resulting in the absorption-induced heating in the sample and oscillation of the sample temperature. The temperature oscillations occurring in each light absorbing layer within the sample launch propagating temperature waves called thermal-waves, which decay strongly as they propagate through the sample. It is this thermal-wave decay process that defines the layer thickness, or sample depth, from which spectral information is obtained in FTIR-PAS analysis. The sampling depth can be increased by decreasing the IR beam modulation frequency imposed by the interferometer. The lower modulation frequency allows a longer time for thermal-waves to propagate from deeper within the sample into the gas. As the sampling depth increases, the saturation of strong bands in PAS spectra increases just as it does in adsorption spectra measured by transmission as sample thickness increases.

The development of photo acoustic techniques was hampered by weak acoustic signals that must be measured due to the very high thermal wave-reflection coefficient at the sample-to-gas interface. A high fraction of the thermal-wave amplitude is reflected back into the sample and is not detected, leading to signal-to-noise problems. Operating in the near- and mid-infrared spectral region, made practical by the high sensitivity of photo acoustic detectors and the multiplexing capability of FTIR systems, has been an area of success for the PAS technique.

The photo acoustic signal contains information on the sample's absorption spectrum and on the depth below the sample's surface from which the signal evolves, allowing the analysis of the surfaces of materials. The most instructive model for general purposes assumes an optically and thermally homogeneous slab sample geometry which is thick on the scale of the thermal wave decay length with the rear sample face thermally grounded and optically non reflective.

FTIR measurements gain information at a depth of up to 45 μ m into the surface of the sample. FTIR can be used to determine the concentration of PEG at the surface of the polymer sample. Song *et al.*¹⁹ reported the use of FTIR-ATR for the surface analysis of plasma modified PSU membranes. Song and coworkers analyzed both PSU and PEG-*g*-PSU membranes. The most important bands of PSU are at 1250 cm^{-1} [$\nu(\phi-o-\phi)$], at 1300-1335 cm^{-1} [$\nu(\text{S}=\text{O})$], an 830 cm^{-1} [$\delta(\text{CH})$]. The most important band of a PEG-*b*-PSU block copolymer will be the band at 1110 cm^{-1} [$\nu(\text{C}-\text{O}-\text{C})$].

7.4.2 Sample preparation

The polymerisation products of the different PEG-*b*-PS and PEG-*b*-PSU were used for FTIR without further treatment. Additionally, PSU and modified PSU membrane samples were prepared as described in Section 7.2.2 were analyzed with FTIR-PAS. The membrane samples were removed from the water and dried in air for 24 h prior to analysis.

7.4.3 Results and discussion

7.4.3.1 PEG-*b*-PS films

Figure 7.7 shows the FTIR spectra of three different PEG-*b*-PS block copolymers, all synthesized using the identical MPEG macro RAFT agent. The only difference in the

Chapter 7: Surface analysis of amphiphilic block copolymers

reaction conditions was the reaction temperature. From the legend in the spectrum it can be seen that the black spectrum represents the block copolymer formed in the reaction of CVADTB MPEG 2000 with styrene at a reaction temperature of 60°C, with the reaction temperatures being 70°C and 80°C for the blue and red spectra, respectively.

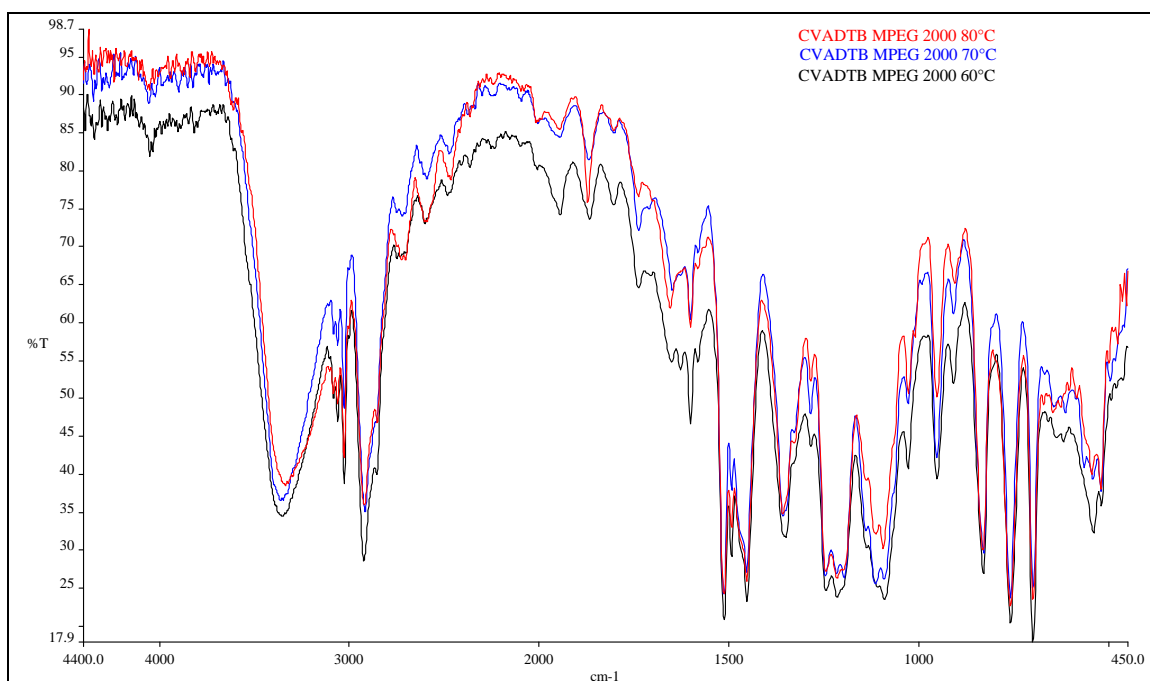


Figure 7.7 FTIR-PAS of PEG-*b*-PS block copolymers.

FTIR analysis is an analysis of the chemical composition of a material. It is therefore important that identical compounds are compared in the spectra. Due to the different chemical composition of the DIBTC based RAFT agents; the spectra will differ from that seen in Figure 7.7, where the similarity in chemical structure of the copolymers is shown. Different functional groups, however, can be compared from sample to sample. Table 7.5 shows the analysis of the different spectra in terms of the integrated peak areas of the aliphatic ether group of PEG (at 1040-1166 cm⁻¹), and the benzene ring of PS (at 668-725 cm⁻¹). A:B refer to the hydrophilic:hydrophobic ratio as determined by integration of the IR peaks of PEG (at 1040-1166 cm⁻¹), and the benzene ring of PS (at 668-725 cm⁻¹).

Chapter 7: Surface analysis of amphiphilic block copolymers

Table 7.5: Results of FTIR analysis of PEG-b-PS block copolymers

Sample	Components	Relative amount (%)	\bar{M}_n g/mol	PDI	PEG (C-O-C)	PS (benzene)	A:B
1	PS	37	11200	1.4	4508	2265	1.99
	PEG-b-PS	52	14600	1.3			
	PEG-PS-PEG	5	14800	1.2			
	PEG2000	6					
2	PS	42	12100	1.3	5045	2524	1.99
	PEG-b-PS	50	16400	1.3			
	PEG2000	8					
3	PS	70	7400	1.3	5173	5464	0.95
	PEG-b-PS	26	9500	1.2			
	PEG2000	4					
4	PS	54	4800	1.3	4728	4310	1.10
	PEG-b-PS	21	6300	1.2			
	PEG-b-PS	16	5600	1.2			
	PEG2000	9					
5	PS	14	6200	1.3	3528	6111	0.58
	PEG-b-PS	56	7900	1.2			
	PEG5000	25					
	PEG-PEG	4					
6	PS	33	9800	1.5	4011	2269	1.77
	PEG-b-PS	40	13900	1.3			
	PEG-PS-PEG	4	17200	1.3			
	PEG2000	23					

The results in Table 7.5 will be compared with both the contact angle measurements and the AFM force-distance measurements.

7.4.3.2 PEG-b-PSU films and membranes

Figure 7.8 shows the FTIR spectra of two different modified PSU membranes. Both Membranes M1106 and M1111 were modified with the addition of a PEG 2000-b-PSU block copolymer added to the casting solution. M1106 and M1111 correspond to Membrane 2 and Membrane 3 in contact angle analysis and AFM force-distance analysis, respectively.

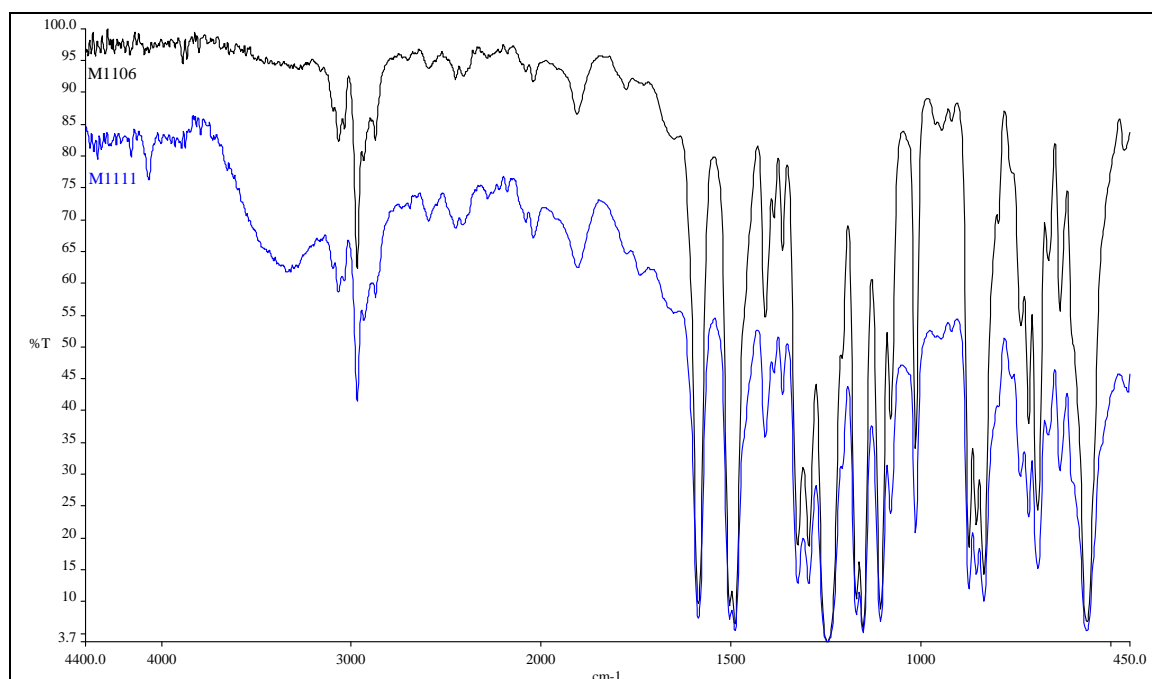


Figure 7.8: FTIR-PAS of PSU membranes modified with PEG2000-b-PSU block copolymers

Similar peak integration to what had been used in Section 7.4.3.1 was used to determine the A:B ratio in both the membranes and the polymer samples. The A:B ratio was then compared to the PEG-content of each sample as determined by $^1\text{H-NMR}$ as shown in Table 7.6 and Table 7.7.

Table 7.6: Results of FTIR analysis of PEG-b-PSU block copolymers

Membrane	\bar{M}_n MPEG (g/mol)	PEG content in PEG-b-PSU (%)	PEG-b-PSU molar mass (g/mol)	PEG (C-O-C)	PS (aromatic)	A:B
1	-	-	-			
2	2000	45	9 171	5468	2616	2.09
3	2000	44	11 691	3326	790	4.21
4	5000	68	ND	5182	2726	1.90

The results in Table 7.6 will be brought into context in Section 7.5, where the different methods of analysis were compared.

Results in Table 7.7 show that the PEG content as determined by $^1\text{H NMR}$ differ from the values obtained by integrating the FTIR data peaks. $^1\text{H NMR}$ and FTIR differ in the sense that $^1\text{H NMR}$ is representative of the complete sample analyzed, while FTIR-PAS is a surface analysis technique, only probing 45 μm into the sample. The FTIR data is therefore more representative of the surface of a material as apposed to the bulk chemical

Chapter 7: Surface analysis of amphiphilic block copolymers

composition analysis of ^1H NMR. With conditioning of the surface of the films to be more hydrophilic, it is therefore possible for the surface to exhibit properties that are different from the bulk properties of the sample. Membrane samples were stored in water, which results in the migration of pendant PEG chains to the surface of the membranes. A higher hydrophilic concentration is therefore expected at the surface of the membrane when compared to the bulk of the sample.

Table 7.7: Results of FTIR analysis of PSU membranes modified with PEG-b-PSU block copolymers

Samples	\bar{M}_n MPEG (g/mol)	PEG content in PEG-b- PSU (%)	PEG-b-PSU molar mass (g/mol)	PEG (C-O-C)	PS (aromatic)	A:B
1	-	-	-			
2	2000	45	9 171	2678	1456	1.83
3	2000	44	11 691	2382	1597	1.49
4	5000	68	ND	3403	2576	1.32

7.5 Summary of results

Table 7.8 and Table 7.9 represents a summary of the results of surface analysis by contact angle measurement, AFM and FTIR.

Table 7.8: Summary of results of surface analysis of PEG-b-PS block copolymers

Sample	Components	Relative amount %	\bar{M}_n g/mol	PDI	Contact angle (θ)	Adhesion force (nN)	A:B FTIR
1	PS	37	11200	1.4	83.3 ± 1.4	263 ± 37.3	1.99
	PEG-b-PS	52	14600	1.3			
	PEG-PS-PEG	5	14800	1.2			
	PEG2000	6					
2	PS	42	12100	1.3	73.9 ± 2.7	218.9 ± 30.5	1.99
	PEG-b-PS	50	16400	1.3			
	PEG2000	8					
3	PS	70	7400	1.3	79.1 ± 1.9	114.3 ± 24.9	0.95
	PEG-b-PS	26	9500	1.2			
	PEG2000	4					
4	PS	54	4800	1.3	66.2 ± 4.0	289.7 ± 11.8	1.10
	PEG-b-PS	21	6300	1.2			
	PEG-b-PS	16	5600	1.2			
	PEG2000	9					
5	PS	14	6200	1.3	82.1 ± 1.6	288.5 ± 20.1	0.58
	PEG-b-PS	56	7900	1.2			
	PEG5000	25					
	PEG-PEG	4					
6	PS	33	9800	1.5	76.9 ± 2.3	ND	1.77
	PEG-b-PS	40	13900	1.3			
	PEG-PS-PEG	4	17200	1.3			
	PEG2000	23					

Contact angle measurements and AFM force-distance analysis are methods used to analyze the surface of a sample, whereas in FTIR the sample is penetrated by the IR beam up to a depth of 45 μm . It is therefore possible that some of the results obtained from the contact angle measurement and AFM might differ from that obtained by FTIR analysis. Further, as AFM measurements are located on small segments of a sample (5 μm x 5 μm) and due to the amphiphilic nature of the PEG-b-PS copolymers, they will phase separate in solution. It is therefore possible that AFM analysis may be localized on

Chapter 7: Surface analysis of amphiphilic block copolymers

a hydrophobic segment in the sample and therefore not give a representative value of the hydrophilicity of that particular sample. The problems associated with the analysis of the PEG 5000-*b*-PS film have been discussed in Section 7.2.3.1.

Table 7.9: Summary of results of surface analysis of modified PSU membranes

Membrane	\bar{M}_n MPEG (g/mol)	PEG content in PEG- <i>b</i> - PSU (%)	PEG- <i>b</i> - PSU molar mass (g/mol)	Contact angle (θ)	Adhesion Force (nN)	A:B
1	-	-	-	81.1 \pm 2.3	55.1 \pm 5.6	
2	2000	45	9171	78.1 \pm 2.9	59.7 \pm 6.8	1.83
3	2000	44	11691	78.3 \pm 1.9	66.2 \pm 13.6	1.49
4	5000	68	ND	71.5 \pm 2.2	60.5 \pm 9.3	1.32

Results of contact angle measurements shown in Table 7.9 show the effective hydrophilization of PSU membranes. This is supported by AFM force-distance analysis, where there is an increase in the adhesion force as shown. Membranes for FTIR analysis had to be dried in an oven to remove all moisture prior to analysis and due to the lower water content in the samples might have influenced the FTIR results.

7.6 Conclusions

Results of the surface analysis of the different films and membranes samples were discussed in Section 7.5. The following conclusions are drawn from the results of the different surface analysis techniques.

- 1 Film preparation and pretreatment had an influence on the hydrophilic: hydrophobic ratio at the surface of the samples.
- 2 For the PEG-*b*-PS films, both the copolymer fraction and molar mass of the copolymer had an influence on the hydrophilicity of the films. An increase in the total PEG fraction resulted in an increase in the contact angle of the films.
- 3 PEG 5000-*b*-PS surface analysis showed lower than expected hydrophilicity. Sample preparation and chain mobility of the large PEG chains resulted in ineffective hydrophilization of the films.
- 4 PEG-*b*-PSU copolymers (from both PEG 2000 and PEG 5000) proved to be effective in hydrophilising PSU membranes as reported by contact angle measurements and AFM force-distance analysis.

Chapter 7: Surface analysis of amphiphilic block copolymers

- 5 Contact angle measurements proved to be the most effective method of hydrophilicity measurement.
- 6 AFM force-distance measurements proved useful in obtaining an indication of the hydrophilicity of the surface of the films and membranes. The technique will have to be adapted to obtain a more representative adhesion force value for the samples.
- 7 FTIR spectroscopy remains an effective method to determine the hydrophilic:hydrophobic ratio of the surface of membrane samples.

7.7 References

1. Bascom, W. D., The wettability of polymer surfaces and the spreading of polymer liquids, *Advances in Polymer Science*, **1988**, 85, 90-124.
2. Johnson, A. E., Analysis of the Young equation and use of the Kelvin equation in calculating the Gibbs excess, *Colloids and Surfaces A: Physicochemical and engineering Aspects*, **2002**, 202, 33-39.
3. Hancock, L. F., Phase inversion membranes with an organised surface structure from mixtures of polysulfone and polysulfone-poly(ethylene oxide) block copolymers, *Journal of Applied Polymer Science*, **1997**, 66, 1353-1358.
4. Hancock, L. F., Fagan, S. M. and Ziolo, M. S., Hydrophilic, semipermeable membranes fabricated with poly(ethylene oxide)-polysulfone block copolymer, *Biomaterials*, **2000**, 21, 725-733.
5. Wei, Z. Q., Wang, C. and Bai, C. L., Surface imaging of fragile materials with hydrophobic atomic force microscope tips, *Surface Science*, **2000**, 467, 185-190.
6. Garcia, R. and Perez, R., Dynamic atomic force microscopy methods, *Surface Science Reports*, **2002**, 47, 197-301.
7. Kim, J. H. and Kim, S. C., Effect of PEO grafts on the surface properties of PEO grafted PU/PS IPN's: AFM study, *Macromolecules*, **2003**, 2867-2872.
8. Albrecht, T. R., Dovek, M. M., Lang, C. A., Grutter, P., Quate, C. F., Kuan, S. N., Frank, C. W. and Pease, R. F. W., Imaging and modification of polymers by scanning tunneling and AFM, *Journal of Applied Physics*, **1998**, 64, 1178-1184.
9. Okabe, Y., Akba, U. and Fujihira, M., Chemical force microscopy of -CH₃ and -COOH terminal groups in mixed self-assembled monolayers by pulse force mode atomic force microscopy, *Applied Surface Science*, **2000**, 157, 398-404.
10. Krottil, H., Stifter, T., Waschipky, H., Weishaupt, K., Hild, S. and Marti, O., Pulsed force mode: a new method of the investigation of surface properties., *Surface and Interface Analysis*, **1999**, 27, 336-340.

Chapter 7: Surface analysis of amphiphilic block copolymers

11. Akari, S., Horn, D., Keller, H. and Schrepp, W., Chemical imaging by scanning force microscopy, *Advanced Materials*, **1995**, 7, 549-551.
12. Frisbie, C. D., Rozsnyai, L. F., Noy, A., Wrighton, M. S. and Lieber, C. M., Functional groups imaging by chemical force microscopy, *Science*, **1994**, 265, 2071-2074.
13. Witec, Calibrating the digital pulsed for mode images, *Manual, version 2.0*, **2003**.
14. Productguide, *Nanoworld*, **2002**.
15. Marti, O., Stifter, T., Waschipky, H., Quintus, M. and Hild, S., Scannig probe microscopy of heterogeneous polymers, *Colloids and Surfaces*, **1999**, 154, 65-73.
16. Spitzig, P., Dynamische Rasterkraftmikroskopie, *PhD dissertation*, **2002**.
17. Sato, F., Okui, H., Akiba, U., Suga, K. and Fujihira, M., A study of topographic effects on chemical force microscopy using adhesive force mapping, *Ultramicroscopy*, **2003**, 97, 303-314.
18. McClelland, J. F., Jones, R. W. and Bajic, S. J., Handbook of Vibrational Spectroscopy, *Wiley & Sons*, **2002**.
19. Song, Y.-Q., Sheng, J., Wei, M. and Yuan, X.-B., Surface modification of polysulfone membranes by low-temperature plasma-graft poly(ethylene glycol) onto polysulfone membranes, *Journal of Applied Polymer Science*, **2000**, 78, 979-985.

Chapter 8

Conclusions and recommendations

8.1 Conclusions

This dissertation forms part of *Project K5/1268* of the Water Research Commission (WRC) of South Africa with the title: *Hydrophilization of hydrophobic Ultrafiltration and Microfiltration Membranes*. The aim of *Project K5/1268* is to improve the properties of commercial PSU UF membranes in terms of the useful lifetime and the separation properties of these membranes.

Certain guidelines are critical for suitable hydrophilizing agents for PSU membranes. These guidelines include:

- the conformational structure of the hydrophilizing agent;
- the precise chemical architecture of the proposed hydrophilizing agents; and
- the most suited method of synthesis.

This led to the need for the synthesis of materials with specific characteristics. Amphiphilic block copolymers possess a chemical architecture making these types of polymers ideal materials for the hydrophilization of PSU UF membranes. Due to the unique properties of PEG, as described in Chapter 1, PEG was selected as the hydrophilic segment of the amphiphilic block copolymer, with PS and PSU being selected as the hydrophobic segments of the different amphiphilic block copolymers to be synthesized.

The RAFT process was selected as a suitable method for the synthesis of PEG-b-PS block copolymers, while PEG-b-PSU block copolymers were synthesized via polycondensation reactions.

With the specific goals of the project being stated in Chapter 1, the following conclusions were made at the completion of the project:

8.1.1 Synthesis and characterisation of hydrophilizing agents

In the controlled free radical homopolymerisation of styrene with the aid of CVADTB and DIBTC as RAFT agents, RAFT agents were effective in producing homopolymers with

narrow MMD. CVADTB was found to be what is termed a “slow” RAFT agent, in that the rate of transfer to and from RAFT agent (addition and fragmentation) was low. The rate of transfer to and from RAFT agent for DIBTC, on the other hand, was fast when compared to CVADTB. In the homopolymerisation of styrene with CVADTB, an increase in reaction temperature resulted in an increase in the rate of the reaction, however, as the reaction temperature was increased, control over the growth of the polymer was compromised in that there was an accompanying increase in the MMD of the polymer. (Although this work is a repetition of published data, it formed part of a systematic study and was useful in the determination of suitable polymerisation conditions for copolymerisation styrene with PEG macro RAFT agents.)

Copolymers were successfully prepared via the RAFT assisted copolymerisation of styrene with PEG-based macro RAFT agents. Analyses by conventional SEC and ^1H NMR were found to be insufficient to characterise these polymers. Both techniques failed to give a chemical composition analysis of the formed copolymer products. A 2D chromatographic system revealed the chemical composition distribution of the formed polymer products. Overlapping of peaks in conventional SEC would have resulted in incorrect conclusions being drawn. In all cases studied, the polymerisation products obtained contained at least three components, PS and PEG homopolymers, as well as PEG-b-PS block copolymer. In certain instances, especially at longer reaction times, and higher fractional conversions, uncontrolled termination reactions led to the formation of PEG-PS-PEG triblock copolymers.

Certain factors proved to have an influence on the products formed. The most important factor is the method of formation of the MPEG macro RAFT agents. PTSA and DMAP are essential to increase the yield of the MPEG macro RAFT agents. Parallel with homopolymerisation, an increase in the reaction temperature resulted in an increase in the polydispersity of the formed polymers. 2D chromatography proved to be instrumental in analyzing the polymer products formed. In accordance with homopolymerisation, CVADTB MPEG macro RAFT agents are termed as “slow” RAFT agents, while DIBTC MPEG macro RAFT agents offered faster rates of transfer and therefore reached higher fractional conversion at corresponding reaction times than the CVADTB macro RAFT agents. The PS homopolymer fraction formed in the reaction with the DIBTC macro RAFT agents was higher compared with the CVADTB counterparts. It therefore appeared that higher yields were obtained in producing CVADTB MPEG macro RAFT agents as opposed to DIBTC MPEG macro RAFT agents.

Copolymers of bis (4-chlorophenyl) sulphone-bisphenol A and MPEG, both MPEG 2000 and MPEG 5000, were successfully synthesized and characterised by both ^1H NMR and ^{13}C NMR. The molar mass of both the bis (4-chlorophenyl) sulphone-bisphenol A polysulphone and the bis (4-chlorophenyl) sulphone-bisphenol A-MPEG copolymers obtained were low, as determined by SEC (relative to narrow MMD polystyrene standards). Longer reactions times and more careful consideration of the stoichiometric imbalance is necessary to optimize the synthetic procedure to produce bis (4-chlorophenyl) sulphone-bisphenol A and MPEG copolymers of higher molar mass.

8.1.2 Surface analysis

Film preparation and pretreatment had an influence on the hydrophilic: hydrophobic ratio at the surface of the samples. For the PEG-b-PS films, both the copolymer fraction and molar mass of the copolymer had an influence on the hydrophilicity of the films. An increase in the total PEG fraction resulted in a decrease in the contact angle of the films. PEG 5000-b-PS surface analysis showed hydrophilicity lower than expected.

PEG-b-PSU copolymers (from both PEG 2000 and PEG 5000) proved to be effective in hydrophilizing PSU membranes as reported by contact angle measurements and AFM force distance analysis.

Contact angle measurements proved to be an effective method of hydrophilicity measurement. AFM force distance measurements proved useful in obtaining an indication of the hydrophilicity of the surface of the films and membranes. The technique, however, will have to be adapted to obtain a more representative adhesion force value for the samples. FTIR spectroscopy remains an effective method to determine the hydrophilic:hydrophobic ratio of the surface of membrane samples.

8.1.3 Model study

Due to the complex composition of the PEG-b-PS copolymerisation products and the inability to successfully isolate the PEG-b-PS fraction, it was not possible to carry out the intended model study on the influence of the chemical composition of the PEG-b-PS block copolymers on the hydrophilicity of these materials. 2D chromatography showed the existence of at least three components (PEG, PS and PEG-b-PS) in each copolymerisation product. With the difficulty experienced in purifying the PEG-b-PS block copolymer, these products were not suitable to be used in a model study as hydrophilizing

agents for PSU UF membranes. However, with the results obtained in the surface analysis of the PEG-b-PS copolymerisation products, conclusions could be made regarding the influence of the hydrophilic fraction in each product.

Contact angle measurements for modified PSU UF membranes showed that the size of the PSU segment did not have an influence on the hydrophilicity of the modified membrane. The governing factor in contact angle analysis appeared to be the size of the PEG segment. An increase in the length of the PEG block of the hydrophilizing agent led to a decrease in the static contact angle of the membrane sample.

8.1.4 Surface analysis of hydrophilized PSU membranes

Flat sheet PSU membranes were cast and evaluated. Surface analysis (contact angle measurements) showed that the governing factor in contact angle analysis appeared to be the size of the PEG segment. An increase in the length of the PEG block of the hydrophilizing agent led to a decrease in the static contact angle of the membrane sample.

In conclusion it can be summarized that:

- The hydrophilizing agents were successfully synthesized and characterised, and
- Surface analysis showed that the hydrophilizing agents were successful in improving the hydrophilicity of the surface of PSU UF membranes.

8.2 Recommendations

The bulk of this investigation focused on the synthesis of PEG-b-PS block copolymers using the MPEG macro RAFT agents. Polymerisations were conducted in bulk, something that will not be practical in scale-up reactions. In terms of the PEG-b-PS block copolymer synthesis, certain recommendations can be made:

- 1 Bulk polymerisation should be avoided and other reaction media will have to be investigated. The RAFT assisted synthesis of these PEG-b-PS block copolymers in emulsion, mini-emulsion or in an appropriate solvent must be investigated. With large fractions of homopolymers forming in the reaction, the efficacy of the RAFT process will have to be evaluated against living anionic polymerisation.

- 2 The successful isolation of the PEG-b-PS block copolymer from the homopolymers in the products is essential in performing a model study on the influence of the hydrophilic:hydrophobic ratio on the surface properties of these block copolymers.

More focus should be placed on the synthesis of PEG-b-PSU block copolymers. Initially it was expected that the products would have a broad MMD and that a model study would not be possible making use of these copolymers. Results have shown that the products obtained have reasonably narrow MMD's, therefore making these copolymers ideal for model study. Recommendations of the synthesis of PEG-b-PSU block copolymers include:

- 1 Block copolymers of higher molar mass have to be synthesized. The introduction of a difunctional PEG will result in an increase in the molar mass of the formed product, as this will lead to the formation of a multi-block copolymer. Bis (4-chlorophenyl) sulphone (CPS) can be replaced with a compound with higher reactivity, like bis (4-fluorophenyl) sulphone (FPS). The effect of a more reactive monomer on the molar mass of the resulting product can be investigated by substituting CPS with FPS. This substitution can range from 0% to 100% to see what influence it might have.
- 2 The influence of the stoichiometric imbalance on the molar mass of the resulting products must be investigated further.

The evaluation of the hydrophilizing agents in terms of their ability to improve the separation properties of PSU membranes will have to be investigated. Although the primary objective of this dissertation is the synthesis and characterisation of polymers with an exact chemical composition distribution, this dissertation forms part of a project with the aim of hydrophilizing PSU UF membranes. Both surface analysis and physical membrane analysis is necessary to determine the hydrophilizing capabilities of these materials. The ratio of PSU:PEG-b-PSU was kept constant in this study. Different concentrations of the hydrophilizing agents will have to be added to the membrane casting solution in order to optimize the hydrophilization process. The distribution of PEG chains at the surface of the membrane will have to be quantified.

Membrane performance is a critical aspect not covered in this investigation. The influence of the length of the hydrophilic segment of the PEG-b-PSU block copolymer on the hydrophilization process was shown. The effect of the length of the hydrophobic segment of the PEG-b-PSU block copolymer will have to be investigated. It has to be investigated

whether there is a critical minimum length of the PSU segment of the PEG-b-PSU block copolymer to ensure molecular entanglement of that segment with the molecules of the PSU membrane substrate. Physical membrane evaluation will determine whether the hydrophilizing agent remains entangled in the PSU membrane matrix, or is washed out of the membrane due to lack of entanglement of molecules of the hydrophobic segment of the PEG-b-PSU block copolymer and the PSU membrane.

Hancock *et al.*¹ reported the use of Tetronic[®] 304 to introduce branch points in the structure of the hydrophilizing agent. This resulted in the process being conducted in three stages. By introducing functional groups on the aromatic rings of CPS, branch points can be introduced into the structure of the hydrophilizing agent whilst maintaining a one-stage process. Care has to be taken that these groups do not deactivate the CPS molecule in terms of nucleophilic substitution. Other multi-functional molecules like pyrogallol and pentaerythritol can be used to introduce branch points into the copolymer structure.

8.3 References

1. Hancock, L. F., Fagan, S. M. and Mullon, C. J.-P., Highly Branched Block Copolymers, *US Patent 6,172,180 B1*, **2001**.

Appendix 1: NMR of PEG-b-PS block copolymers

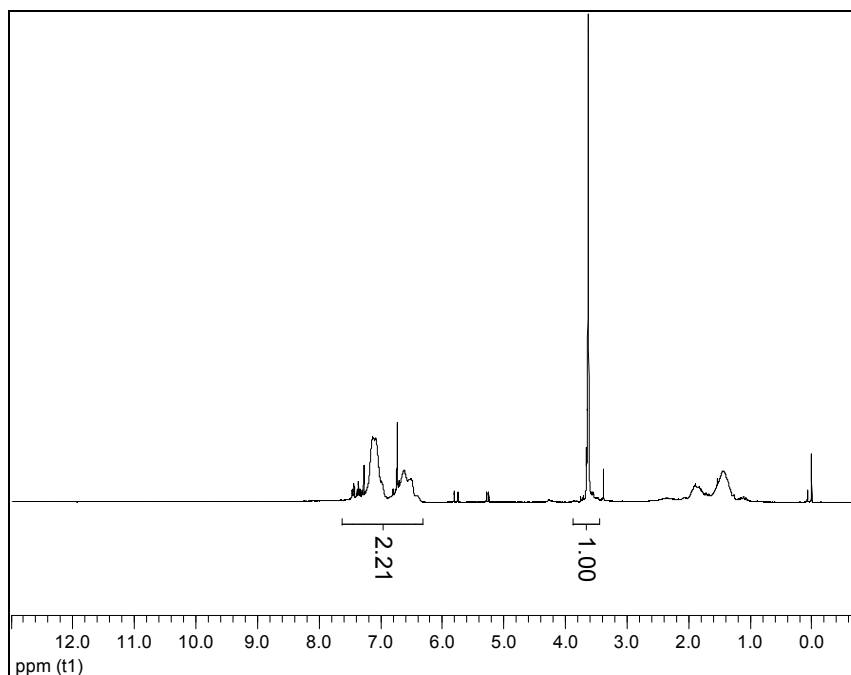


Figure A1: ¹H NMR spectrum for the copolymerisation of styrene with CVADTB MPEG 2000 at 60°C (reaction time: 22 h).

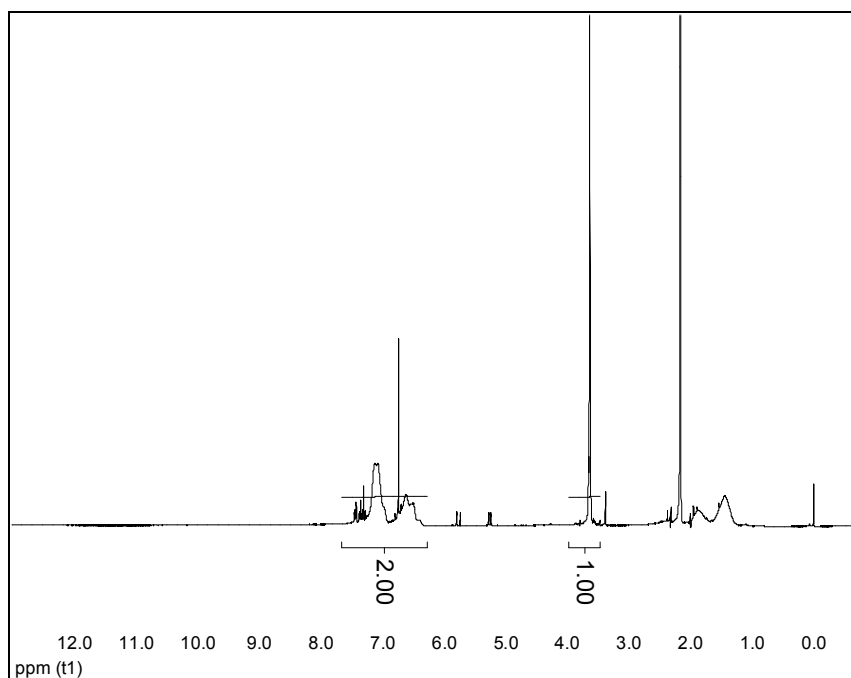


Figure A2: ¹H NMR spectrum for the copolymerisation of styrene with CVADTB MPEG 2000 at 70°C (reaction time: 24 h, Method 1).

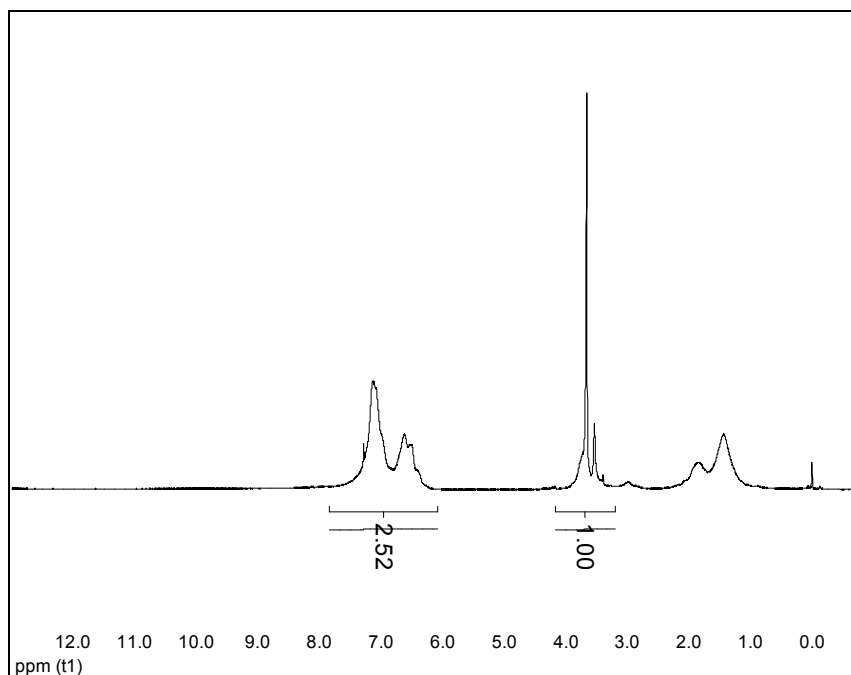


Figure A3: ¹H NMR spectrum for the copolymerisation of styrene with CVADTB MPEG 2000 at 70°C (reaction time: 11 h, Method 2).

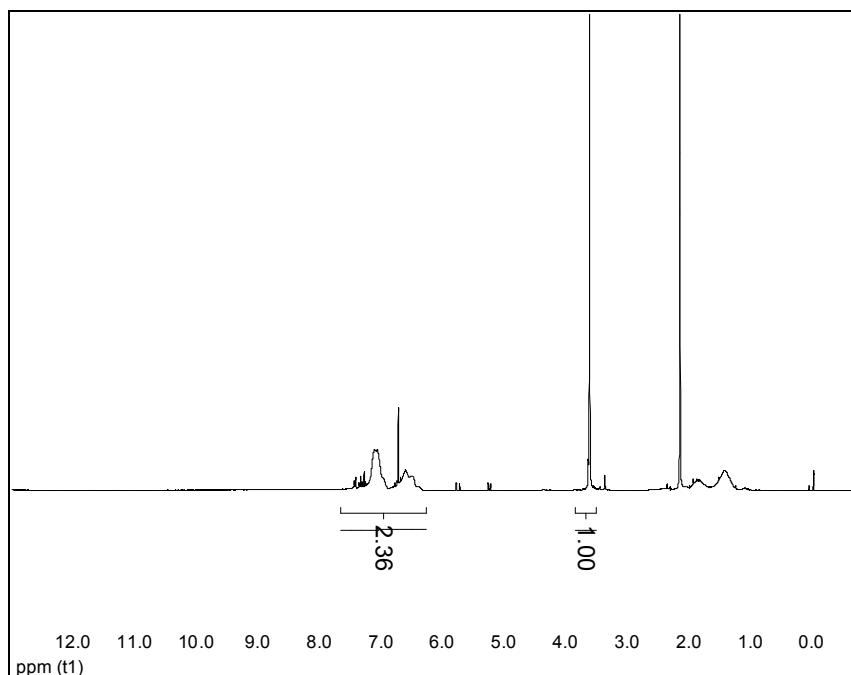


Figure A4: ¹H NMR spectrum for the copolymerisation of styrene with CVADTB MPEG 2000 at 80°C (reaction time: 22 h).

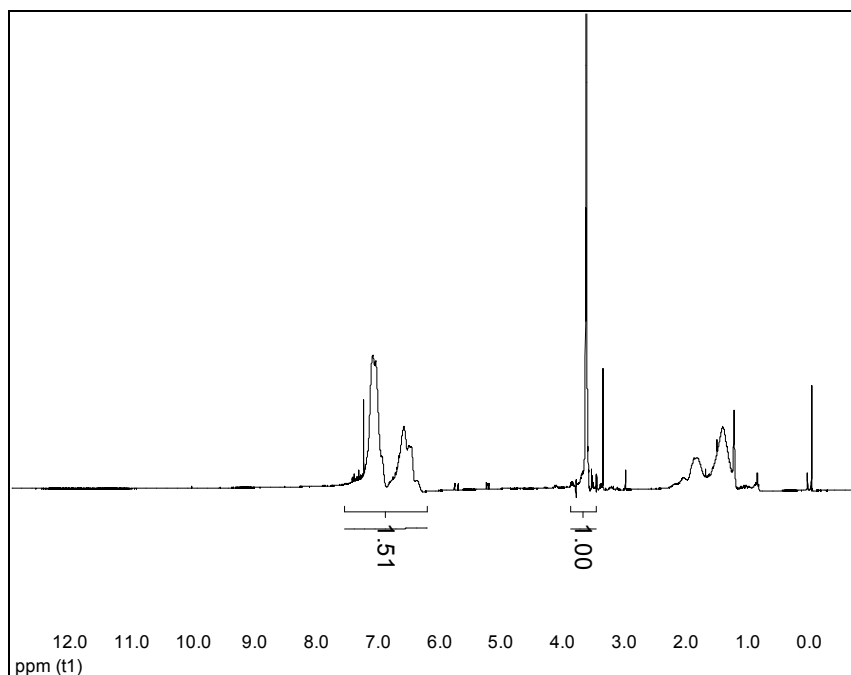


Figure A5: ^1H NMR spectrum for the copolymerisation of styrene with DIBTC MPEG 2000 at 70°C (reaction time: 6.5 h).

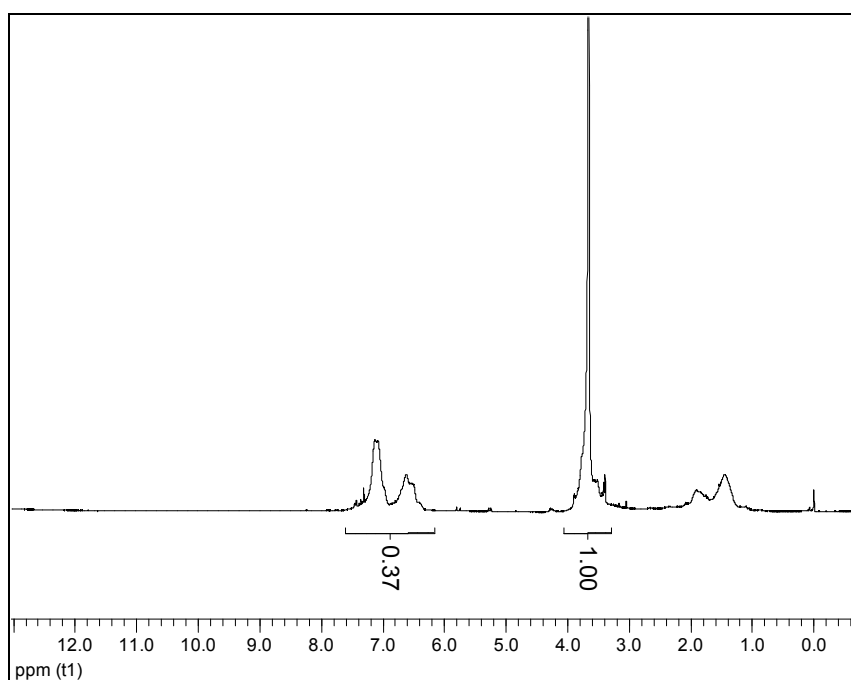


Figure A6: ^1H NMR spectrum for the copolymerisation of styrene with CVADTB MPEG 5000 at 70°C (reaction time: 6.5 h).

